GFZ German Research Centre for Geosciences
DOI: 10.2312/gfz.4.8.2019.004

Deliverable	D4.1 – Rock Properties
Work package	WP4 - Microscale
Type	R (document, report)
Dissemination level	PU (public)
Licence information	This publication is licensed under a Creative Commons License, International Attribution 4.0: CC BY
Due date	February 28th 2019
Actual submission date	March 01st 2019
Lead author (affiliation)	Richard R. Bakker (TUD)
Contributors	Christian Kluge (GFZ), Guido Blöcher (GFZ), Thomas Reinsch (GFZ), David Bruhn (TUD), Maiya Medetbekova (DTU), Helle Foged Christensen (GEO/DTU), Hamidreza M. Nick (DTU), and Auke Barnhoorn (TUD)
Change History	

Recommended Citation:

Bakker, R. R., Kluge, C., Blöcher, G., Reinsch, T., Bruhn, D. F., Medetbekova, M., Christensen, H. F., Nick, H. M., and Barnhoorn, A. (2019): The Horizon 2020 SURE Project: Deliverable 4.1 - Report on rock properties. Potsdam: GFZ German Research Centre for Geosciences, DOI: 10.2312/gfz.4.8.2019.004

The data associated to this report can be accessed via:

Bakker, R. R., Kluge, C., Blöcher, G., Reinsch, T., Bruhn, D. F., Medetbekova, M., Christensen, H. F., Nick, H. M., and Barnhoorn, A. (2019): The Horizon 2020 SURE Project: Deliverable 4.1 - Data on rock properties. GFZ Data Services, DOI: 10.5880/GFZ.4.8.2019.004

The SURE project has received funding from the European Union's Horizon 2020 research and innovation programme under grant agreement No 654662.

Table of Contents

The SURE project has received funding from the European Union's Horizon 2020 research and innovation programme under grant agreement No 654662.

The SURE project has received funding from the European Union's Horizon 2020 research and innovation programme under grant agreement No 654662.

The SURE project has received funding from the European Union's Horizon 2020 research and innovation programme under grant agreement No 654662.

GFZ German Research Centre for Geosciences
DOI: 10.2312/gfz.4.8.2019.004

1. Executive Summary

To assess the ability to produce a borehole with jet drilling technology, several different rock properties were measured on a suite of rock types. Test include: Uniaxial Compressive Strength (UCS); Acoustic wave speeds (v_p & v_s, unconfined); Triaxial deformation tests, Tensile strength tests; porosity measurements; and permeability measurements amongst others. The tests have been done at the rock deformation laboratories at GFZ, TU Delft and DTU. In some cases, duplicate tests have been done to check for consistency across facilities. As the SURE project advanced, a focus to some specific rock types emerged. These include: Gildehaus (Bentheim) Sandstone, used as benchmark rock type; Flechtinger sandstone, lateral equivalent for the Rotliegend sandstone, a reservoir rock in the Netherlands and Germany; Kohlenkalk (limestone), a target for ultra-deep geothermal (UDG) projects; Interlayered sediments in lava-sequences, a target for jetting in a field-test in Iceland; and Buntsandstein (sandstone), particularly from Bad-Dürkheim, as analogue rocks for Triassic sandstone reservoirs in the Netherlands; and Austin and Welton chalk as analogue rocks for chalk reservoirs. However, more rock types have been tested, but not to the same level of completeness. The data itself might still be useful for other projects, and is therefore also reported here.
A comprehensive overview of all data (averaged when applicable) is depicted in the table below (section 2). This is followed by notes on the used methods and apparatuses (section 3), followed by detailed description of individual tests (section 4). In case of multiple tests, curves of representative tests are shown here.

2. Comprehensive Data Tables

2.1. Porosity

Rock type	Porosity [%]	range (+/-) [%]	# samples
Ruhrsandstein (SRS6-DO)	9.0	2.5	5
Massenkalk (Saurland) (CMA6-WU)	2.3	1.0	4
Quartzite (Friedrichsdorf) (SQZ6-FR)	0*	0*	2
Granit (Odenwald) (PGR6-RI)	0.6	0.2	1
Bad Dürkheim sandstone (SBS6-BD)	19.0	5.0	24
Roter Mainsandstein (SRM6-MI)	14.0	4.0	11
Gildenhaus Sandstone (SGH6-GI)	24.0	1.0	3
Bebertal / Flechtinger sandstone (SBT6-BE)	8.5	3.3	16
Kohlenkalk (CKO6-AA)	0.8	0.2	5
Oberkirschner sandstein (SWD6-OK)	17.0	2.0	2
Friedewalder sandstone (SBS6-FR)	18.6	1.0	1
Ruethener Gruensandstein (SRG6-RU)	25.0	2.0	6

The SURE project has received funding from the European Union's Horizon 2020 research and innovation programme under grant agreement No 654662.

Interlayered sediments (VIB8-IC)	22.5	2.5	3
Iceland Basalt (VBA6-IC)	5.3	1.0	1
Austin Chalk	30.5	1.4	10
Welton chalk	16.1	2.3	8

* below detection limit

2.2. Permeability

Note: for rocktypes where multiple measurements are done, a representative value (order of magnitude) is given. Here the x,y direction is along/parallel to the bedding and the z-direction perpendicular to bedding.

Rock type	direction	Permeability (water; @ σ_3 = 25-15 MPa)	# samples
		[m^2]	
Bad Dürkheim sandstone (SBS6-BD)	x,y	3.0E-15	5
	z	3.0E-16	5
Roter Mainsandstein (SRM6-MI)	x,y	3.0E-15	2
	z	1.0E-15	1
Gildenhaus Sandstone (SGH6-GI)	n/a	2.3E-13	1
Bebertal / Flechtinger sandstone (SBT6-BE)	x,y	2.0E-16	*[2]
Kohlenkalk (CKO6-AA)	x	2.0E-19*[1]	4
	z	2.0E-19*[1]	5
Oberkirschner sandstein (SWD6-OK)	x,y	2.0E-15	1
Ruethener Gruensandstein (SRG6-RU)	x,y	4.0E-13	1
Interlayered clays (VIB8-IC)	n/a	1.63E-18*[1]	2
Iceland Basalt (VBA6-IC)	n/a	8.1E-18*[1]	1
Austin chalk	n/a	5.8E-15	4
Welton chalk	n/a	1.3E-16	4

Samples with direction "n/a" are considered isotropic.

* pulse decay method (gas permeameter)

*[2] see Pei et al., 2016 (detailed ref. in section 5.8)

2.3. Uniaxial test to derive UCS and the elasic modulii (Young's modulus and Poisson's ratio)

Rock type	UCS	Young's modulus	Poisson's ratio	# samples
	[MPa]	[GPa]	[-]	
Ruhrsandstein (SRS6-DO)	93.5-99.1	12.7-15.4	0.12-0.14	2
Massenkalk (Saurland) (CMA6-WU)	137-152	66.5-66.8	0.25-0.29	2
Quartzite (Friedrichsdorf) (SQZ6-FR)	307.0	46.6-56.7	0.09-0.11	2

The SURE project has received funding from the European Union's Horizon 2020 research and innovation programme under grant agreement No 654662.

Granit (Odenwald) (PGR6-RI)	120-142	39.9-47.6	0.19-0.26	2
Bad Dürkheim sandstone (SBS6-BD)	34.0	7.3	0.21	1
	22.5	4.8	0.26	1
Roter Mainsandstein (SRM6-MI)	66.5	11.7	0.32	1
	50.9	10.2	0.24	1
Gildenhaus Sandstone (SGH6-GI)	39-42	13.9-14.3	0.31-0.37	2
Bebertal / Flechtinger sandstone (SBT6-BE)	56.45	14.9	0.285	*2
Kohlenkalk (CKO6-AA)	116-158	41-46	0.28-0.30	2
	124-152	34.2-36.1	0.25-0.36	2
Oberkirschner sandstein (SWD6-OK)	75	15.6	0.33	1
	63	13.72	0.21	1
Friedewalder sandstone (SBS6-FR)	42-43	8.33-8.91	0.23-0.25	2
	44-60	8.70-9.75	0.170-0.19	2
Ruethener Gruensandstein (SRG6-RU)	13.5	4.4	0.03	1
	*1	4.7	*1	
Interlayered clays (VIB8-IC)	58 – 68	9.3 – 11.4	0.15-0.20	4
Iceland Basalt (VBA6-IC)	146-149	16.5-17.4	0.21-0.24	3
Austin chalk	10.4	5.7	0.23	6
Welton chalk	15.6	8.0	0.15	4

*1, radial strain poorly measured, only axial data available. No clear peak stress, rock too weak for accurate measurement

*2 see Pei et al., 2016 (detailed ref. in section 5.8)

2.4. Tiaxial strength

Rock type	Triaxial compressive strength	Cohesion	Internal friction angle	#
	[MPa]	[MPa]	[°]	
Massenkalk (Saurland) (CMA6-WU)		46.20	24.69	4
Bad Dürkheim sandstone (SBS6-BD)		8.65	27.95	5
Roter Mainsandstein (SRM6-MI)		21.50	20.71	4
Bebertal / Flechtinger sandstone (SBT6-BE)	$\sigma_3 = 5$; $\sigma_1 = 94.7$ $\sigma_3 = 10$; $\sigma_1 = 126.3$ $\sigma_3 = 20$; $\sigma_1 = 179.7$	15.80	43.20	3
Kohlenkalk (CKO6-AA)	$\sigma_3 = 20$, $\sigma_1 = 197$; $\sigma_3 = 30$, $\sigma_1 = 229$; $\sigma_3 = 40$, $\sigma_1 = 306$	46.40	20.81	4

The SURE project has received funding from the European Union's Horizon 2020 research and innovation programme under grant agreement No 654662.

	σ_3 = 20, σ_1 = 205; σ_3 = 30, σ_1 = 203 σ_3 = 40, σ_1 = 228 σ_3 = 50, σ_1 = 241	31.60	37.60	5
Oberkirschner sandstein (SWD6-OK)	σ_3 = 20, σ_1 = 151.5			
Interlayered clays (VIB8-IC)*	σ_3 = 10; σ_1 = 108.1 σ_3 = 20; σ_1 = 135.0	16.3	35.37	
Austin chalk	σ_3 = 2, σ1 = 17.2 σ_3 = 4, σ_1 = 21.6 σ_3 = 6, σ_1 = 24.3	7.8	41	3
Welton chalk	σ_3 = 2, σ_1 = 38.7 σ_3 = 4, σ_1 = 46.0 σ_3 = 6, σ_1 = 49.0	21.3	46	3

* More test are pending

2.5. Tensile strength and fracture toughness

Rock type	Tensile strength	range (+/-)*[1]	Fracture toughness K_{1c}	range (+/-) *[1]	direction *[2]	# samples
	[MPa]	[MPa]	[MPa $m^{0.5}$]	[MPa $m^{0.5}$]		
Ruhrsandstein (SRS6-DO)	5.25	1.73	0.670	0.146	ab	3
	6.58	1.61	0.474	0.156	pb	3
	8.46	3.07	0.875	0.368	uz	5
Massenkalk (Saurland) (CMA6-WU)	10.98	4.52	1.182	0.468		8
Quartzite (Friedrichsdorf) (SQZ6-FR)	17.47	7.28	1.396	1.308		4
Granit (Odenwald) (PGR6-RI)	11.85	3.37	1.347	0.291		4
Bad Dürkheim sandstone (SBS6-BD)	2.25	0.20	0.215	0.020		7
	2.70	0.35	0.245	0.030		6
Roter Mainsandstein (SRM6-MI)	2.91	0.66	0.350	0.077	ab	3
	5.85	0.36	0.641	0.003	pb	3
Gildenhaus Sandstone (SGH6-GI)	3.15	0.61	0.370	0.083		16
Bebertal / Flechtinger sandstone (SBT6-BE)	3.82		0.480			19

The SURE project has received funding from the European Union's Horizon 2020 research and innovation programme under grant agreement No 654662.

Kohlenkalk (CKO6-AA)	15.3	2.5	1.1	0.2	uz	3
	8.7	1.0	0.5	0.1	ab	3
	14.3	0.3	0.8	n/a	pb	2
Friedewalder sandstone (SBS6-FR)	3.74	1.14				
	3.66	0.22				
Interlayered clays (VIB8-IC)	8.00	2.00	0.711	0.153		18
Iceland Basalt (VBA6-IC)	7.16	0.41	0.962	0.080		8
Austin Chalk	1.75	0.08				6
Welton chalk	2.78	0.7				6

*[1] maximum range of data (not enough experiments for standard errors etc.)

*[2] directions (discs for tensile strength): ab, along bedding; pb, perpendicular to bedding; uz, unknown (z-direction core)

2.6. Acoustic Wave Speeds

Rock type	direction	v_p	v_{sh}	v_{sv}
		[km/s]	[km/s]	[km/s]
Ruhrsandstein (SRS6-DO)	y	3.66	2.51	2.38
	z	3.25	2.34	2.36
Massenkalk (Saurland) (CMA6-WU)	n/a	6.41	3.38	3.38
Quartzite (Friedrichsdorf) (SQZ6-FR)	n/a	5.36	3.56	3.58
Granit (Odenwald) (PGR6-RI)	n/a	4.77	3.06	2.85
Bad Dürkheim sandstone (SBS6-BD)*2	x,y	2.95	1.95	
	z	2.96	1.99	
Roter Mainsandstein (SRM6-MI)*2	x	3.03	2.00	
	z	4.09	2.01	
Gildenhaus Sandstone (SGH6-GI)	n/a	2.61	1.75	1.74
Oberkirschner sandstein (SWD6-OK)	x	2.87	2.00	1.93
	z	3.05	2.01	2.02
Friedewalder sandstone (SBS6-FR)	x	2.63	1.75	1.73
	z	2.50	1.71	1.71
Ruethener Gruensandstein (SRG6-RU)	x	2.54	1.66	
	z	2.64	1.73	

The SURE project has received funding from the European Union's Horizon 2020 research and innovation programme under grant agreement No 654662.

Interlayered clays (VIB8-IC)	n/a	3.40	2.06	
Iceland Basalt (VBA6-IC)	n/a	3.68	2.36	2.37
Austin chalk	n/a	3.12	1.62	
Welton chalk	n/a	4.22	2.07	

Samples with direction “n/a” are considered isotropic.

2.7. Thermal properties

Rock type	Thermal Effusivity	Thermal Conductivity
	[W*√(s)/((m^2)K)]	[W/mK]
Ruhrsandstein (SRS6-DO)	2957	4.005
Massenkalk (Saurland) (CMA6-WU)	2723	3.498
Quartzite (Friedrichsdorf) (SQZ6-FR)	3781	6.003
Granit (Odenwald) (PGR6-RI)	2444	2.918
Bad Dürkheim sandstone (SBS6-BD)*	3087	4.298
Roter Mainsandstein (SRM6-MI)*	2922	3.928
	2858	3.790
Gildenhaus Sandstone (SGH6-GI)	3233	4.640
Kohlenkalk (CKO6-AA / CMA6-KM)	2633	3.306
Friedewalder sandstone (SBS6-FR)	1569	1.294
Interlayered clays (VIB8-IC)	1971	2.005
Iceland Basalt (VBA6-IC)	2080	2.206

* results vary strongly per block, more samples have been tested, posted here are representative values

The SURE project has received funding from the European Union’s Horizon 2020 research and innovation programme under grant agreement No 654662.

3. Notes on samples and data processing:

Within WP5, several blocks were collected from various quarries, these include large samples (>50 x 50 x 50 cm) which were generally used for jetting tests, and smaller samples, used for hydraulic and mechanical characterization within WP4. In some cases, core samples from the larger block samples were taken. Core samples were drilled using diamond-tip drill bits while flushed with water, and cut plan-parallel to the length required for the test using diamond-edge saw blades. Experiments were conducted at the rock mechanics laboratories of GFZ and TU Delft, with the exception of Chalk-lithologies, which were conducted at DTU / GEO.

Figure 1, example of the provided a provided sample block (this case: VIB8_IC_01), with locations of the drilled cores indicated on the block. Note the ruler for scale.

In general, if anisotropic features could be determined beforehand (from sample blocks), cores were drilled in certain directions are labelled with X, Y, or Z, where x and y directions are both along the bedding plane, z direction is perpendicular to bedding plane. For all samples, no further distinction between x and y directions is further made prior to drilling the samples, as no particular paleo-flowdirection (or equivalent) could be determined from the individual blocks. It is therefore assumed that cores drilled in x and y directions are equivalent.

3.1. Sample codes and references to IGNS database

Rock type	Internal code	IGSN
Ruhrsandstein	SRS6-DO	GFTRE0099
Massenkalk (Saurland)	CMA6-WU	GFTRE0014
Quartzite (Friedrichsdorf)	SQZ6-FR	GFTRE0075

The SURE project has received funding from the European Union's Horizon 2020 research and innovation programme under grant agreement No 654662.

Granit (Odenwald)	PGR6-RI	GFTRE0033
Bad Dürkheim sandstone	SBS6-BD	GFTRE0035
Roter Mainsandstein	SRM6-MI	n.a.
Gildenhaus Sandstone	SGH6-GI	GFTRE0065
Bebertal / Flechtinger sandstone	SBT6-BE	
Kohlenkalk	CKO6-AA / CMA6-KM	GFTRE0000
Oberkirschner sandstein	SWD6-OK	GFTRE0119
Friedewalder sandstone	SBS6-FR	GFTRE0057
Interlayered clays	VIB8-IC	n.a.
Iceland Basalt	VBA6-IC	n.a.
Austin Chalk	n.a.	n.a.
Welton Chalk	n.a.	n.a.

n.a.: not available.

3.2. Porosity

3.2.1. TU Delft

Porosity was determined using a helium pycnometer installed at the TU Delft GSE lab. Samples are flushed prior to pycnometer runs. In post-processing outliers are manually excluded from averaging. The porosity is defined as the percentage of pore space, and is calculated as:

$$porosity = \left(1 - \frac{v_{pycnometer}}{v_{cylinder}}\right) \cdot 100\% \qquad (1)$$

where $v_{pycnometer}$ is the volume derived from the pycnometer (i.e., volume of grains) and $v_{cylinder}$ is the bulk volume of the sample (often a cylinder as the samples are subsequently used for other tests).

The SURE project has received funding from the European Union's Horizon 2020 research and innovation programme under grant agreement No 654662.

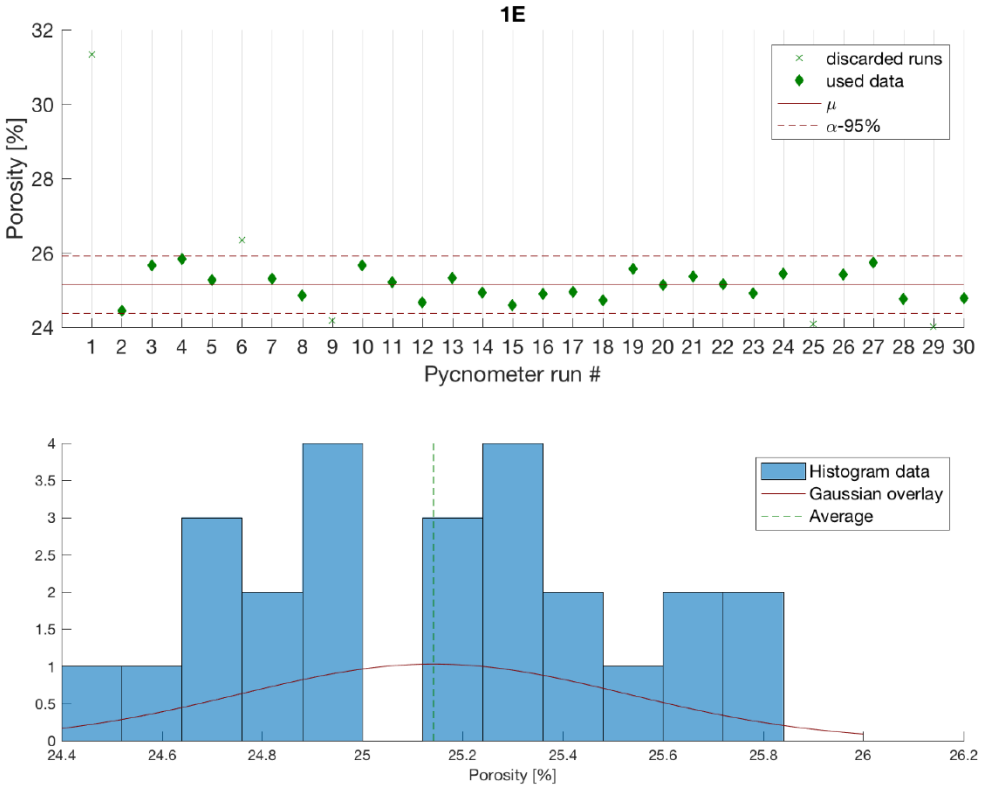

Figure 2, example results of pycnometry on sample VIB8_IC_01_1

3.2.2. GFZ

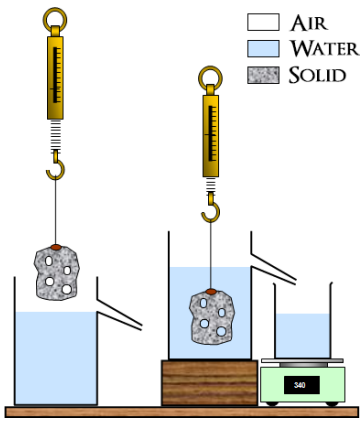

Figure 3: http://www.schoolphysics.co.uk, modified

At the Rock Deformation Laboratory of GFZ the porosity is measured by comparing the weight of the same core in oven-dry and saturated (distilled water) conditions. Using the weight difference and the density of distilled water the pore space is thereby calculated. Using

The SURE project has received funding from the European Union's Horizon 2020 research and innovation programme under grant agreement No 654662.

this Archimedes principle, the sample will be weighted under dry conditions. Afterwards the sample is saturated and the weight of the saturated sample is measured. If the fluid density and the bulk volume of the sample are known, the porosity can be calculated as follows:

$$m_{Air} = m_s \quad (2)$$

$$m_{Water} = m_s - V_s * \rho_f \quad (3)$$

$$\rho_s = \frac{m_s}{V_s} = \frac{m_{Air} * \rho_f}{m_{Air} - m_{Water}} \quad (4)$$

$$\varphi = \frac{V_b - V_s}{V_b} \quad (5)$$

3.3. UCS

Samples with a length to diameter ratio of 2.5:1 were deformed at a constant displacement rate, such that the engineering strain rate was 10^{-5} s^{-1}. Axial displacement was logged using two linear variable differential transducers (LVDTs), and used to calculate axial strain by:

$$\varepsilon = \frac{\Delta l}{l_0} \quad (6)$$

where ε is the engineering strain, Δl the change in length of the sample, and l_0 the initial length of the sample. Axial LVDT's are placed around the sample, avoiding corrections for apparatus compliance. The samples were fitted with a chain-gap type LVDT to measure radial displacement. Load is measured with a load cell, and converted to axial stress by dividing to the initial cross sectional area normal to the load direction. As "barreling"-effects were limited (radial strain <1%), no corrections for increased cross sectional area were performed. Elastic properties are determined by fitting axial stress vs axial strain as well as axial stress vs radial strain curves by a 1st order polynomial. Fit area is chosen such to limit influence of crack closure / machine settling at early stages of the experiment and also not to include the regime where subcritical crack growth is expected. The slope of the axial stress with axial strain is taken as Young's' Modulus. Poisson's ratio is determined by dividing the negative of the Young's Modulus by the value of the slope of the axial stress with radial strain. This method was chosen instead of evaluating the lateral and axial strain at 50% of maximum load, to avoid unrealistic high (axial) strain values due to crack closure and / or machine settling. Errors of the elastic properties are determined by using the associated errors of the linear regressions, determined by an alpha-95 prediction interval.

3.4. Brazil disk indirect tensile strength / Fracture Toughness

Core samples cut to discs, with length equal to half of the radius of the samples were used. These were diametrically loaded by line loads using specially designed jogs (according to ASTM standards), assuming an effective angle of load of 10˚. Samples were deformed at a loading rate such that failure occurred within half a minute. To avoid high deformation rates during failure (overshoot), the machine was operated in constant displacement mode instead of loading rate. Moreover, by logging the load and displacement, fracture toughness could be determined using the method of Guo et al., 1993.
For samples with clear anisotropic features (e.g., bedding, foliation) orientations of the discs with respect to the load direction have been taken into account. If no such information is available the sample is considered isotropic, and all data is used for averaging.

The SURE project has received funding from the European Union's Horizon 2020 research and innovation programme under grant agreement No 654662.

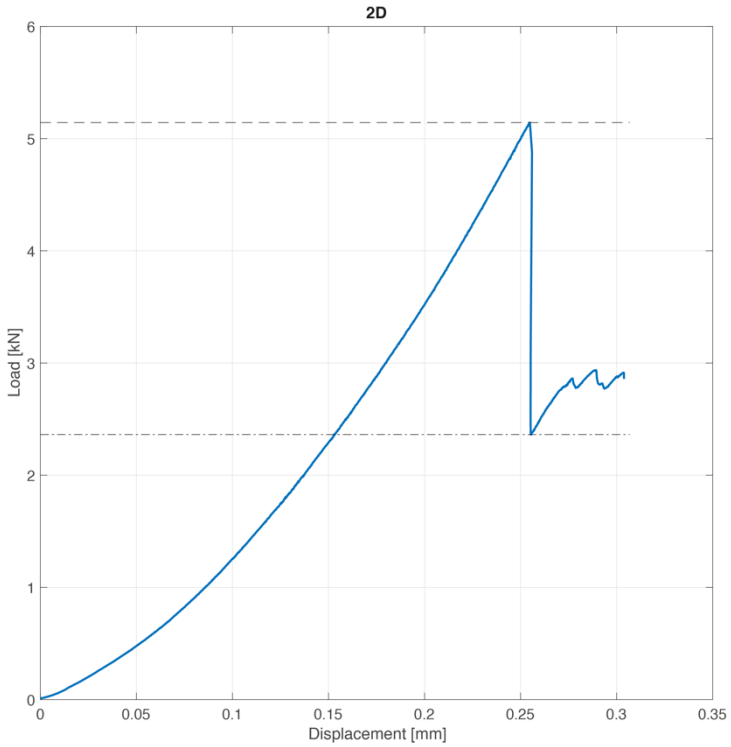

Figure 4, example of a load vs displacement curve of sample ViB8_IC_01_2D, used to calculate tensile strength (maximum load, dashed line), and p_{min} (dash-dot line).

3.5. Permeability

3.5.1. TU Delft

Permeability (k) is measured inside a triaxial deformation vessel (TerraTek) as installed in the rock mechanics laboratory of TU Delft, based on the principle of Darcy's law:

$$k = \frac{Q\mu L}{A\Delta P} \qquad (7)$$

where Q is the flowrate in m^3/s, μ is the viscosity of water at a certain temperature, in Pa.s, L is the sample length in meters, A is the cross sectional area in m^2 and ΔP is the pressure difference in Pascal.

Samples are radially confined using pressurized oil, separated by a rubber (EPDM) jacket. This type of jacket provides a good seal from low confining stress onward, preventing leakage between the sample wall and jacket. Axial confinement is brought to the sample by means of steel pistons and an axially applied load, measured with a load cell. These pistons have pore fluid lines embedded in them, and the end faces have grooves to allow equal distribution of fluid into the sample. Prior to measurements, samples are vacuumed, then flushed with CO_2, then flooded with distilled water. The distilled water is pressurized to dissolve any leftover CO_2, ensuring saturation.

The SURE project has received funding from the European Union's Horizon 2020 research and innovation programme under grant agreement No 654662.

Permeability measurements are conducted by flushing water through the sample at a known flowrate, and measuring the pressure difference across the sample. All measurements presented here are conducted with the constant flow method, using water at room temperature, at effective hydrostatic pressure and a pore pressure of 25 bar (regulated at outflow pump (i.e., backpressure)). Flow rates are chosen such to limit the resulting pressure difference to less than 5% of the confining pressure. An example of a run at constant confining pressure, collecting 5 data points is shown in figure 2.
Errors in permeability are calculated as the result of machine precision for flowrate, measurement errors for length and diameter (corrected for changes due to confining pressure), and standard deviation of pressure difference within a certain time window where a constant flowrate is imposed.

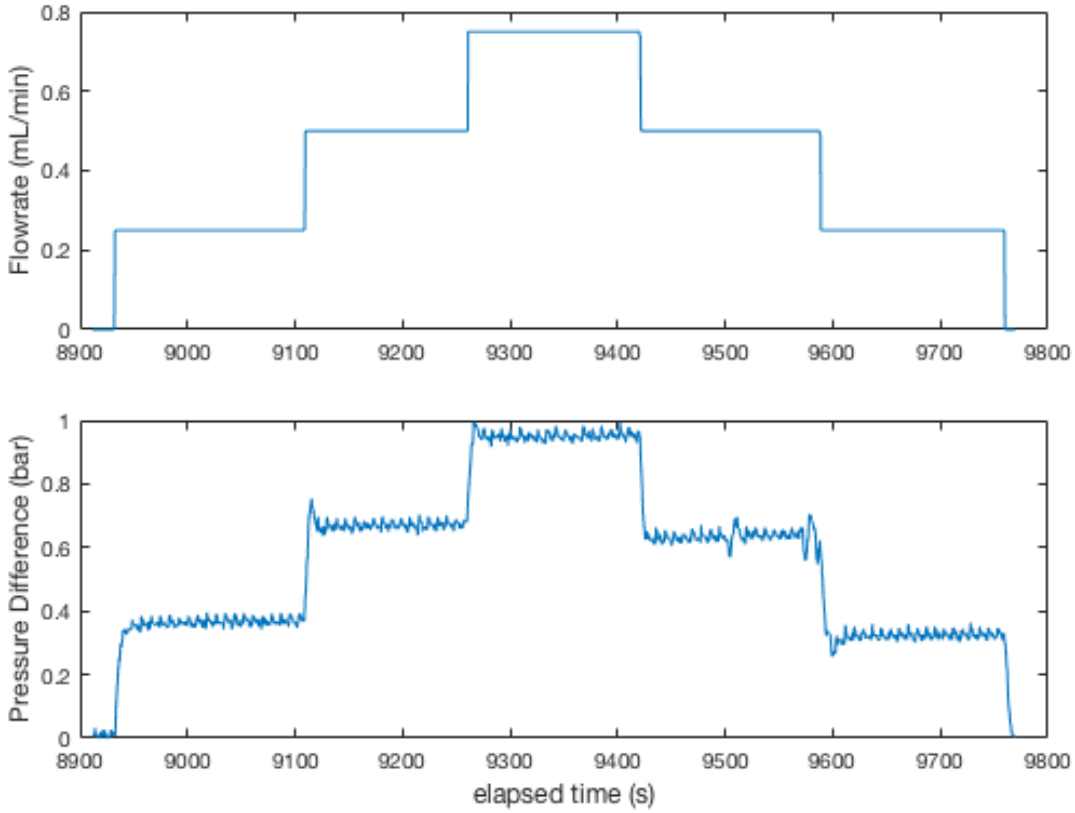

Figure 2, example of flowrate and resulting pressure difference.

3.5.2. GFZ

Tri-axial cell
The permeability determination is based on Darcy's law by the flow of distilled water. The permeability is determined for all samples at a confining pressure of 2 MPa and a fixed outlet pressure in the range of 0.1 to 0.2 MPa. Constant flow rates were in the order of 0.001 to 0.01 ml/min.

The SURE project has received funding from the European Union's Horizon 2020 research and innovation programme under grant agreement No 654662.

GFZ German Research Centre for Geosciences
DOI: 10.2312/gfz.4.8.2019.004

To quantify the effect of the effective pressure on the permeability, a constant flow is applied during the increase of confining pressure. The effective pressure is determined based on the effective pressure theory of Terzaghi (1936):

$$P_{eff} = P_{con} - P_{pore} \quad (8)$$

Where the mean pore pressure is assumed as:

$$P_{pore} = P_{out} + 0.5(P_{in} - P_{out}) \quad (9)$$

Gas permeameter

A cylindrical rock sample with a height of 40 or 50 mm and a diameter of 25 mm is put in a neoprene rubber jacket. Afterwards, the sample is placed in a hollow steel cylindrical chamber. Between the specimen and the threaded steel cylinder there is a space for hydraulic fluid to adjust the confining pressure. The recording frequency of the pressures and flow rates is 0.1 s-1. By controlling the flow and setting a constant confining pressure of 5 MPa and an outlet pressure of ~0.15 MPa, the inlet pressure at the top of the sample is monitored over time. After achieving a constant inlet pressure at a certain flow rate, the flow rate is increased for the next step. In total four steps of different flow rates are performed to obtain the permeability. The intrinsic permeability is described by Darcy's law by:

$$k = -\frac{Q\mu}{A}\frac{dL}{dP} \quad (10)$$

where Q is the flow rate [m^3/s], A is the cross sectional area of the flow [m^2], k the intrinsic permeability [m^2], μ the viscosity of the pore fluid [Pa*s], dP the pressure difference between the top and bottom of the specimen [Pa] and dL the length of the rock specimen [m]. This equation only holds for liquid fluids. For the use of gas, there are mainly two complications: compressibility and gas slippage. Gas is a compressible fluid and the application of high pressure during the gas permeameter test causes compression. The modified flow equation for compressible fluids is expressed by:

$$Q = -A\frac{k_{gas}}{\mu L}\frac{(P_{in}^2 - P_{out}^2)}{2P_{out}} \quad (11)$$

Klinkenberg (1941) discovered a higher gas permeability with respect to liquid permeability and attributed this to the slippage of gas molecules along grains. In comparison to a liquid, the average velocity of gas in the vicinity of pore walls is nonzero and therefore contributes to the flow. The Klinkenberg correction translates the gas permeability obtained by equations (12 and 13) into the equivalent liquid permeability by:

$$k_{gas} = k_{liquid}\left(1 + \frac{b}{P}\right) \quad (12)$$

$$b = \left(\frac{c\kappa T}{\pi\sqrt{2}r^3}\right) \quad (13)$$

Where b is the Klinkenberg slip factor (Pa), P the average pressure of the sample (Pa), c a constant, T the temperature (K), r the sample radius and κ the Boltzmann's constant (JK^{-1}). For high pressures the liquid permeability is equal to the gas permeability if $2/(P_{in}+P_{out}) = 0$. Extrapolation of the k_{gas} is performed by linear extrapolation. Based on a maximum pressure difference of 5 MPa and a minimum measurable flowrate of 0.02 mL/min, this method can measure the permeability down to 10 nD.

The SURE project has received funding from the European Union's Horizon 2020 research and innovation programme under grant agreement No 654662.

3.6. Triaxial tests

3.6.1. TU Delft

The Terratek apparatus described above is additionally used for tri-axial testing. Tests were either run room-dry, or under drained conditions, using constant back-pressure. The later also allows for monitoring of pore space destruction (pore collapse) or creation (microcracks). Radial strain is based on a chain-type LVDT similar to the UCS tests, corrected for (changing) jacket wall thickness during tests. Axial strain is determined using two LVDT's, mounted around the sample avoiding corrections for machine compliance. The Terratek apparatus is can handle maximum confining pressure up to 500 bar, and maximum axial loads of 300 kN.

3.6.2. GFZ

All tensile, uniaxial and tri-axial strength tests as well as some hydraulic tests were performed using the MTS 815 apparatus. This mechanical testing system (MTS) is a servo controlled compressive machine with 2000 kN vertical loading capacity. The apparatus consists of a stiff loading frame with a closed tri-axial cell, a set of independently operating Quizix 6000-Series pumps and a data-monitoring and acquisition system. In situ conditions can be simulated by hydrostatic pressures up to 140 MPa and temperatures up to 150 °C using oil as the confining medium. The axial strain and lateral strain of the core samples are measured by two Linear Variable Differential Transformers (LVDTs) and a circumferential chain extensometer, respectively. The resolution of the vertical and circular extensometer is 1*10-3 mm resulting in an axial strain resolution of $2*10^{-5}$ mm/mm and a lateral strain resolution of $1*10^{-6}$ mm/mm. The temperature is continuously monitored by two thermocouples, installed at the top and bottom of the specimen. Pore pressure is simulated by the use of two independent up- and downstream Quizix pumps. These pumps operate in constant pressure or constant flow rate mode and monitor accurately the volume change of the sample as a result of changing temperature or stress. The pressure difference over the sample is determined by a differential pressure sensor within the range of 0.01 to 1 MPa.

The SURE project has received funding from the European Union's Horizon 2020 research and innovation programme under grant agreement No 654662.

GFZ German Research Centre for Geosciences
DOI: 10.2312/gfz.4.8.2019.004

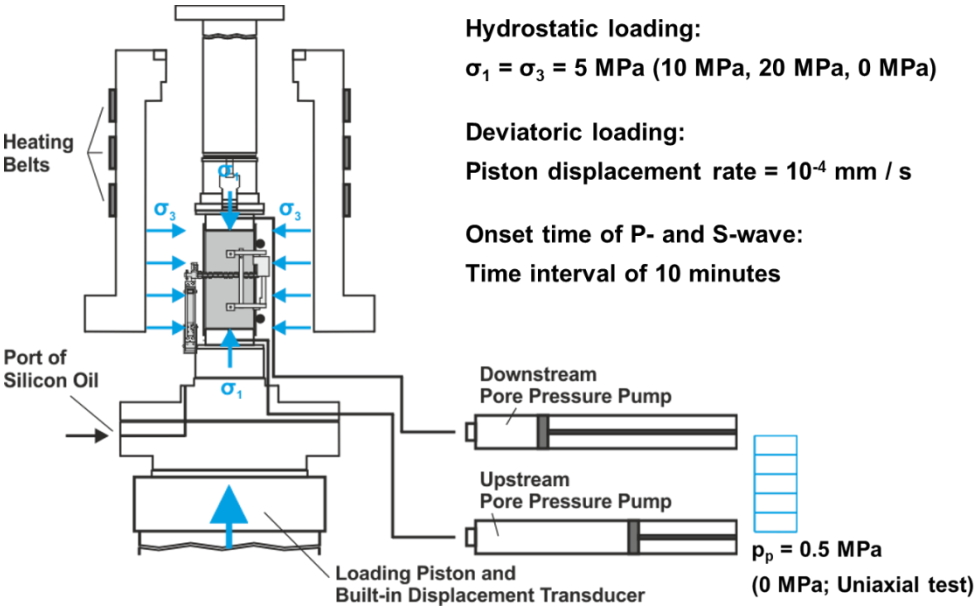

The SURE project has received funding from the European Union's Horizon 2020 research and innovation programme under grant agreement No 654662.

3.7. Acoustic wave speed

Acoustic wave speeds are determined using a set of transducers designed for a peak response frequency of 1 MHz. A single sine wave pulse is sent from a sender each 10 ms, which is in turn picked up by the receiver. This is repeated for at least 50, and the data is stacked to filter out noise effects. Picking first arrival is done graphically using the waveform itself as well as by using the spectrogram (see figure 3 for example of p-wave arrival). The latter is particularly useful when the influence arising from v_s-v_p conversion is relatively high (see figure 4 for example of s-wave arrival). As a result, time-picking errors are in the order of 0.1 µs.

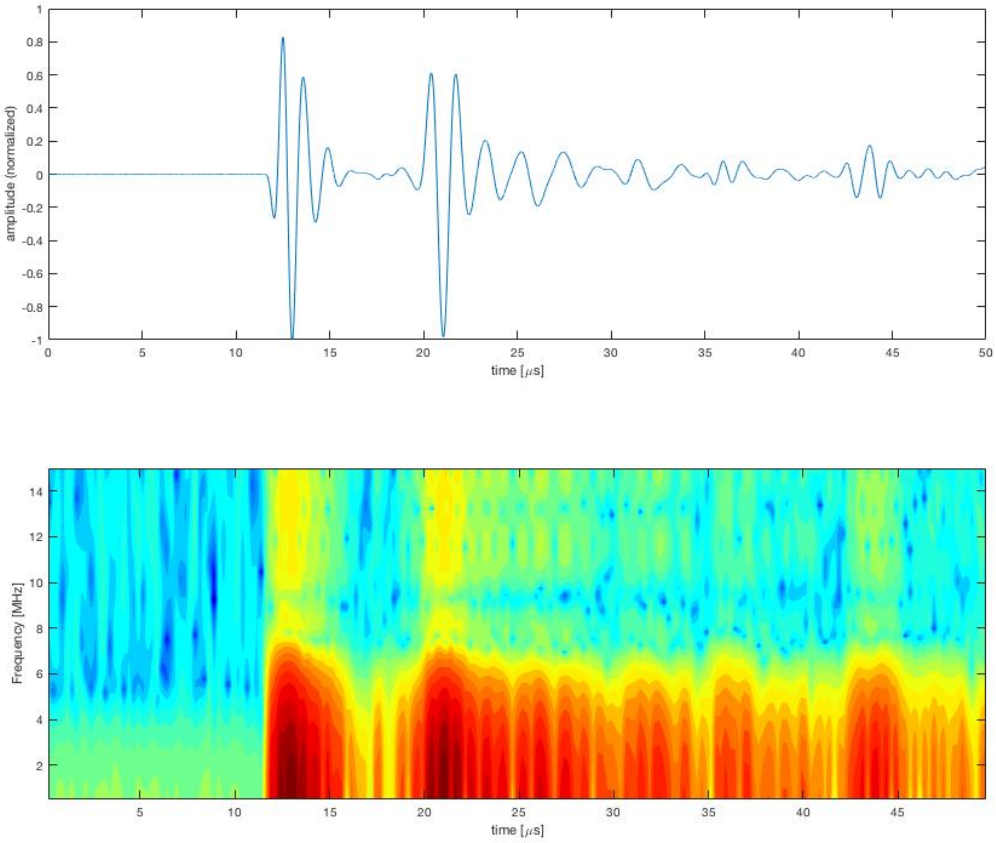

Figure 3, Example for a p-wave arrival, Sample: CMA6_WU_50_1

The SURE project has received funding from the European Union's Horizon 2020 research and innovation programme under grant agreement No 654662.

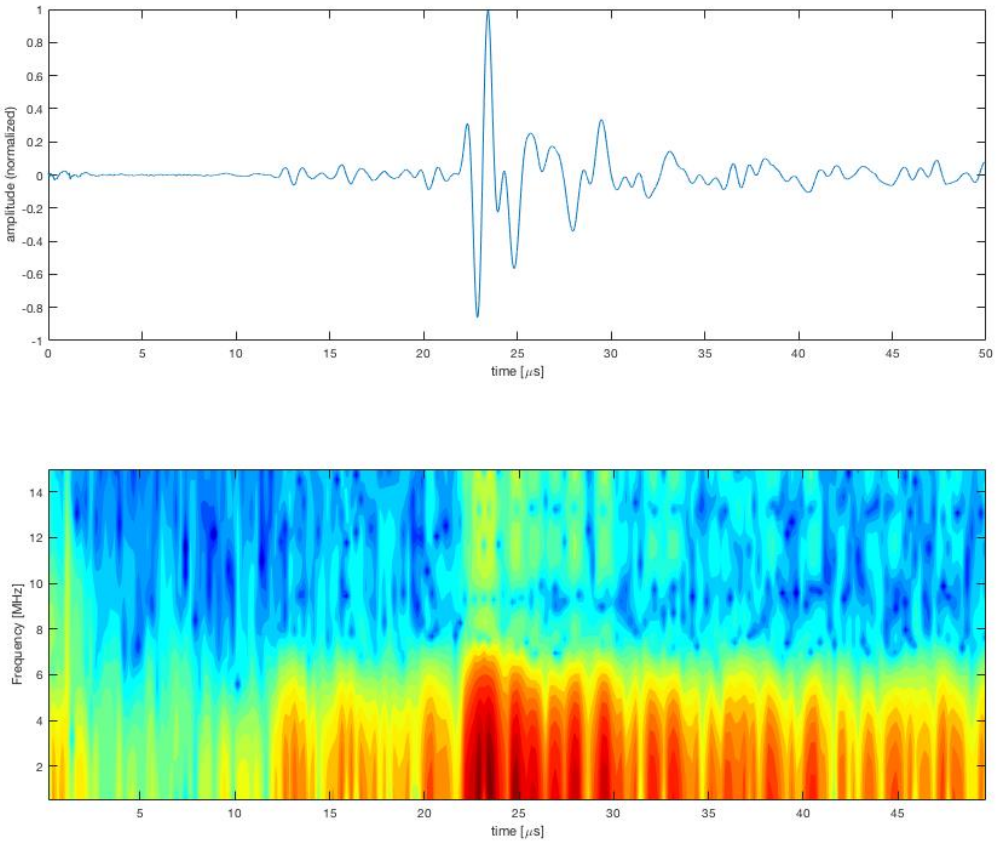

Figure 4, Example for a s-wave arrival, Sample: CMA6_WU_50_1

3.8. XRD & XRF

3.8.1. TU Delft

Both mineral composition and chemical composition (major oxides) of samples was determined at the faculty of Mechanical, Maritime and Materials Engineering (3mE), Department of Materials Science and Engineering. Samples consist of pressed pills, made up from ground-up starting material (often saw-cuts that were not viable for mechanical testing). For X-ray diffraction (XRD, mineral composition) the following instrument (and settings) was used: Bruker D8 Advance diffractometer Bragg-Brentano geometry with graphite monochromator and Vantec position sensitive detector. Co Kα radiation. Divergence slit 6M16 V12, scatter screen height 8 mm, 45 kV 35 mA. Sample spinning. Measurements were conducted with the following parameters: Coupled θ -2θ scan 10° -130°, step size 0.041 o 2θ, counting time per step 1 s. Data evaluation is conducted using Bruker software Diffrac Suite, EVA vs 4.2.
Chemical composition (major oxides) was determined using: Panalytical Axios Max WD-XRF spectrometer. Data evaluation was done with SuperQ5.0i/Omnian software.

3.8.2. Microprobe (GFZ)

An electron probe microanalyzer (EPMA) is used to determine the mineral composition, grain size, grain geometry and microcrack structure. Within the EPMA, an electron beam is transmitted to the 30 µD thin sections. As a response, each element in the sample emits a

The SURE project has received funding from the European Union's Horizon 2020 research and innovation programme under grant agreement No 654662.

characteristic X-ray which is detected by the electron microprobe. A high resolution image is generated which gives the opportunity to identify the textural structure on a micro scale level (1 µm). By the use of point analysis, the chemical composition of almost every single mineral can be determined. However, before conducting point analyses a standard should be used to calibrate the instrument. The analyses presented in this thesis are not point analyses but back-scatter detector (BSE) spectra where the intensity of each single element is plotted in a spectrum. The resulting analyses will calculate the mineral composition norming all the oxides at 100%, not considering water which may occur in some mineral phases. The different minerals within the sample differ in their brightness related to the atomic weight of the elements forming the mineral. ImageJ software is used in order to estimate the mineral fraction of the thin sections.

3.9. Thermal properties

Thermal conductivity (in W/mK) and effusivity (in $Ws^{0.5}/m^2K$) were determined using a C-Therm TCI Thermal Conductivity Analyzer, as installed at the Material Physics Lab, faculty of Aerospace Engineering, department of Aerospace Structures and Materials. For all samples, distilled water was used as contact fluid. As distilled water would move into pore space due to capillary effects, all measurements were conducted on saturated material.

3.10. Mercury Porosimetry

3.10.1. GFZ

In general, the capillary pressure is given by Laplace / Washburn Equation as follows:

$$p_c = p_a - p_w = \frac{2\gamma}{r_m} = \frac{2\gamma cos\theta}{R},$$

with p_a - atmospheric pressure, p_w - hydrostatic pressure, p_c - equivalent pressure due to capillary forces, γ - surface tension, and θ - contact angle.
Therefore, the capillary pressure can be linked to the pore radiuas as exemplary shown in Figure 5.

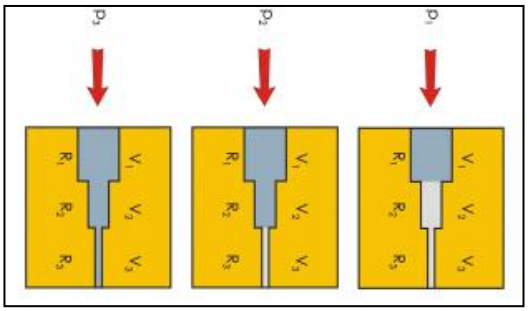

Figure 5: Different pores with certain radius will be wetted by mercury related to different pressure stages (source unknown).

Mercury intrusion porosimetry (MIP) is therefore an experimental technique used for the characterization of pore size distribution (Figure 6). By penetrating mercury into the pores of

The SURE project has received funding from the European Union's Horizon 2020 research and innovation programme under grant agreement No 654662.

a specimen, the volume of penetrated liquid metal as a function of pressure is measured. The mercury volume that intrudes at each pressure increment, corresponds to the volume of pores of each size class. Since mercury is a non-wetting fluid, an externally imposed pressure is required to intrude the liquid into the pores of the rock sample. Besides the determination of the pore size distribution, the total porosity is determined from the total intruded volume mercury. It is measured by a mercury penetrometer (an electrical capacitance dilatometer) and has an accuracy of 0.1 µL.

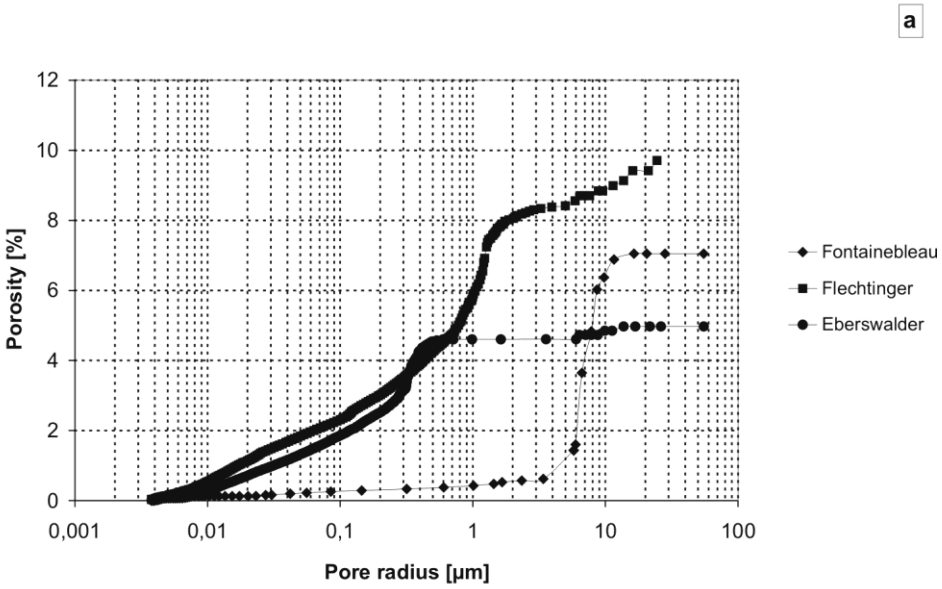

Figure 6: Pore size distribution of three kind of sandstone after Milsch, H., Blöcher, G., Engelmann, S. (2008): The relationship between hydraulic and electrical transport properties in sandstones: An experimental evaluation of several scaling models.

The SURE project has received funding from the European Union's Horizon 2020 research and innovation programme under grant agreement No 654662.

4. Details per rocktype

4.1. SRS6_DO - Ruhrsandstein

4.1.1. UCS

Sample: SRS6_DO_50_Y2B

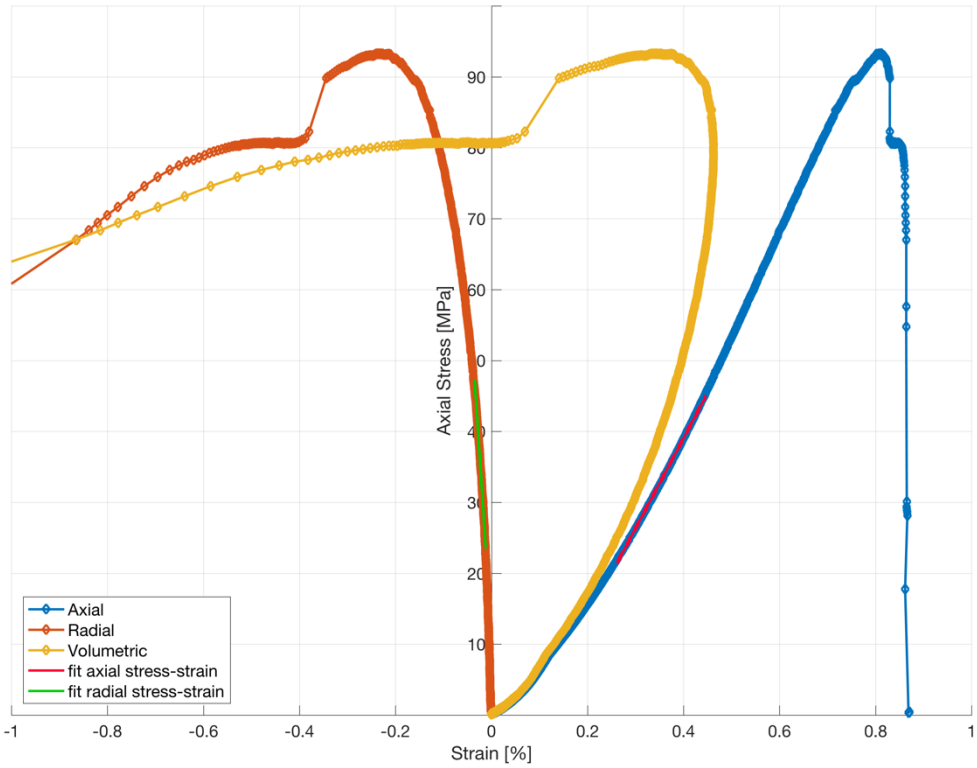

Peak stress: 93.5 [MPa]
Yield stress: 85.4 [MPa]
Young's Modulus: 12.7118 +/- 0.034699 [GPa]
Poisson's ratio: 0.12402 +/- 0.0012402, [-]

The SURE project has received funding from the European Union's Horizon 2020 research and innovation programme under grant agreement No 654662.

Sample: SRS6_DO_50_Y3A

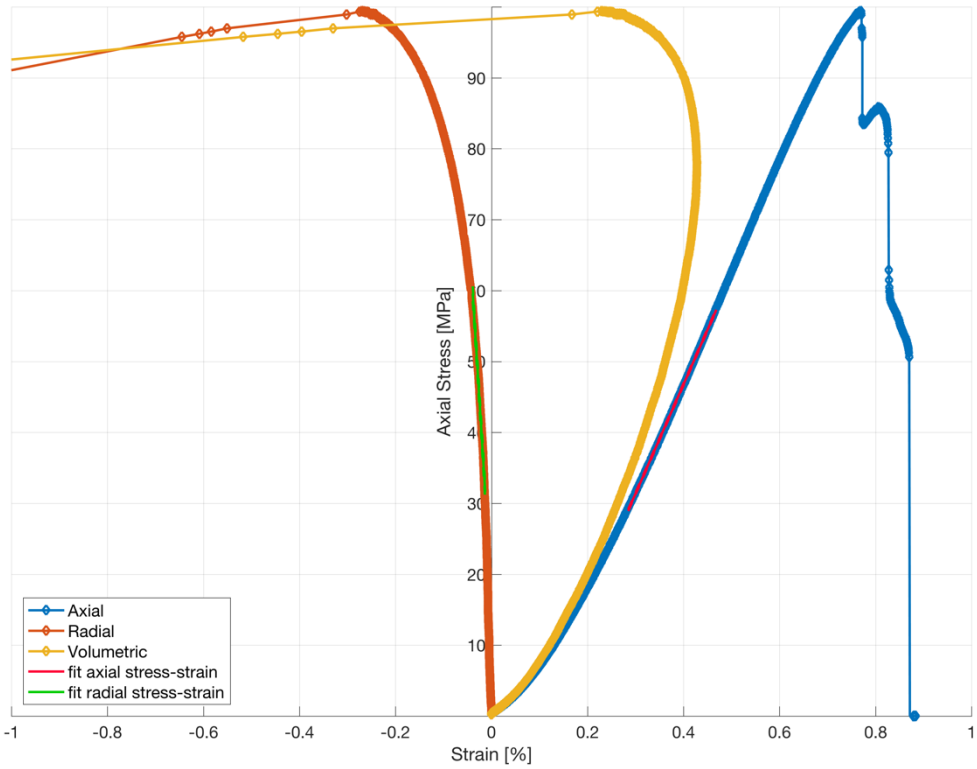

Peak stress: 99.1 [MPa]
Yield stress: 89.9 [MPa]
Young's Modulus: 15.4031 +/- 0.023255 [GPa]
Poisson's ratio: 0.1433 +/- 0.0017582, [-]

4.1.2. Brazil disk indirect tensile strength

Tensile failure along to bedding plane* (block: SRM6_DO_50):
Tensile Strength Mean: 5.2453 [MPa]
Standard deviation: 1.5227 [MPa]
Data range: 4.1017 – 6.9738 [MPa]
Number of samples: 3

Tensile failure perpendicular to bedding plane* (block: SRM6_DO_50):
Tensile Strength Mean: 6.5843 [MPa]
Standard deviation: 1.4306 [MPa]
Data range: 4.9741 – 7.7090 [MPa]
Number of samples: 3

Tensile failure unknown orientation (z-direction cores)* (block: SRM6_DO_50):
Tensile Strength Mean: 8.4588 [MPa]
Standard deviation: 1.7821[MPa]

The SURE project has received funding from the European Union's Horizon 2020 research and innovation programme under grant agreement No 654662.

Data range: 7.1711 – 11.5249 [MPa]
Number of samples: 5

* Based on CT scan data, what is identified as bedding plane could be a foliation plane. More research needed to confirm.

4.1.3. Acoustic velocities

Sample code	v_p [km/s]	v_{s1} [km/s]	v_{s2} [km/s]
SRS6_DO_50_Y2B	3.6303	2.4912	2.2295
SRS6_DO_50_Y3A	3.6877	2.5345	2.5290
SRS6_DO_50_Z3	3.2457	2.3352	2.3590

The SURE project has received funding from the European Union's Horizon 2020 research and innovation programme under grant agreement No 654662.

4.2. CMA6_WU – Massenkalk (Saurland)

4.2.1. UCS

Sample: CMA6_WU_50_1

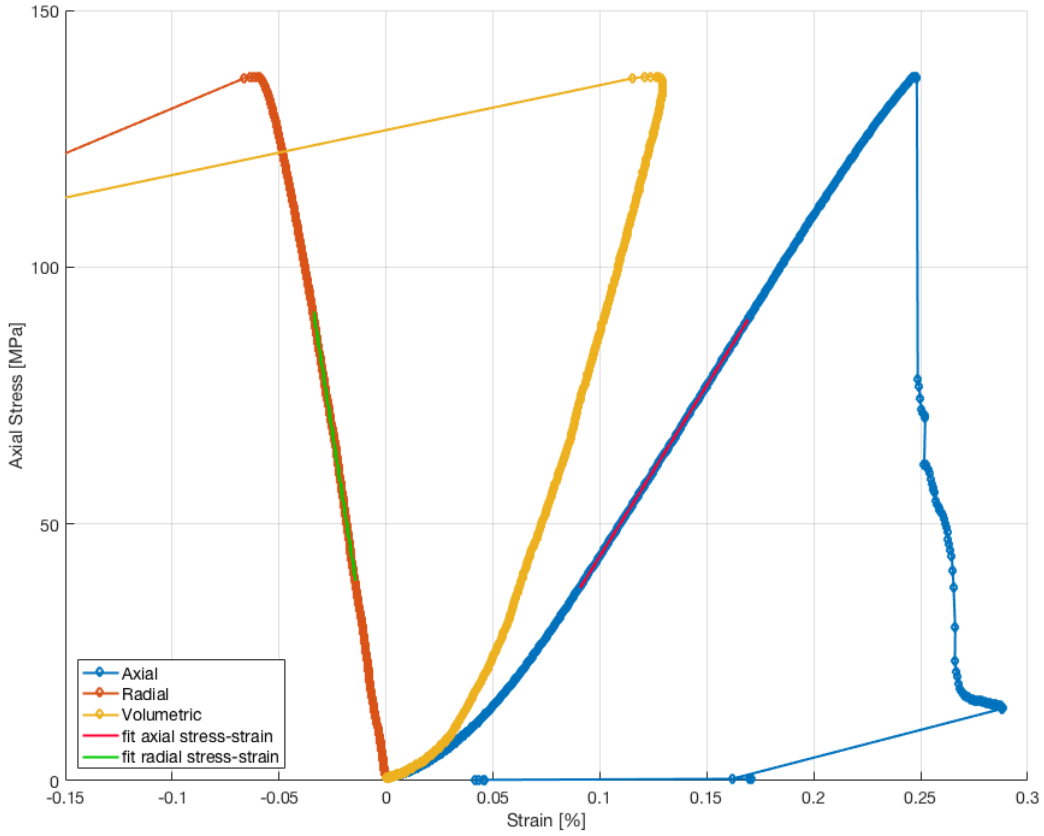

Peak stress: 137 [MPa]
Yield stress: 131 [MPa]
Young's Modulus: 66.5285 +/- 0.058798 [GPa]
Poisson's ratio: 0.24984 +/- 0.0017462, [-]

The SURE project has received funding from the European Union's Horizon 2020 research and innovation programme under grant agreement No 654662.

Sample: CMA6_WU_50_2

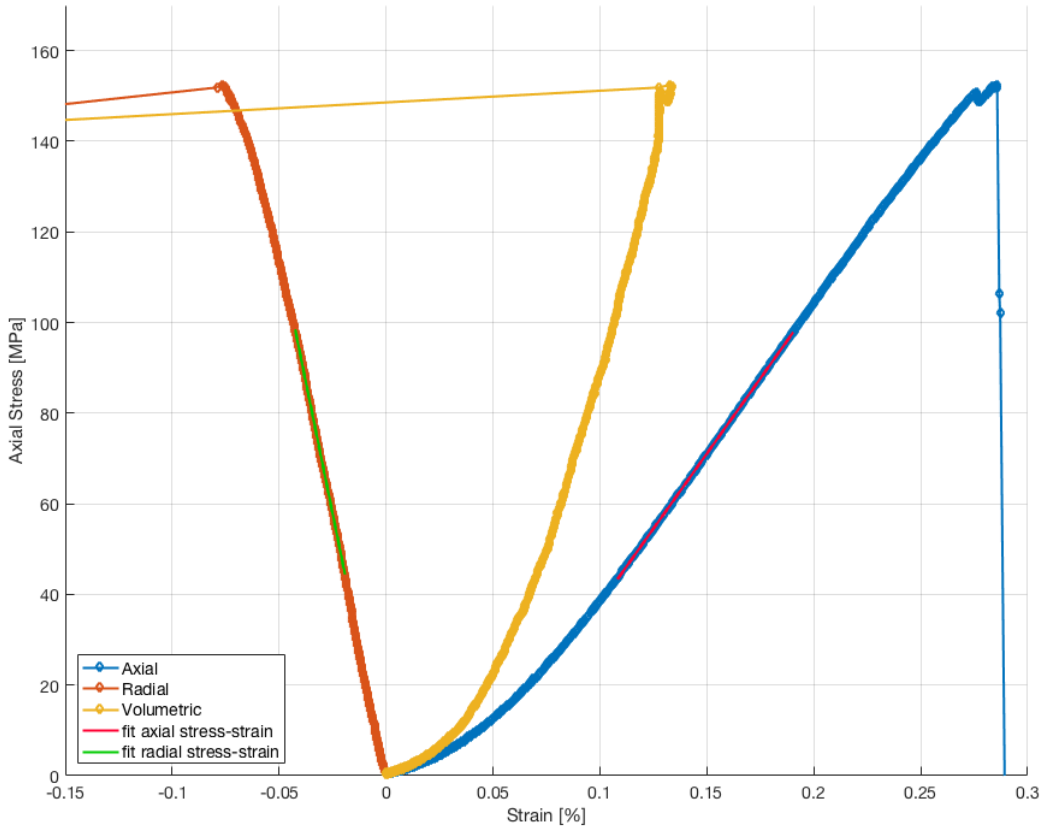

Peak stress: 152 [MPa]
Yield stress: 139 [MPa]
Young's Modulus : 66.3156 +/- 0.065231 [GPa]
Poisson's ratio : 0.28626 +/- 0.0010265, [-]

4.2.2. Brazil disk indirect tensile strength

Tensile Strength Mean: 11.30 [MPa]
Standard deviation: 2.30 [MPa]
Data range: 7.14 – 14.47 [MPa]
Number of samples: 8

4.2.3. Acoustic velocities

Sample code	v_p [km/s]	v_{s1} [km/s]	v_{s2} [km/s]
CMA6_WU_50_01	6.5016	3.4287	3.4295
CMA6_WU_50_02	6.3260	3.3412	3.3318

The SURE project has received funding from the European Union's Horizon 2020 research and innovation programme under grant agreement No 654662.

4.2.4. Tri-axial deformation

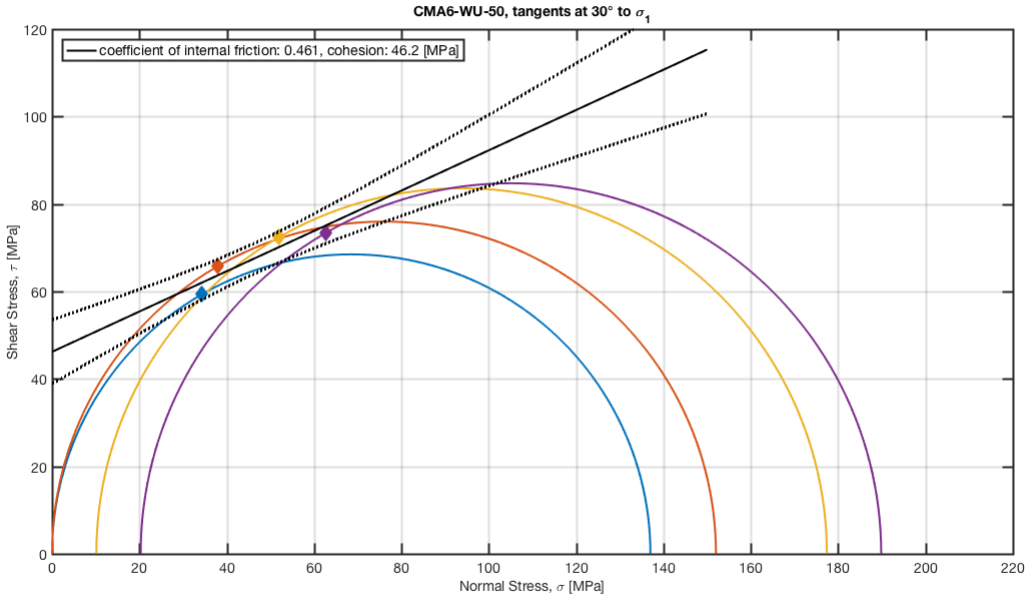

Mohr circles based on combined UCS and triaxial experiments. Note that due to intra-sample variability and lack of data the coefficients might differ greatly, as indicated by the bounds Mohr-Coulomb envelope (dotted lines) in above figure. For current best fit:
Internal friction coefficient: 0.461 [-]
Cohesion: 46.2 [MPa]

Triaxial experiment details:
Sample: CMA6_W_50_03
P_c: 10.14 [MPa]
Peak stress: 177.4 [MPa]
Young's Modulus: 54.2851 +/- 0.11485 [GPa],
Poisson's ratio: 0.17066 +/- 0.0010306 [-]

Sample: CMA6_W_50_04
P_c: 20.2874 [MPa]
Peak stress: 189.8437 [MPa]
Young's Modulus: 59.3188 +/- 0.08718 [GPa],
Poisson's ratio: 0.21252 +/- 0.0010741 [-]

The SURE project has received funding from the European Union's Horizon 2020 research and innovation programme under grant agreement No 654662.

4.3. SQZ6_FR – Quarzite (Friedrichsdorf)

4.3.1. UCS

Sample: SQZ6_FR_50_1A
Note: sample had a visible crack running roughly along sample axis. Failure occurred along that crack as well. Data to be handled with caution. Only elasticity parameters are deducted from experiment.

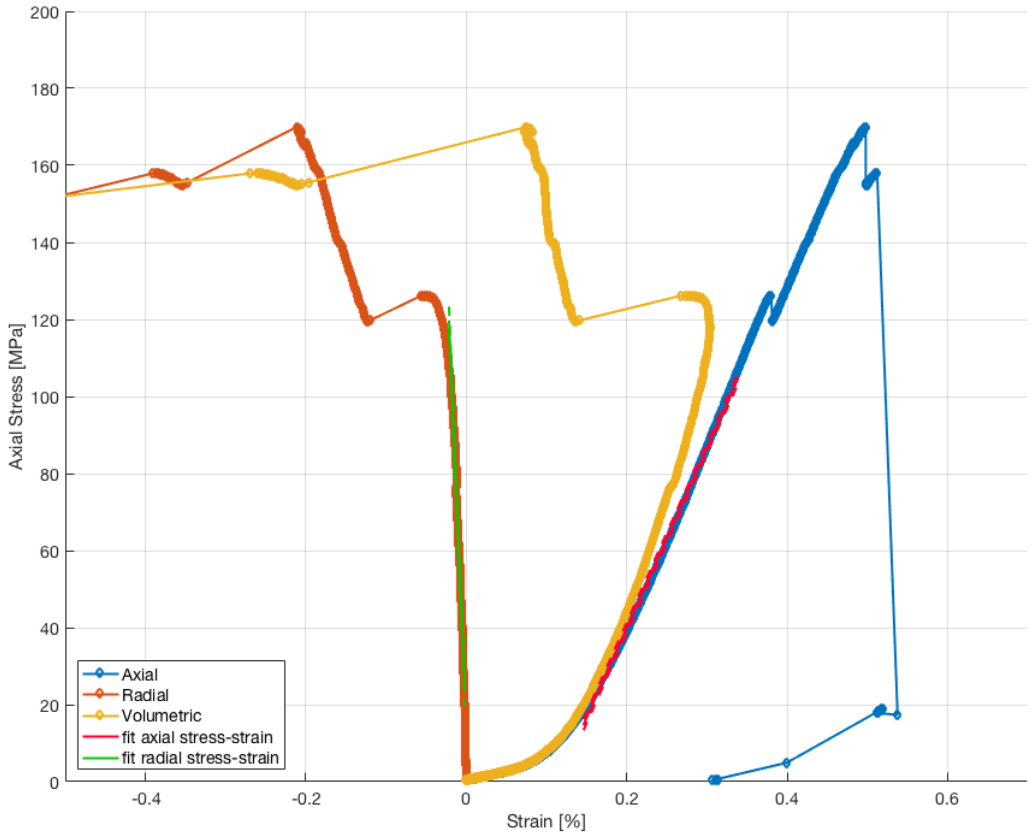

Peak stress: not identified
Yield stress: not identified
Young's Modulus: 46.6644 +/- 0.20667 [GPa]
Poisson's ratio: 0.094888 +/- 0.0014789, [-]

The SURE project has received funding from the European Union's Horizon 2020 research and innovation programme under grant agreement No 654662.

Sample: SQZ6_FR_50_2A

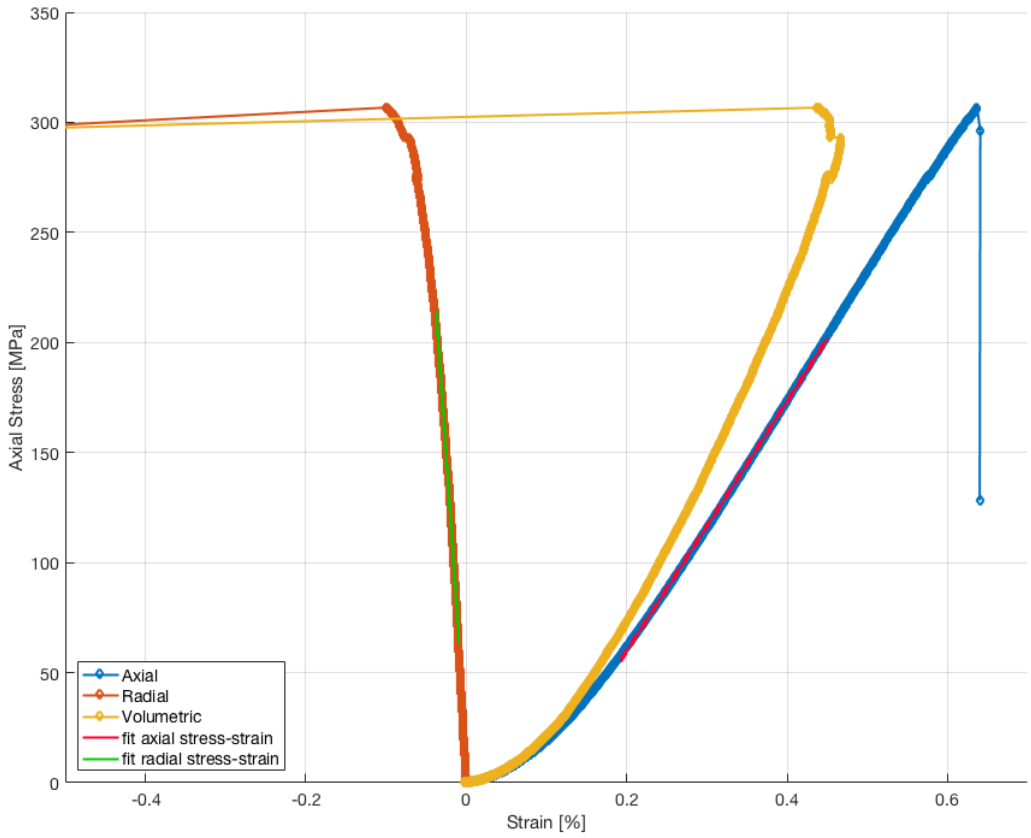

Peak stress: 307 [MPa]
Yield stress: 271 [MPa]
Young's Modulus: 56.7102 +/- 0.084071 [GPa]
Poisson's ratio: 0.10817 +/- 0.00075785, [-]

4.3.2. Brazil disk indirect tensile strength

Tensile Strength Mean: 17.4700 [MPa]
Standard deviation: 5.4929 [MPa]
Data range: 10.1860 – 23.1244 [MPa]
Number of samples: 4

4.3.3. Acoustic velocities

Sample code	v_p [km/s]	v_{s1} [km/s]	v_{s2} [km/s]
SQZ6_FR_50_1A	5.2827	3.4927	3.5896
SQZ6_FR_50_2A	5.4449	3.6215	3.5662

The SURE project has received funding from the European Union's Horizon 2020 research and innovation programme under grant agreement No 654662.

4.4. PGR6-RI – Granit (Odenwald)

4.4.1. UCS

Sample: PGR6_RI_50_01

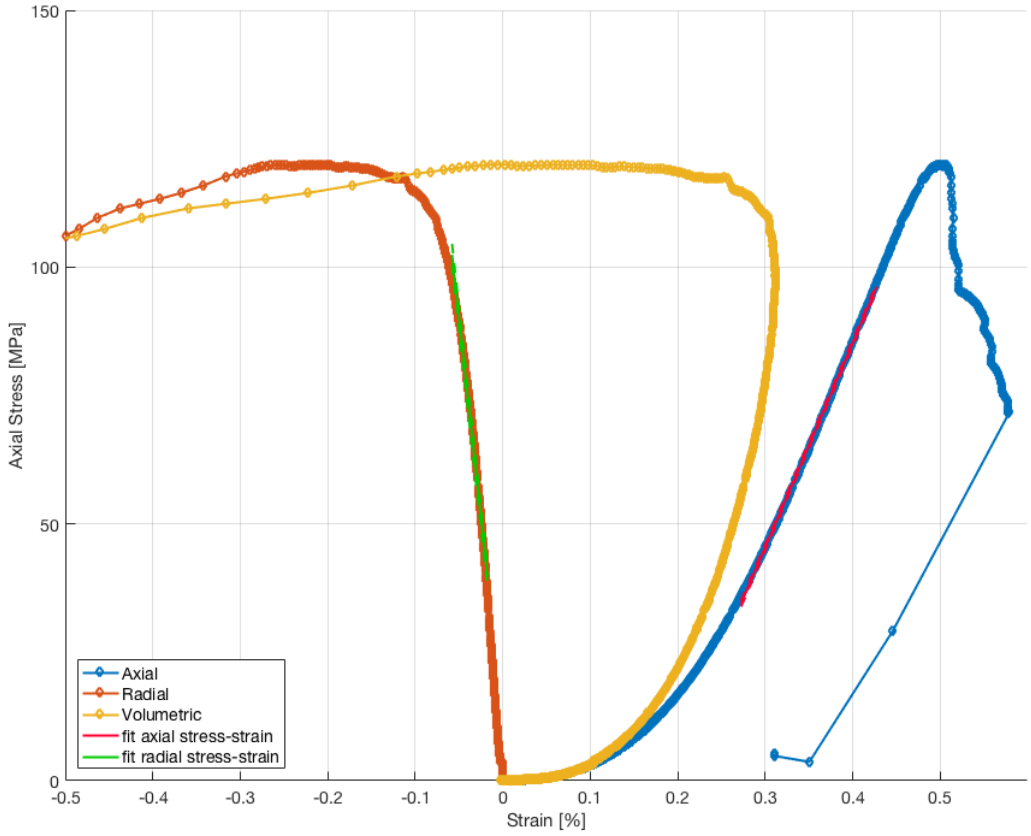

Peak stress: 120 [MPa]
Yield stress: 104 [MPa]
Young's Modulus: 39.7989 +/- 0.12412 [GPa]
Poisson's ratio: 0.25701 +/- 0.0034852, [-]

The SURE project has received funding from the European Union's Horizon 2020 research and innovation programme under grant agreement No 654662.

Sample: PGR6_RI_50_02

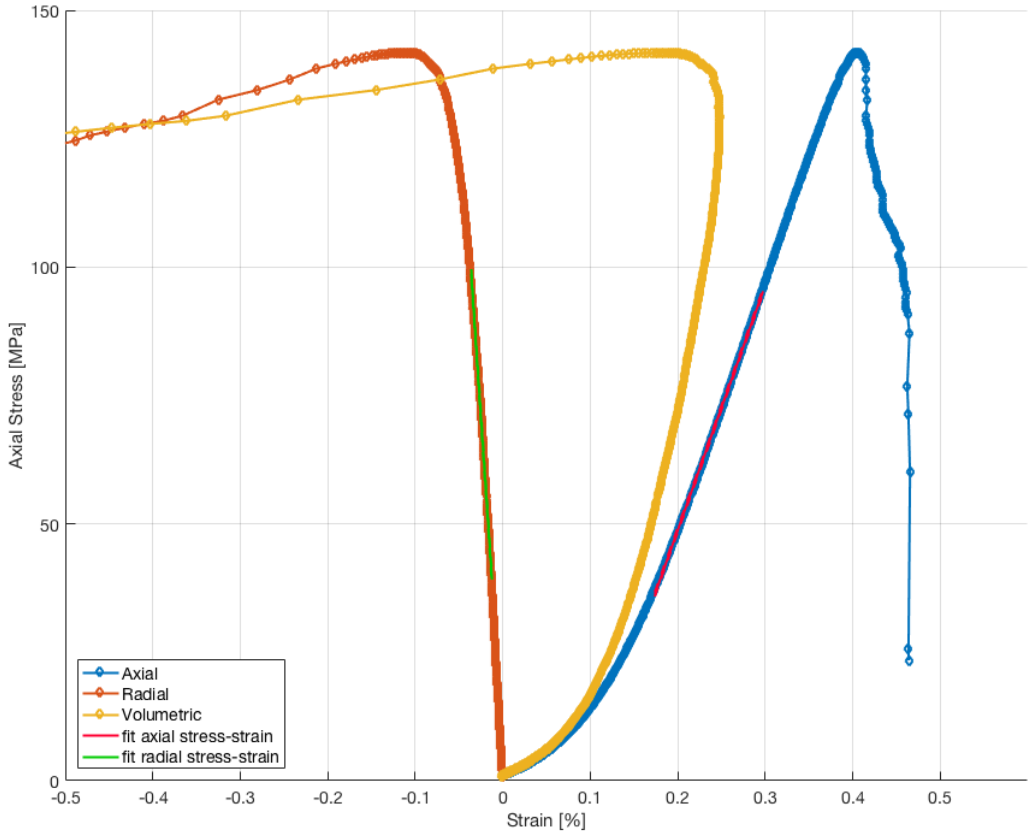

Peak stress: 142 [MPa]
Yield stress: 129 [MPa]
Young's Modulus: 47.68 +/- 0.12518 [GPa]
Poisson's ratio: 0.18973 +/- 0.0016739, [-]

4.4.2. Brazil disk indirect tensile strength

4.4.3. Acoustic velocities

Sample code	v_p [km/s]	v_{s1} [km/s]	v_{s2} [km/s]
PGR6_RI_50_01	4.5194	2.9393	2.7517
PGR6_RI_50_02	5.0181	3.1710	2.9567

The SURE project has received funding from the European Union's Horizon 2020 research and innovation programme under grant agreement No 654662.

4.5. SBS6_BD – Buntsandstein (Bad Dürkheim)

There is relatively large variation expected between sample blocks, based on visual inspection of the blocks the grain size varies, and thereby porosity / strength etc.

4.5.1. UCS

Sample: SBS6_BD_51_02_zdir

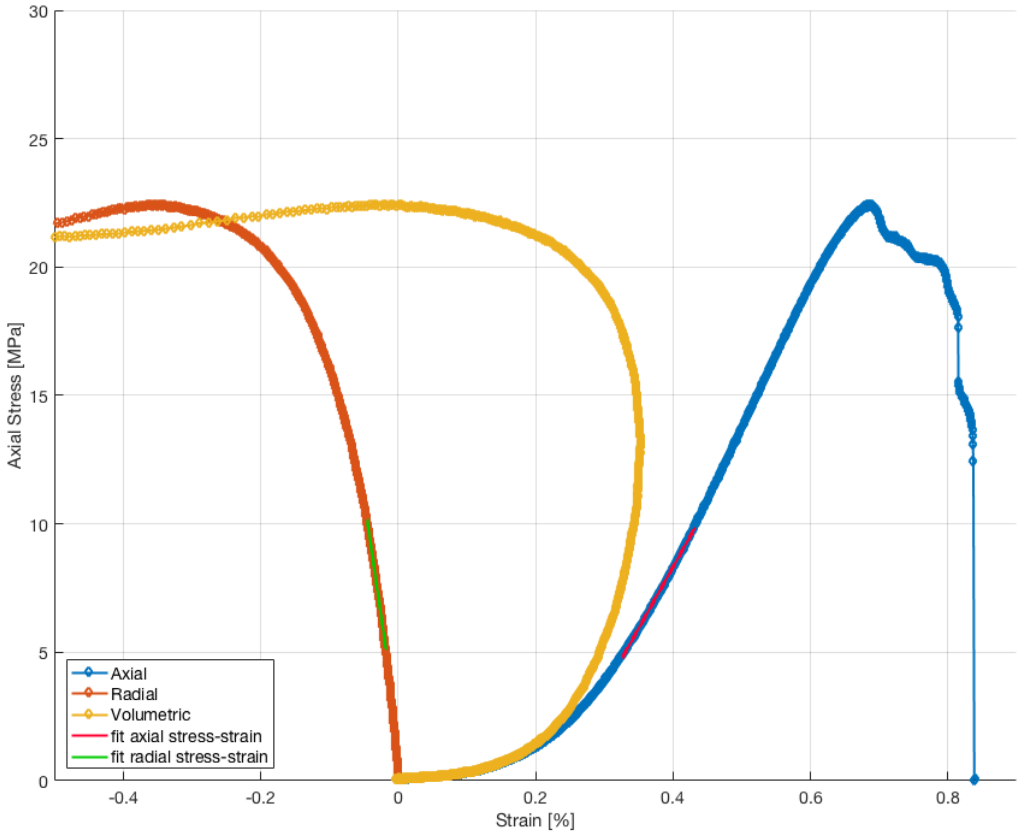

Peak stress:	22.5 [MPa]
Yield stress:	20.4 [MPa]
Young's Modulus:	4.7904 +/- 0.020706 [GPa]
Poisson's ratio:	0.26114 +/- 0.0031368, [-]

The SURE project has received funding from the European Union's Horizon 2020 research and innovation programme under grant agreement No 654662.

Sample: SBS6_BD_51_04_xdir

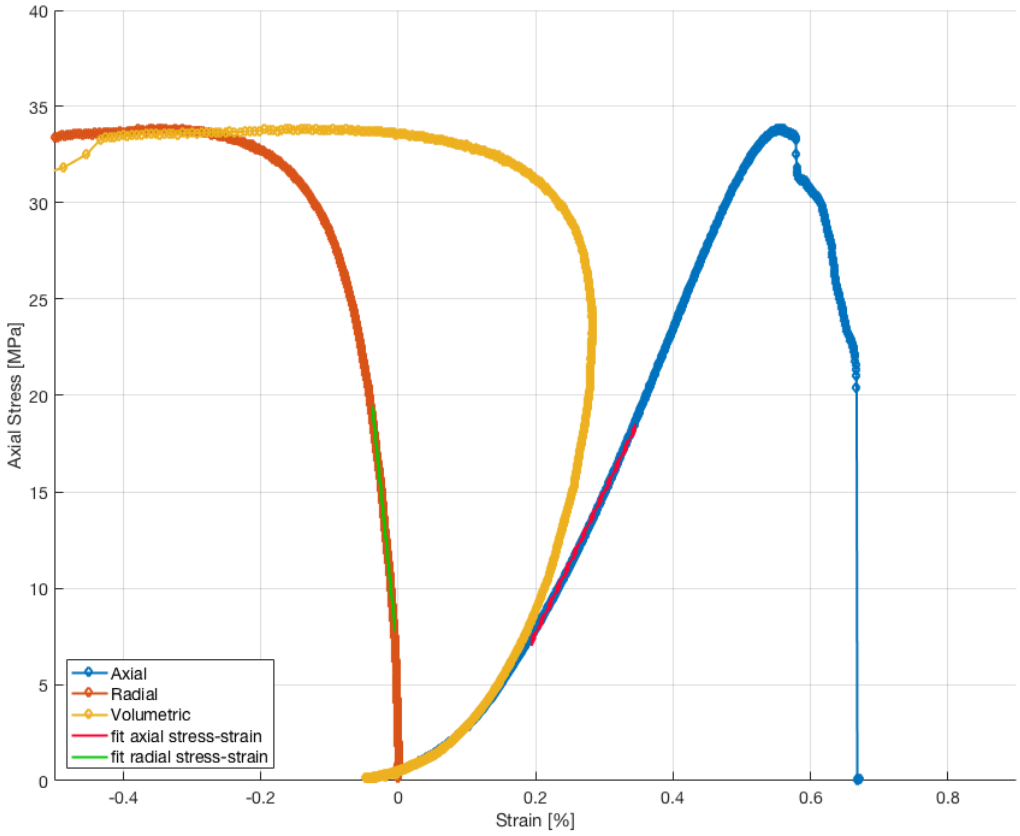

Peak stress:	34.0 [MPa]
Yield stress:	30.9 [MPa]
Young's Modulus:	7.3831 +/- 0.034307 [GPa]
Poisson's ratio:	0.21008 +/- 0.0024813, [-]

The SURE project has received funding from the European Union's Horizon 2020 research and innovation programme under grant agreement No 654662.

4.5.2. Permeability

Sample SBS6_BD_50_Y1:

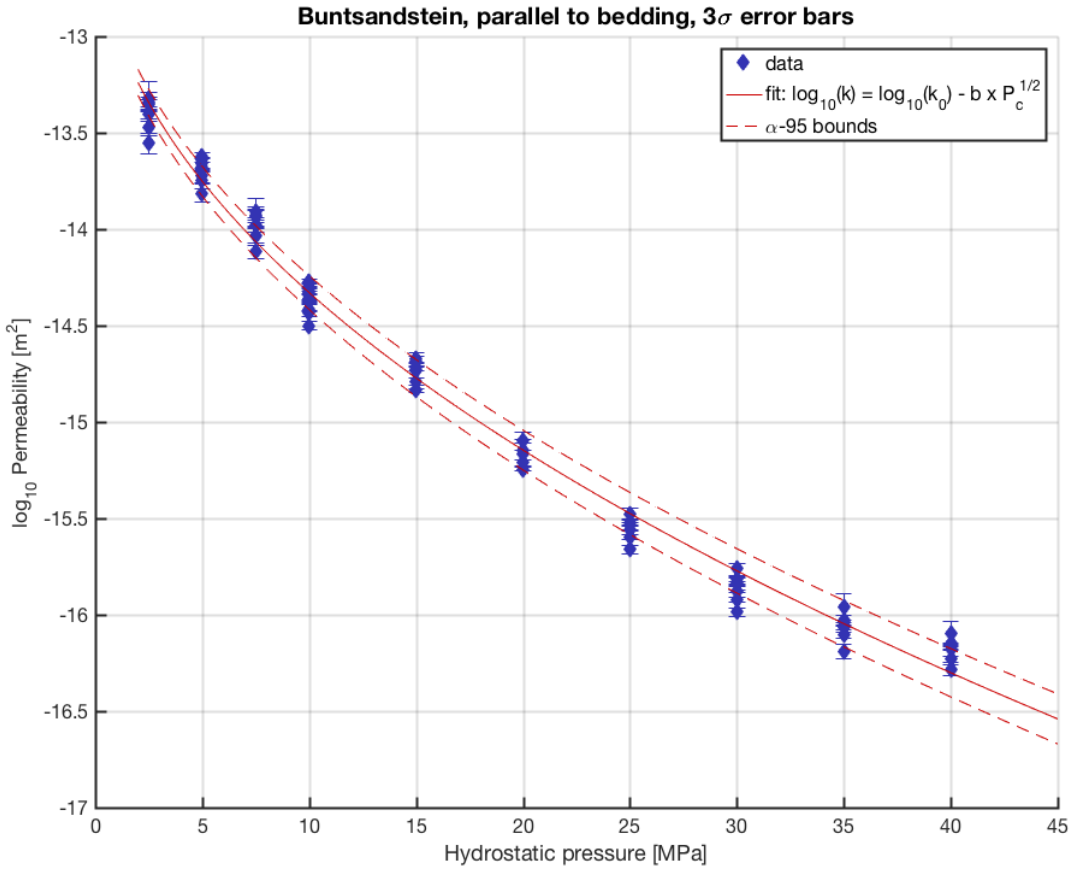

The SURE project has received funding from the European Union's Horizon 2020 research and innovation programme under grant agreement No 654662.

Sample SBS6_BD_50_Z1:

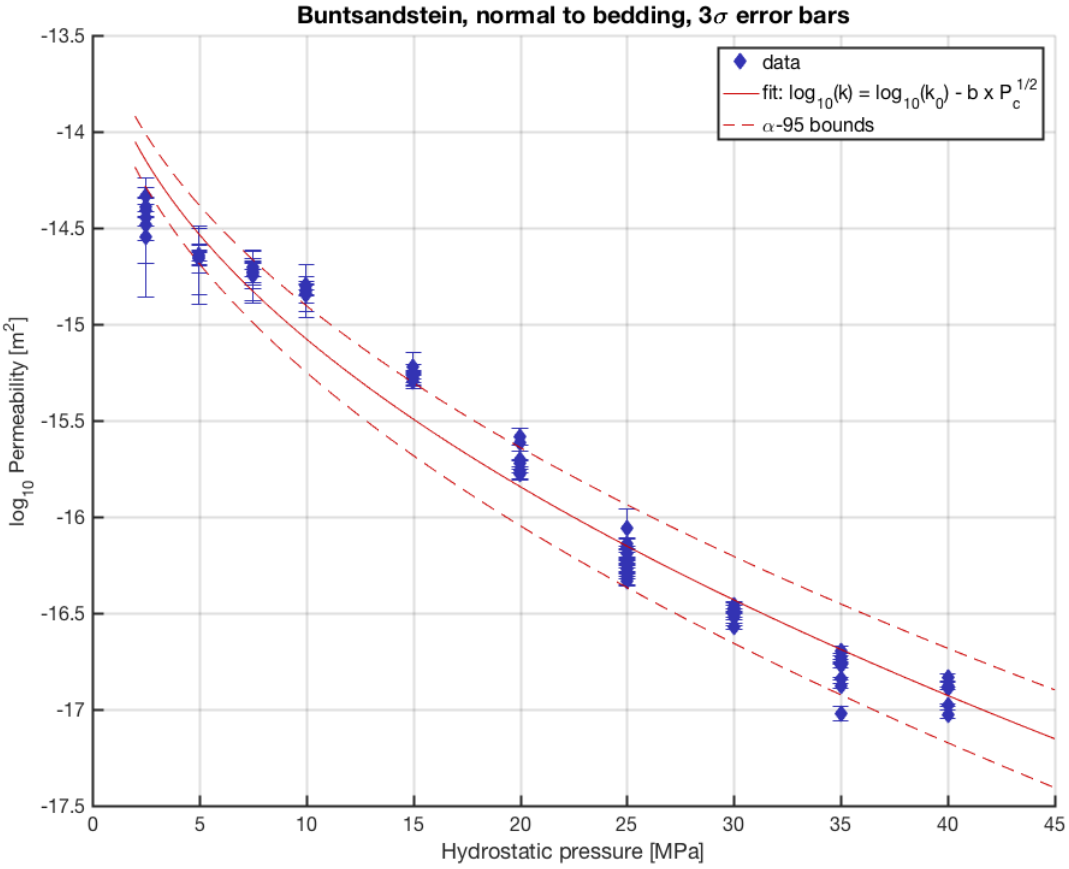

4.5.3. Brazil disk indirect tensile strength

Averages

Sample block	Core direction	Orientation of applied load towards bedding	$\sigma_t \pm$ SD [MPa]	$F_{max} \pm$ SD [kN]	$P_{min} \pm$ SD [kN]	$K_{IC} \pm$ SD [MN/m$^{1.5}$]
SBS6-BD52	Z	n.a	2.7 ± 0.4	2.0 ± 0.4	1.5 ± 0.2	0.25 ± 0.04
	X	n.a	2.5 ± 0.3	1.7 ± 0.1	1.4 ± 0.1	0.24 ± 0.03
SBS6-BD53	Z	n.a	2.7 ± 0.3	2.0 ± 0.2	1.3 ± 0.1	0.24 ± 0.01
	X	n.a	2.0 ± 0.1	1.5 ± 0.1	1.1 ± 0.05	0.19 ± 0.01

Data from the MSc. Thesis of Thomas Hinkofer (TU Delft, supervised by Bakker, Bruhn and Barnhoorn). Full dataset can be accessed via the TU Delft thesis repository.

The SURE project has received funding from the European Union's Horizon 2020 research and innovation programme under grant agreement No 654662.

4.5.4. Acoustic velocities

Sample code	v_p [km/s]	v_s [km/s]
SBS6_BD_50_Y4*	3.1189	
SBS6_BD_50_Z2*	2.9184	
SBS6_BD_52_X1B	2.7228	1.8741
SBS6_BD_52_Z2	2.8725	1.8655
SBS6_BD_53_X2B	2.7251	1.8928
SBS6_BD_53_Z2B	2.6296	1.8836
SBS6_BD_54_X3A	3.2502	2.0890
SBS6_BD_54_Z2A	3.4394	2.2333

* sample used for coda wave interferometry-type experiment, therefore v_p available only

The SURE project has received funding from the European Union's Horizon 2020 research and innovation programme under grant agreement No 654662.

4.6. SRM6_MI – Roter Mainsandstein

4.6.1. UCS

Sample: SRS6_MI_51_X1

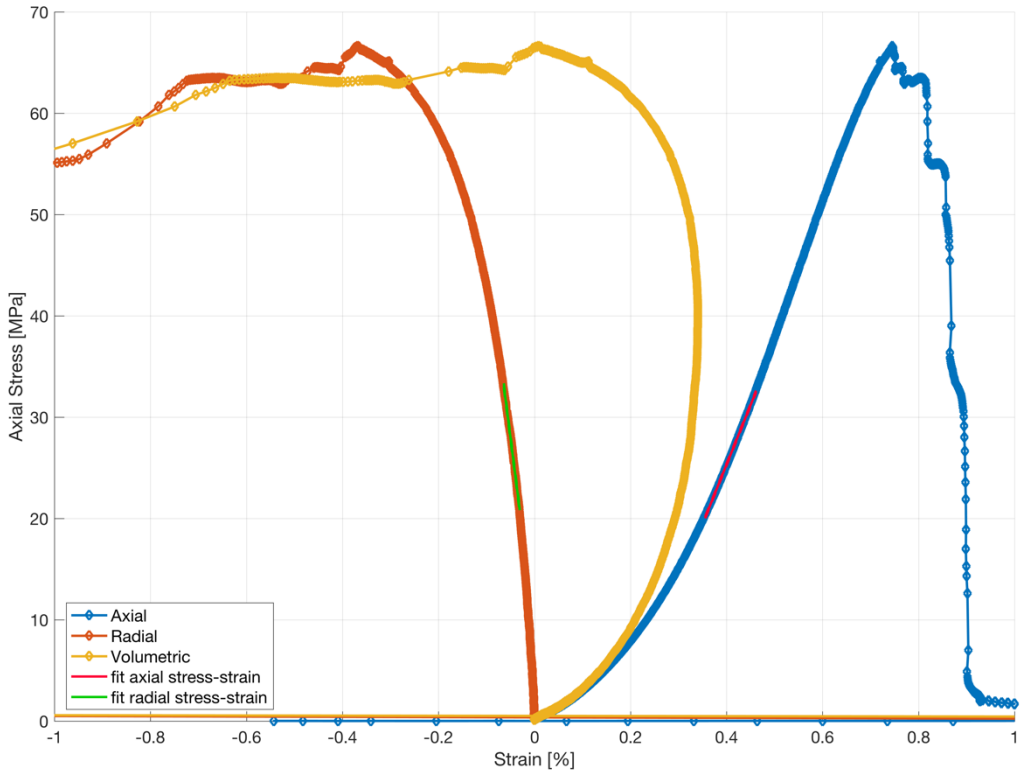

Peak stress: 66.5 [MPa]
Yield stress: 59.4 [MPa]
Young's Modulus: 11.7318 +/- 0.044707 [GPa]
Poisson's ratio: 0.31738 +/- 0.0039295 [-]

The SURE project has received funding from the European Union's Horizon 2020 research and innovation programme under grant agreement No 654662.

Sample: SRS6_MI_50_Z9

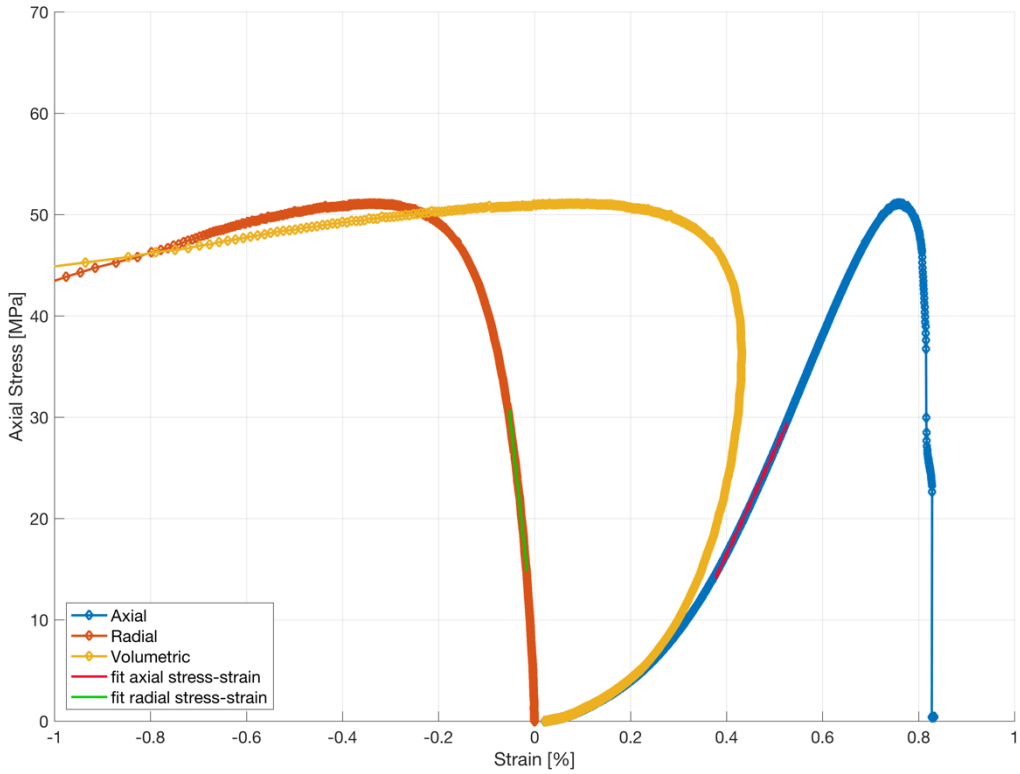

Peak stress: 50.9 [MPa]
Yield stress: 44.1 [MPa]
Young's Modulus: 10.2171 +/- 0.034638 [GPa]
Poisson's ratio: 0.2395 +/- 0.0027461 [-]

4.6.2. Brazil disk indirect tensile strength

Tensile failure along bedding plane (block: SRM6_MI_52):
Tensile Strength Mean: 2.9090 [MPa]
Standard deviation: 0.6642 [MPa]
Data range: 2.1433 – 3.3293 [MPa]
Number of samples: 3

Tensile failure perpendicular to bedding plane (block: SRM6_MI_52):
Tensile Strength Mean: 5.8543 [MPa]
Standard deviation: 0.3122 [MPa]
Data range: 5.6603 – 6.2144 [MPa]
Number of samples: 3

The SURE project has received funding from the European Union's Horizon 2020 research and innovation programme under grant agreement No 654662.

4.6.3. Permeability – hydrostatic

Sample: SRM6_MI_50_Y1

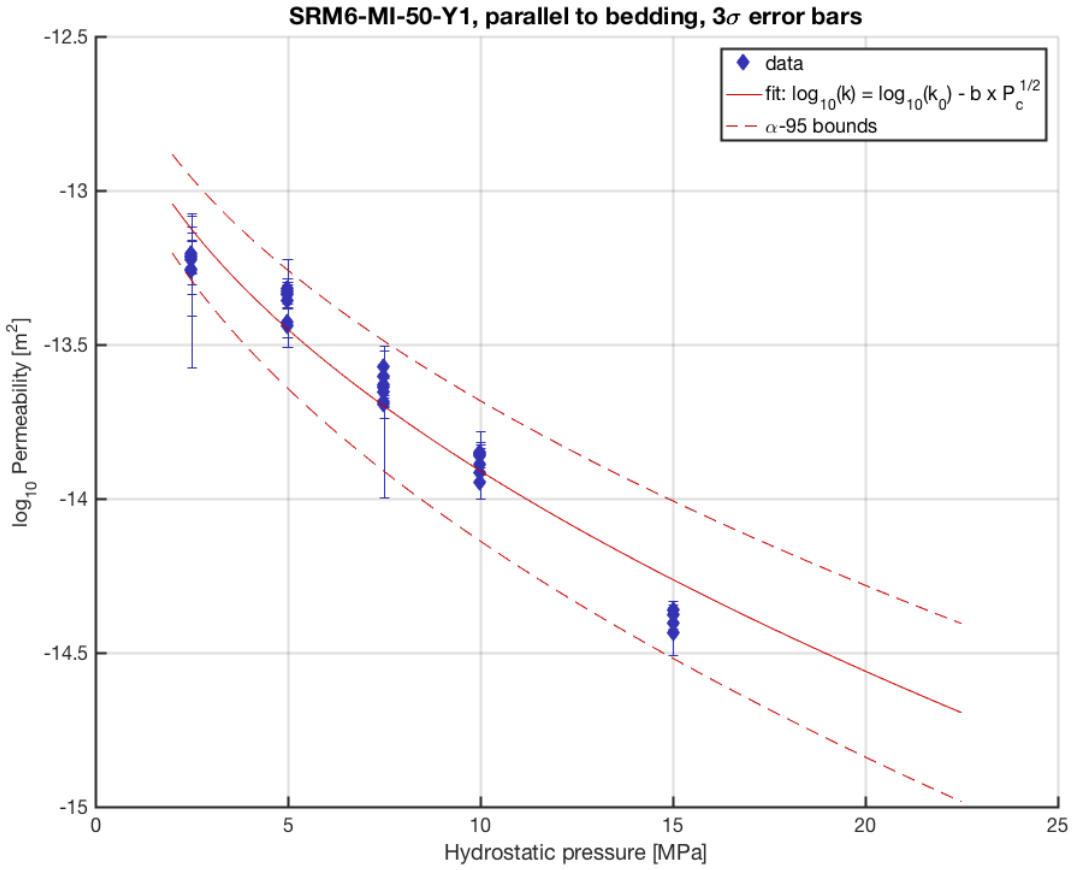

The SURE project has received funding from the European Union's Horizon 2020 research and innovation programme under grant agreement No 654662.

Sample: SRM6_MI_50_Y2

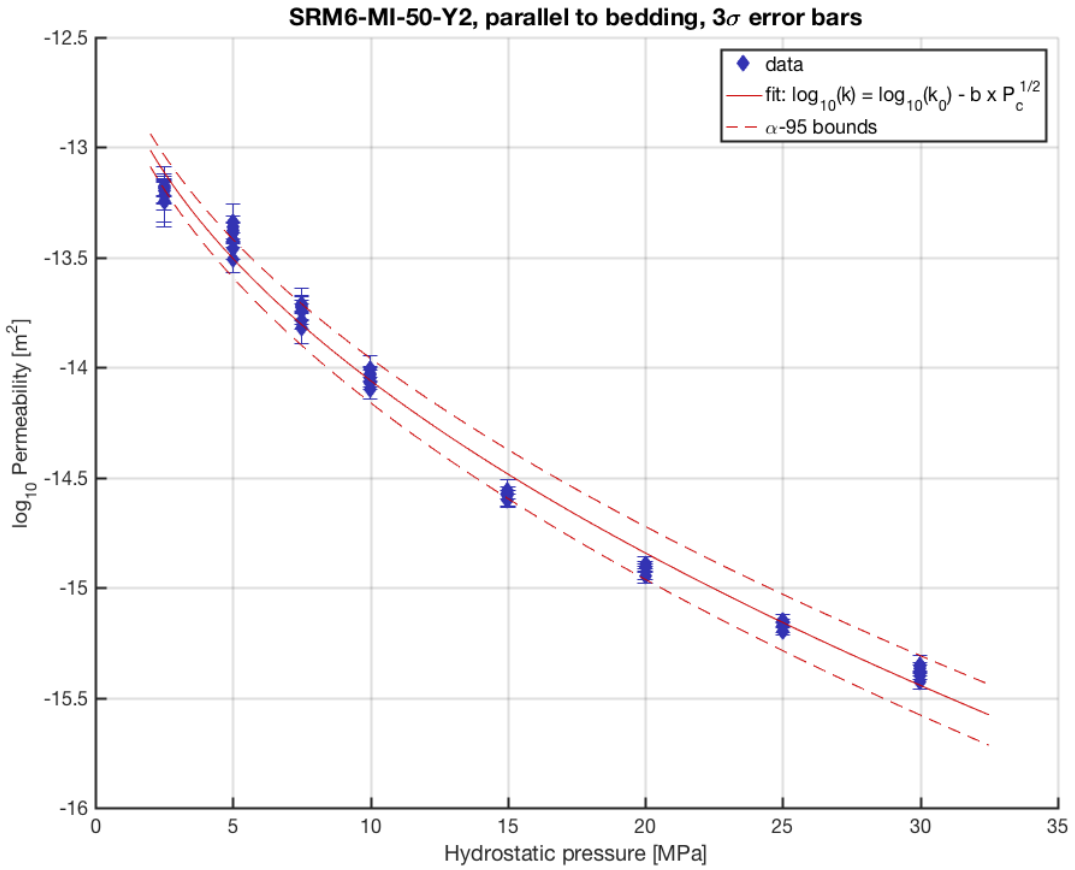

The SURE project has received funding from the European Union's Horizon 2020 research and innovation programme under grant agreement No 654662.

Sample: SRM6_MI_50_Z8:

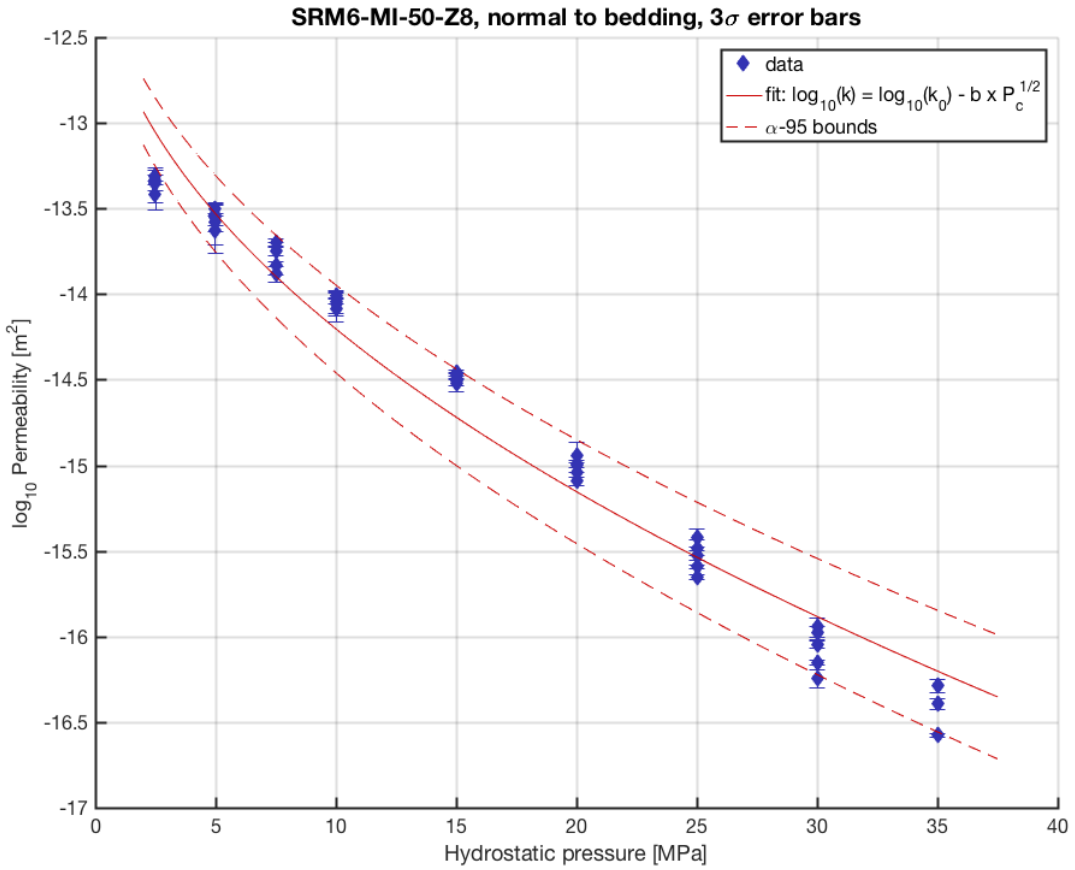

4.6.4. Tri-axial deformation

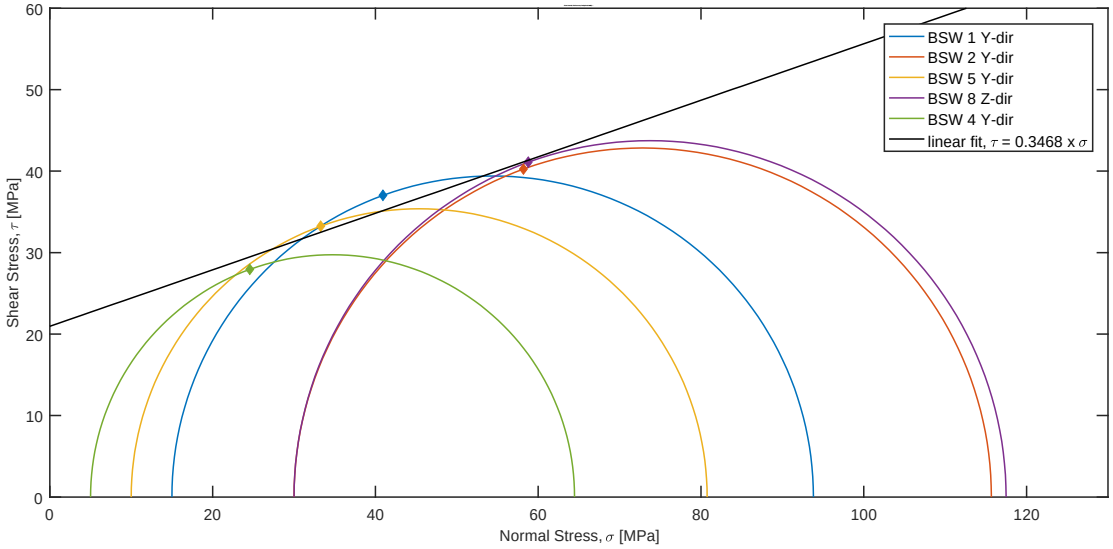

The SURE project has received funding from the European Union's Horizon 2020 research and innovation programme under grant agreement No 654662.

Mohr circles based on triaxial experiments, local notation is used. All samples derived from block SRM6_MI_50. Note that due to intra-sample variability and lack of data the coefficients might differ greatly. For current best fit:
Internal friction coefficient: 0.3468 [-]
Cohesion: 21.5 [MPa]

4.6.5. Acoustic velocities

Sample: SRM6_MI_51_X1
v_p = 3.0316 [km/s]
v_s= 2.0024 [km/s]

The SURE project has received funding from the European Union's Horizon 2020 research and innovation programme under grant agreement No 654662.

4.7. SGH6_GI – Gildehaus Sandstone

4.7.1. UCS

Sample: SGH6_GI_50_01

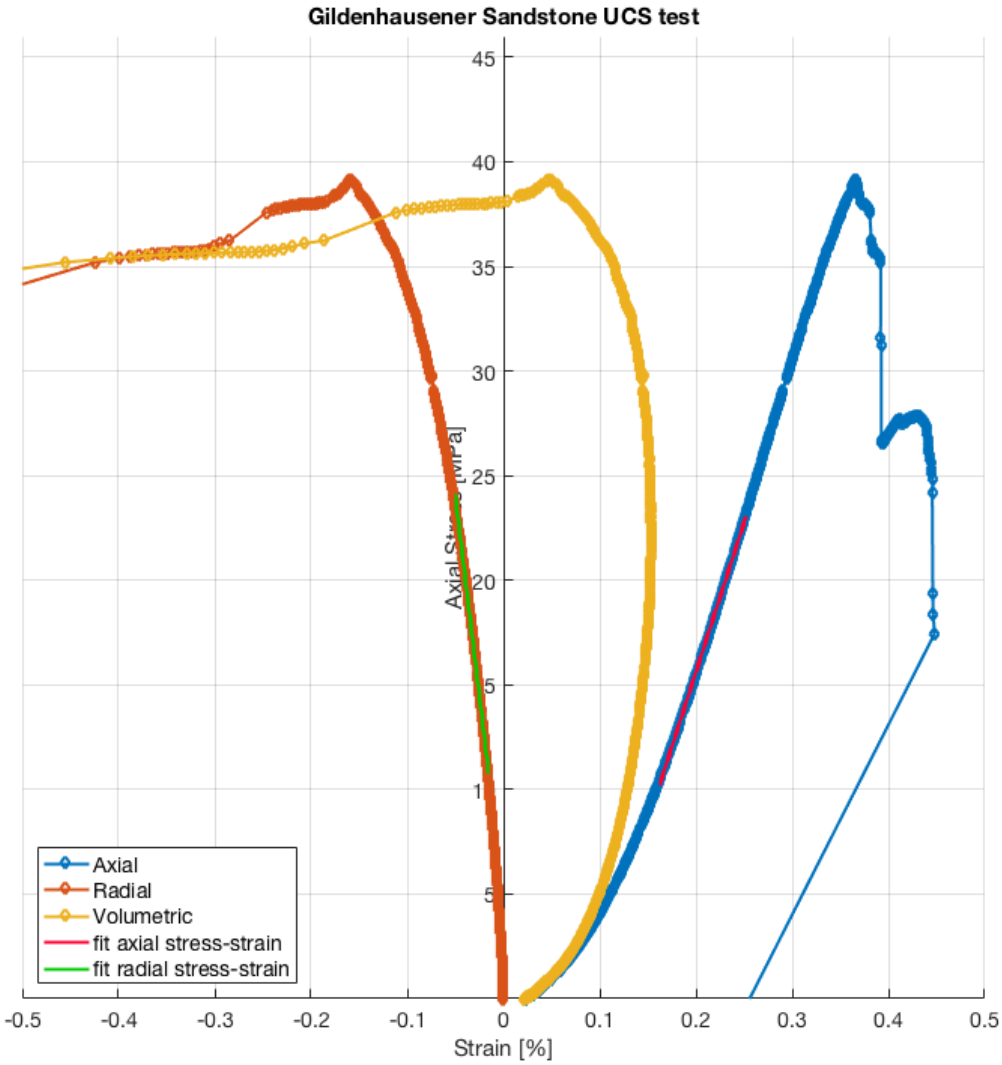

Peak stress: 39 [MPa]
Yield stress: 36 [MPa]
Young's Modulus: 14.2807 +/- 0.051268 [GPa]
Poisson's ratio*: 0.37445+/- 0.0045275 [-]
* linear part not readily identifiable, samples seem to have an increasing radial strain rate with increasing axial strain. Elastic part assumed at low stresses.

The SURE project has received funding from the European Union's Horizon 2020 research and innovation programme under grant agreement No 654662.

Sample: SGH6_GI_50_02

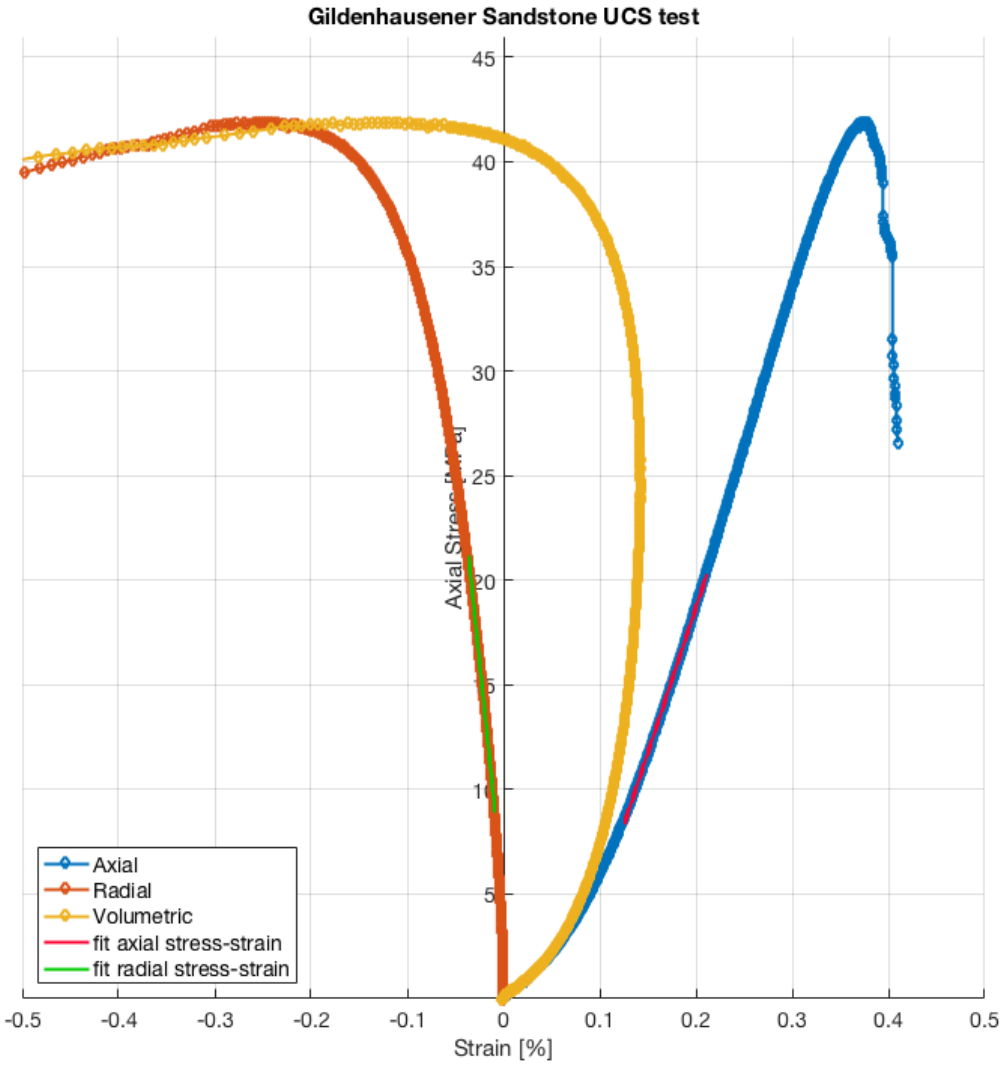

Peak stress: 42 [MPa]
Yield stress: 40 [MPa]
Young's Modulus: 13.8878 +/- 0.059725 [GPa]
Poisson's ratio*: 0.31174+/- 0.0038193 [-]
* linear part not readily identifiable, samples seem to have an increasing radial strain rate with increasing axial strain. Elastic part assumed at low stresses.

The SURE project has received funding from the European Union's Horizon 2020 research and innovation programme under grant agreement No 654662.

Sample: SGH6_GI_50_03

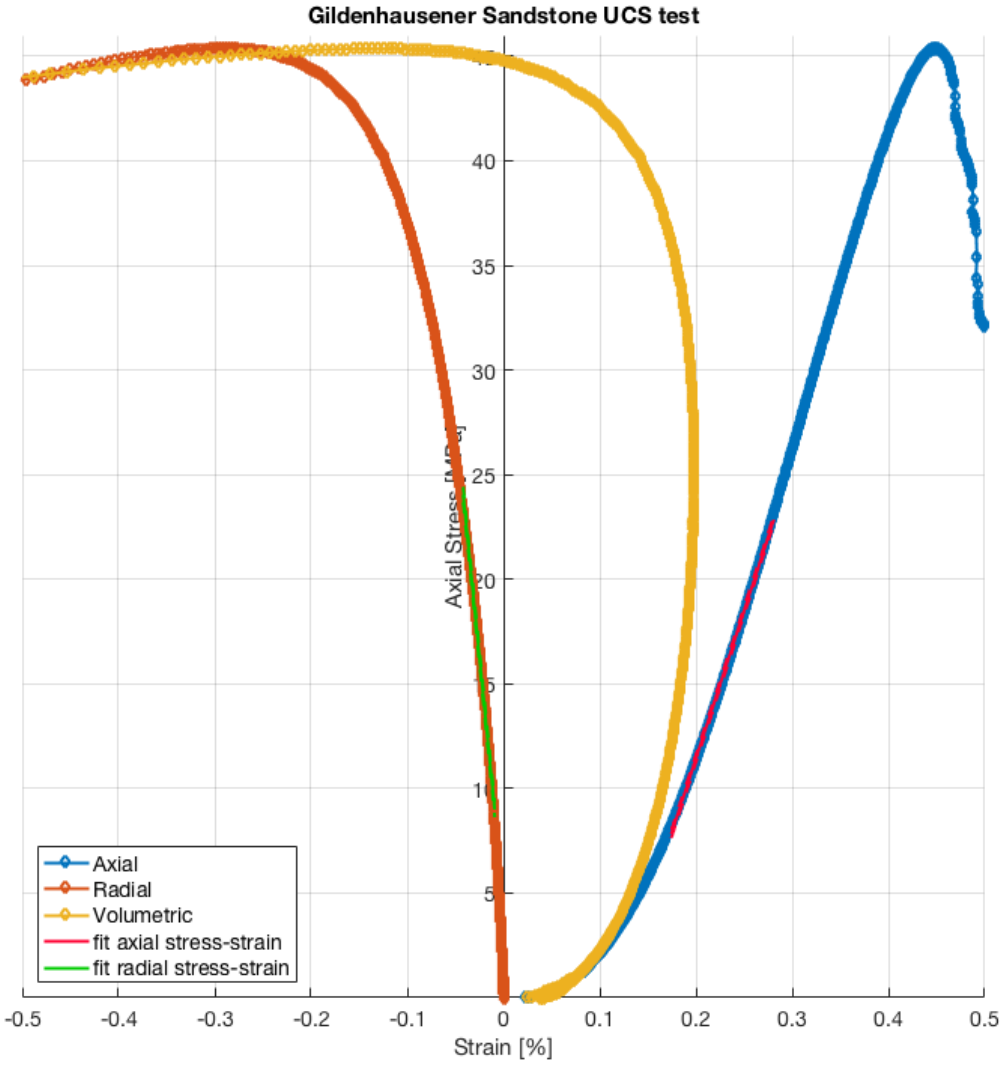

Peak stress: 45 [MPa]
Yield stress: 40 [MPa]
Young's Modulus: 14.1004 +/- 0.070085 [GPa]
Poisson's ratio*: 0.30663+/- 0.0044034 [-]
* linear part not readily identifiable, samples seem to have an increasing radial strain rate with increasing axial strain. Elastic part assumed at low stresses.

4.7.2. Brazil disk indirect tensile strength

Tensile Strength Mean: 3.1687 [MPa]
Standard deviation: 0.3059 [MPa]
Data range: 2.5333 – 3.7126 [MPa]

The SURE project has received funding from the European Union's Horizon 2020 research and innovation programme under grant agreement No 654662.

Number of samples: 16

4.7.3. Permeability

No significant pressure dependence could be measured. Permeability average for sample SGH6_GI_50_04: 2.25 x 10^{-13} m^2

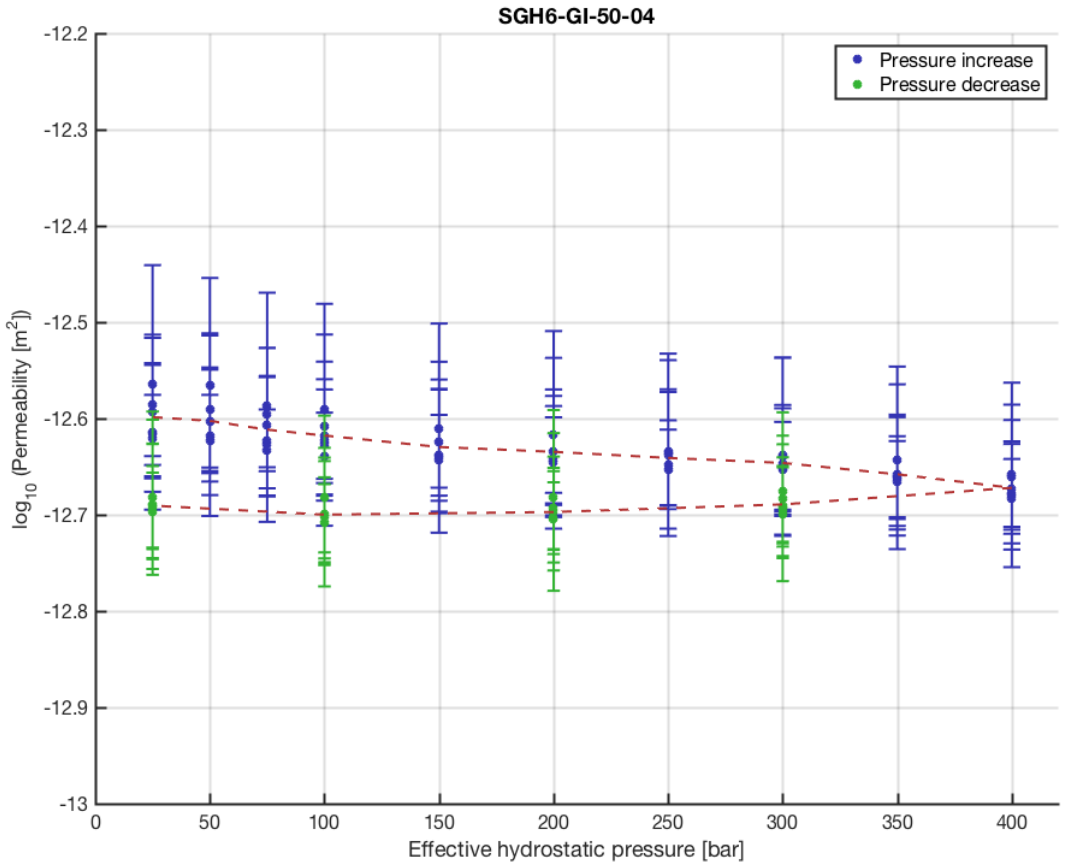

4.7.4. Acoustic velocities

Sample code	v_p [km/s]	v_{s1} [km/s]	v_{s2} [km/s]
SGH6_GI_50_17	2.5892	1.7404	1.7352
SGH6_GI_50_19	2.6289	1.7611	1.7441

The SURE project has received funding from the European Union's Horizon 2020 research and innovation programme under grant agreement No 654662.

4.8. SBT6_BE – Bebertal / Flechtinger Sandstone

For a more detailed description on the methods the reader is referred to Pei et al. (2016) (detailed below). Depicted here are key findings and a summary of average parameters (table, section 5.8.2). Further data can be found in Blöcher et al. (2014) and references therein

References:

Pei, L., Blöcher, G., Milsch, H., Deon, F., Zimmermann, G., Rühaak, W., ... & Huenges, E. (2016). Thermal strain in a water-saturated limestone under hydrostatic and deviatoric stress states. *Tectonophysics*, *688*, 49-64.

Blöcher, G., Reinsch, T., Hassanzadegan, A., Milsch, H., & Zimmermann, G. (2014). Direct and indirect laboratory measurements of poroelastic properties of two consolidated sandstones. *International Journal of Rock Mechanics and Mining Sciences*, *67*, 191-201.

4.8.1. Triaxial strength

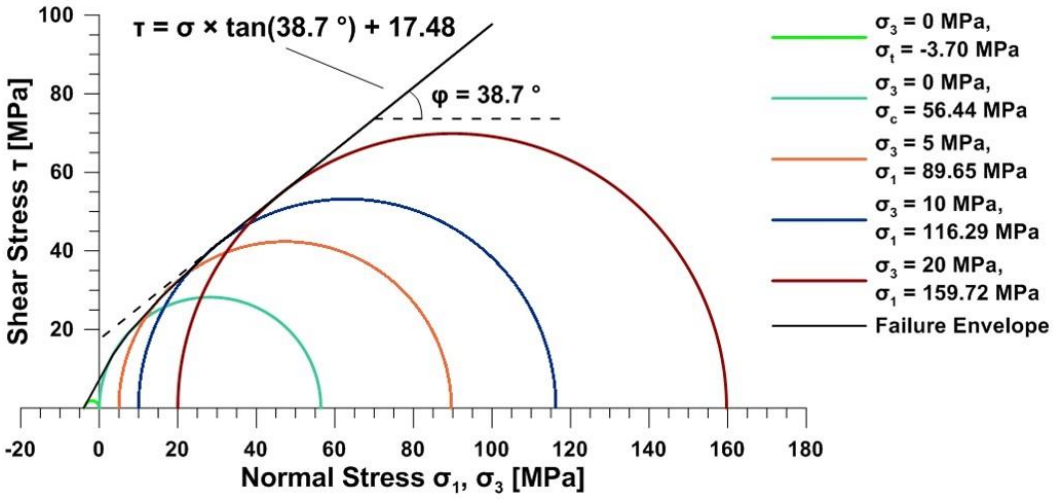

The failure envelope was constructed from tri-axial experiments at confining stress ranging from 0 to 20 MPa. The cohesion was found to be approximately 17.48 MPa, the internal friction angle is 38.7°.

The SURE project has received funding from the European Union's Horizon 2020 research and innovation programme under grant agreement No 654662.

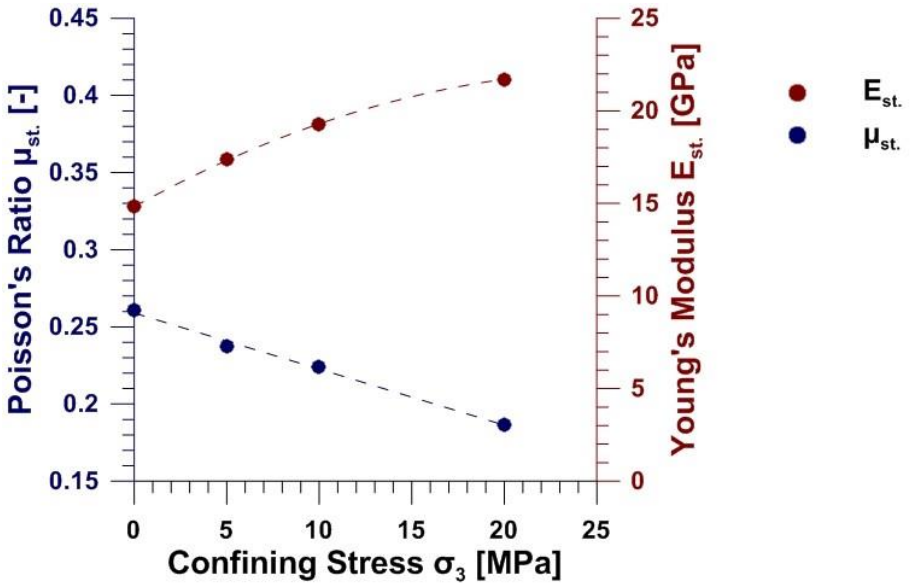

The static Poisson ratio and Young's modulus were calculated from the linear slope of the stress-strain curve, as well as the axial-lateral curve in the linear elastic domain, in separate experiments.

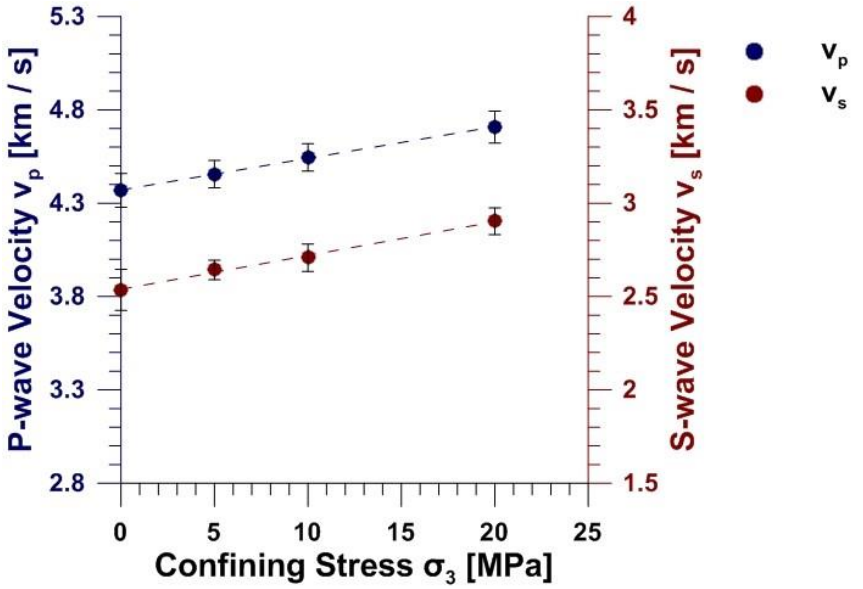

The SURE project has received funding from the European Union's Horizon 2020 research and innovation programme under grant agreement No 654662.

The dynamic elastic properties were calculated from the measured p and s-wave velocities during the experiment. The P and S-wave velocity was measured depending on the confining stress and show a linear increase for increasing confining stress.

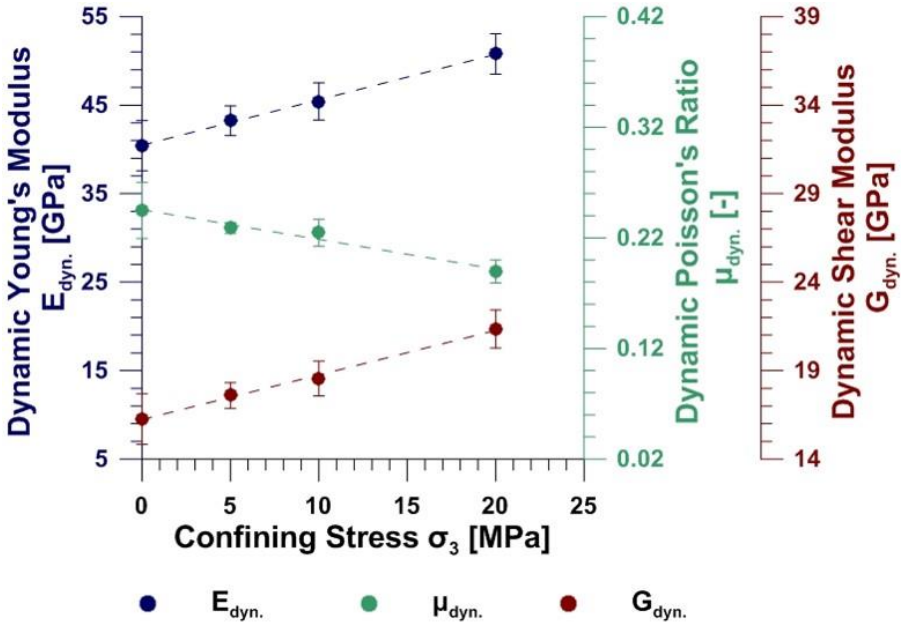

From the acoustic velocities, the dynamic Young's modulus, Poisson Ratio and Shear Modulus was calculated. The Poisson ratio decreases while the Shear and Youngs modulus increase with increasing confining pressure. The trend is the same as for the static elastic properties although the magnitudes for the Young's modulus differ.

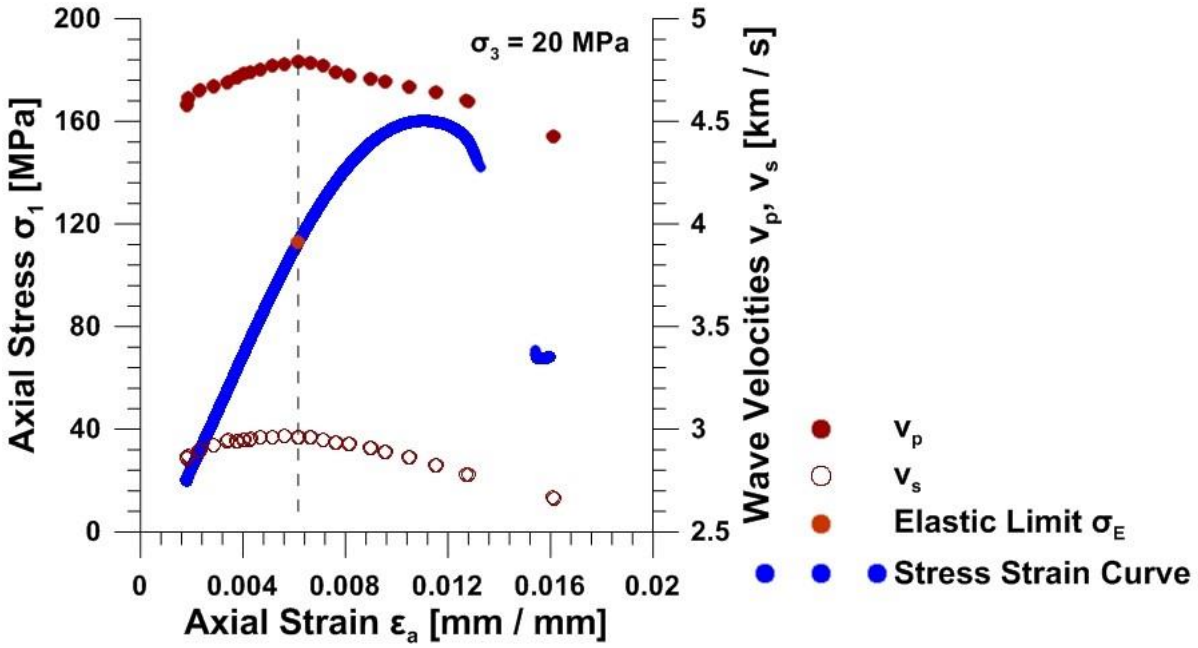

The SURE project has received funding from the European Union's Horizon 2020 research and innovation programme under grant agreement No 654662.

The wave velocities show dependence on axial stress during deviatoric loading in uniaxial testing conditions.

4.8.2. Table of Rock Properties

In total 43 experiments were performed on the Flechtingen sandstone (SBT6-BE). The results are summarized in the following table.

Property [unit]	**Value / Range**
E_{st} *[GPa]*	14.8 to 21.7
μ_{st} *[-]*	0.19 to 0.26
v_p *[km/s]*	4.1 to 4.8
v_s *[km/s]*	2.4 to 3.0
E_{dyn} *[GPa]*	35.5 to 52.9
G_{dyn} *[GPa]*	14.1 to 22.3
μ_{dyn} *[-]*	0.17 to 0.29
UCS [MPa]	56.5
TS [MPa]	3.82
KIc [MPa $m^{2/3}$*]*	0.482
KIIc [MPa $m^{2/3}$*]*	2.037
porosity [%]	8.5
permeability (at 15 MPa) [m²]	$2.0e^{16}$

The SURE project has received funding from the European Union's Horizon 2020 research and innovation programme under grant agreement No 654662.

4.9. CKO6_AA – Kohlenkalk

4.9.1. Brazilian Disk Testing

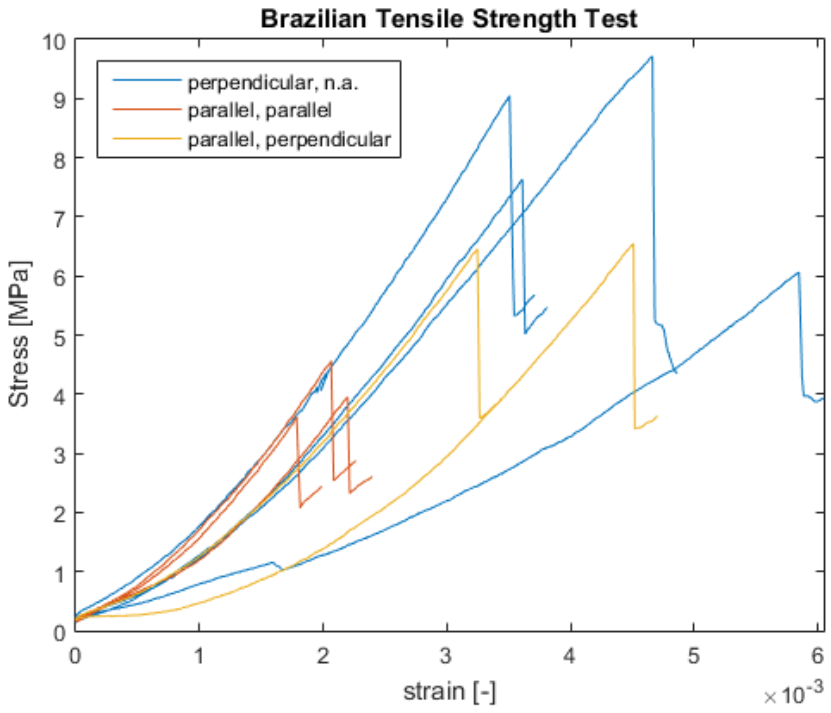

The discs with their bedding orientation parallel to the vertical load show a tensile strength of 4.1 MPa. In the case of the other orientations, the load is perpendicular to the bedding. These samples show a tensile strength of 7.6 and 6.5 MPa, which is 2 times larger compared to the samples with the load parallel to the bedding.

Sample code	Pmax [kN]	Pmin [kN]	σ_t [MPa]	K_{IC} [MN/m$^{1.5}$]	bedding orientation w.r.t. tensile stress
CK06-AA-01-02-07s	15,9	10,4	8,3	1,3	*n.a.*
CK06-AA-01-02-03s	17,2	10,1	8,3	1,1	*n.a.*
CK06-AA-01-02-12s	12,8	8,2	6,1	0,9	*n.a.*
CK06-AA-01-02-11s	22,1*	*n.a.*	*n.a.*	*n.a.*	*n.a.*
Average + Standard deviation	*15,3 \ 1,85*	*9,6 \ 1,00*	*7,6 \ 1,06*	*1,1 \ 0,15*	
CK06-AA-01-03-09p	8,5	5,0	3,9	0,5	parallel
CK06-AA-01-03-11p	9,9	5,5	4,6	0,6	parallel
CK06-AA-01-03-08p	7,7	4,4	3,6	0,5	parallel
Average + Standard deviation	*8,7 \ 0,91*	*5,0 \ 0,45*	*4,1 \ 0,39*	*0,5 \ 0,04*	
CK06-AA-01-03-12p	14,0	7,3	6,5	0,8	perpendicular
CK06-AA-01-03-10p	14,5	8,1	6,5	0,8	perpendicular
Average + Standard deviation	*14,3 \ 0,23*	*7,7 \ 0,38*	*6,5 \ 0,05*	*0,8 \ 0,02*	

The SURE project has received funding from the European Union's Horizon 2020 research and innovation programme under grant agreement No 654662.

4.9.2. Unconfined Compressive Strength Experiments

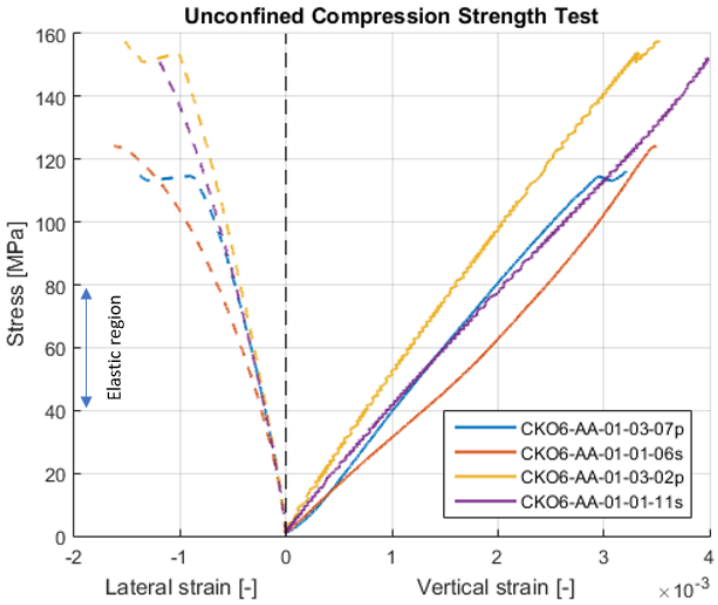

Four UCS tests are performed, two on the x/y-oriented and two on the z-oriented samples. The x/y oriented samples showed a UCS of 116 MPa and 158 MPa, the z-oriented samples 124 MPa and 152 MPa (Table 5). The stress - strain curves in Figure 5.6 are almost linear for all samples, indicating a fully elastic region until ultimate compressive failure.

Sample code	UCS [MPa]
CKO6-AA-01-03-07p	116
CKO6-AA-01-03-02p	158
CKO6-AA-01-01-06s	124
CKO6-AA-01-01-11s	152
Average + Standard deviation	*138 \ 20*

The SURE project has received funding from the European Union's Horizon 2020 research and innovation programme under grant agreement No 654662.

4.9.3. Confined Compressive Strength Experiments

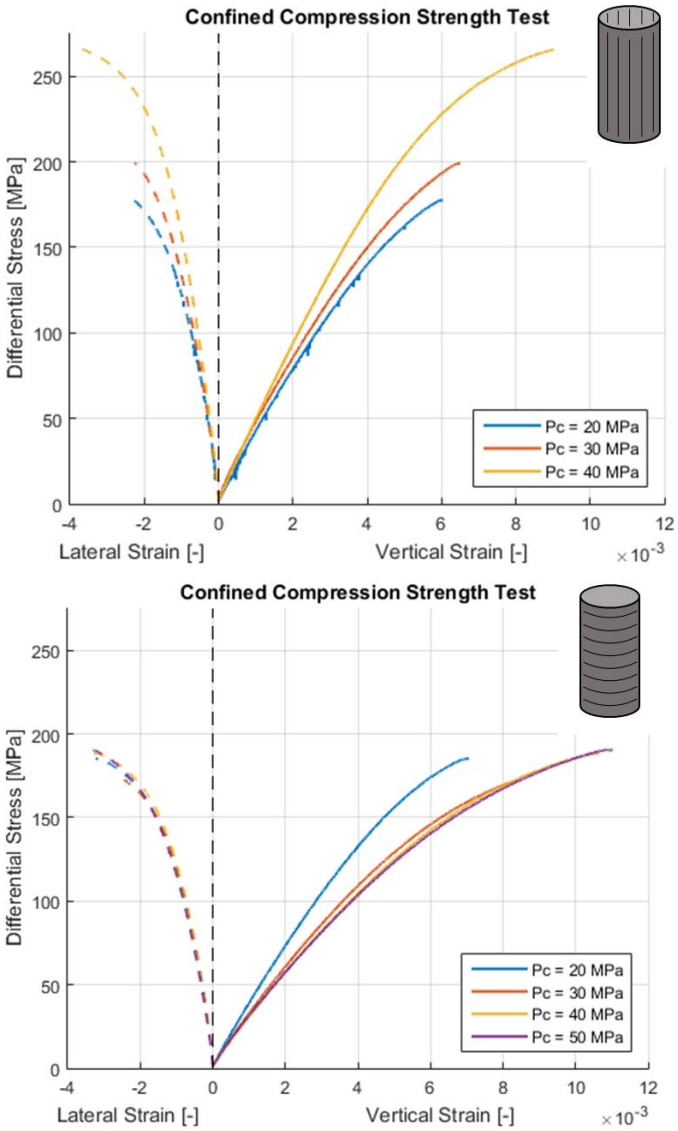

Tri-axial loading is performed with seven samples, at the confinement pressures of 20, 30, 40 and 50 MPa. Table 6 shows the compressive strength obtained from the loading tests. The x/y-oriented cores show a clear increase in compressive strength as the confining pressure increases. At the confining pressure of 20 MPa, the rock sample shows an UCS of 197 MPa which is significantly lower compared to the UCS of 306 MPa at 40 MPa. The z-oriented cores on the other hand show no significant difference as a function of the confining pressure. Their UCS is slightly increasing at a higher confining pressure, however, based on the differential pressure there is almost no increase in compressive strength. The samples with a confining pressure of 20 MPa show a different fracture structure in comparison to the tests performed at higher confining pressures. The CKO6- AA-01-03-06p has 3 main diagonal

The SURE project has received funding from the European Union's Horizon 2020 research and innovation programme under grant agreement No 654662.

fractures and the CKO6-AA-01-02-01s one main fracture interrupted by a complex conjugate fracture structure. All samples with a confining pressure of at least 30 MPa showed one main diagonal shear fracture. During the axial loading, the axial and lateral strain were monitored by the extensometers.

Sample code	Confining Pressure [MPa]	σ_{max} [MPa]
CKO6-AA-01-03-06p	20	197
CKO6-AA-01-03-01p	30	229
CKO6-AA-01-03-05p	40	306
CKO6-AA-01-02-01s	20	205
CKO6-AA-01-02-08s	30	203
CKO6-AA-01-02-10s	40	228
CKO6-AA-01-02-05s	50	241

4.9.4. Mohr Failure Envelope

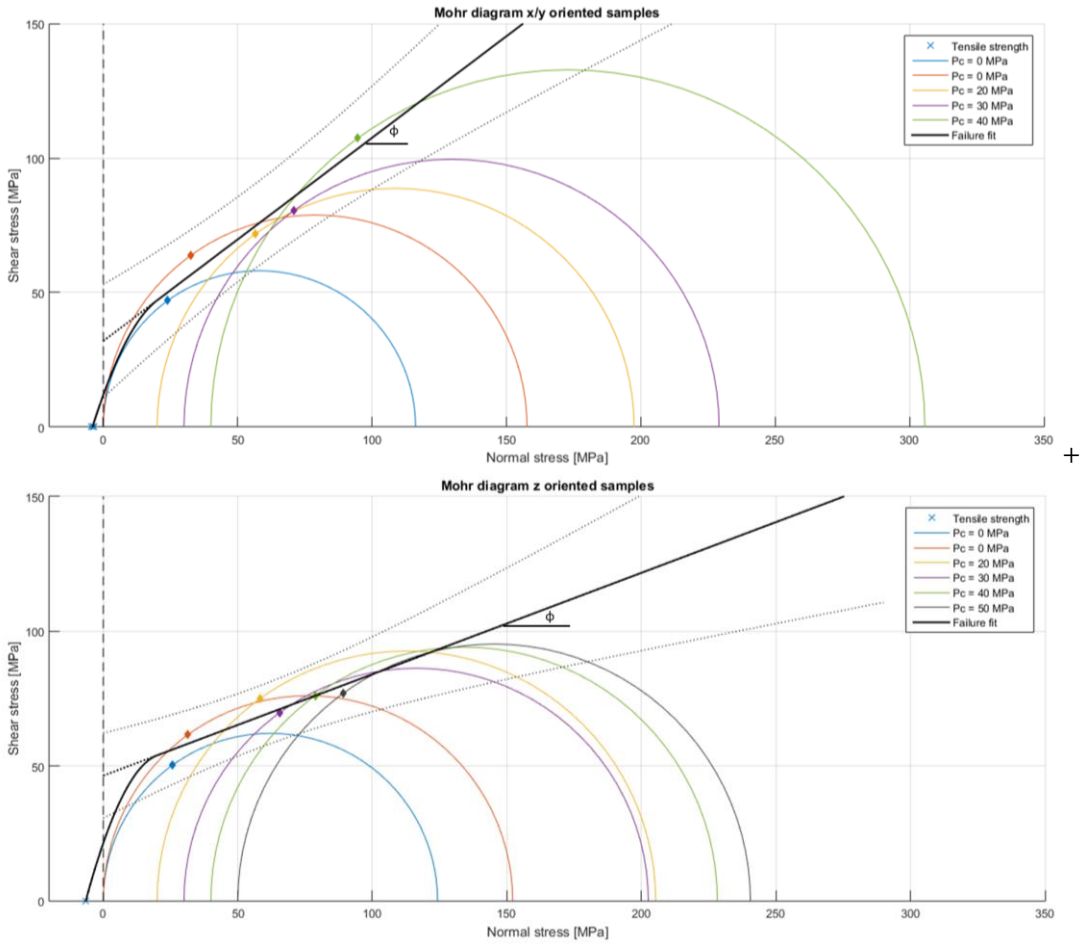

For the construction of the failure envelopes, a failure angle of 27° is assumed based on the measured failure angles of the deformed samples and a best fit of the failure envelope itself. A

The SURE project has received funding from the European Union's Horizon 2020 research and innovation programme under grant agreement No 654662.

difference in the friction coefficient between the different orientations is clearly shown by failure envelopes. The friction coefficient of the parallel samples with 0.38 is significantly lower compared to a friction coefficient of 0.77 of the perpendicular samples.

Orientation	Cohesion [MPa]	Friction coefficient [-]	Failure angle [°]
x/y-orientation	46.4	0.38	~ 27
z-orientation	31.6	0.77	~ 27

4.9.5. Elastic Moduli at Elevated Confining Stress

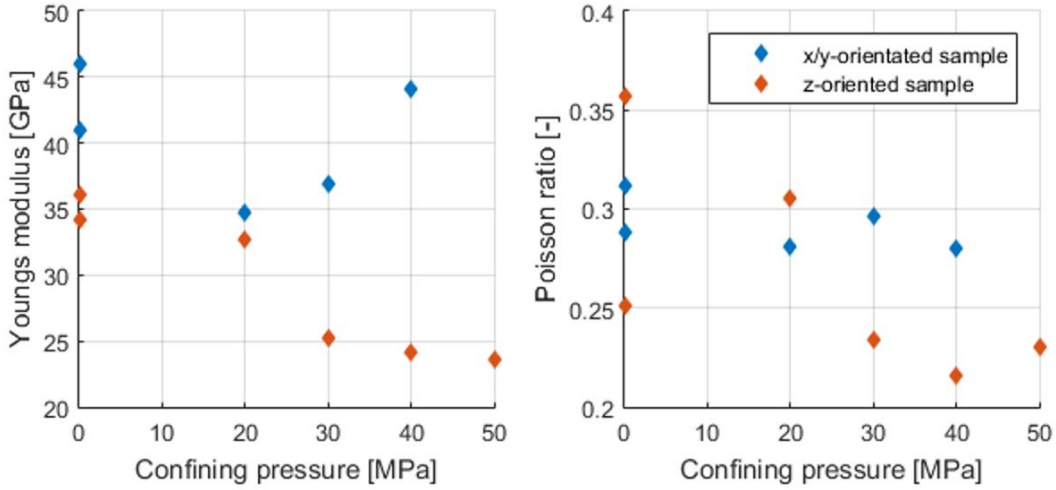

Both the Poisson's ratio and Young's modulus are determined within the elastic region of the stress strain curve of both the unconfined and tri-axial compressive tests. Due to micro-crack closure of pre-existing cracks, the strain shows a non-linear behavior at vertical stresses below 25% of the failure strength. Plasticity starts to have an effect at vertical stresses of over 75% of the failure strength. The interval between the vertical stress of 40 MPa and 80 MPa is chosen, because the non-linear behavior of the rock is not affecting the determination of the elastic moduli.

Sample code	Confining Pressure [MPa]	Young's modulus [GPa]	*Poisson's ratio* [-]
CKO6-AA-01-03-07p	0	41,0	0,296
CKO6-AA-01-03-02p	0	46,0	0,280
CKO6-AA-01-03-06p	20	34,8	0,312
CKO6-AA-01-03-01p	30	36,9	0,289
CKO6-AA-01-03-05p	40	44,1	0,281
CKO6-AA-01-01-06s	0	34,2	0,357
CKO6-AA-01-01-11s	0	36,1	0,251
CKO6-AA-01-02-01s	20	32,6	0,305
CKO6-AA-01-02-08s	30	25,2	0,234

The SURE project has received funding from the European Union's Horizon 2020 research and innovation programme under grant agreement No 654662.

CKO6-AA-01-02-10s	40	24,1	0,216
CKO6-AA-01-02-05s	50	23,6	0,230

4.9.6. Porosity and Pore Size Distribution

Two MIP experiments are performed to determine the porosity and pore size distribution. Two half cylindrical rock fragments are evaluated in terms of total mercury intrusion volume as a function of pressure. Figure 5.19 shows the rough data of the experiment. Both curves show an intrusion of ~0.4 mm 3 /g at around 0.1 bar. Mercury started to penetrate the pores of the CKO6-AA-MIP2 sample between 60 and 200 bar. Within the CKO6-AA-MIP1 the mercury intrusion started at around 200 bar, showing an exponential increase until a pressure of 2000 bar. Using the relation of Washburn (1921), the pore diameter distribution is obtained. The CKO6-AA-MIP1 shows a main pore diameter in the range of 0.01 – 0.05 µm, for the CKO6-AA-MIP2 a diameter of between 0.05 and 0.3 µm is found.

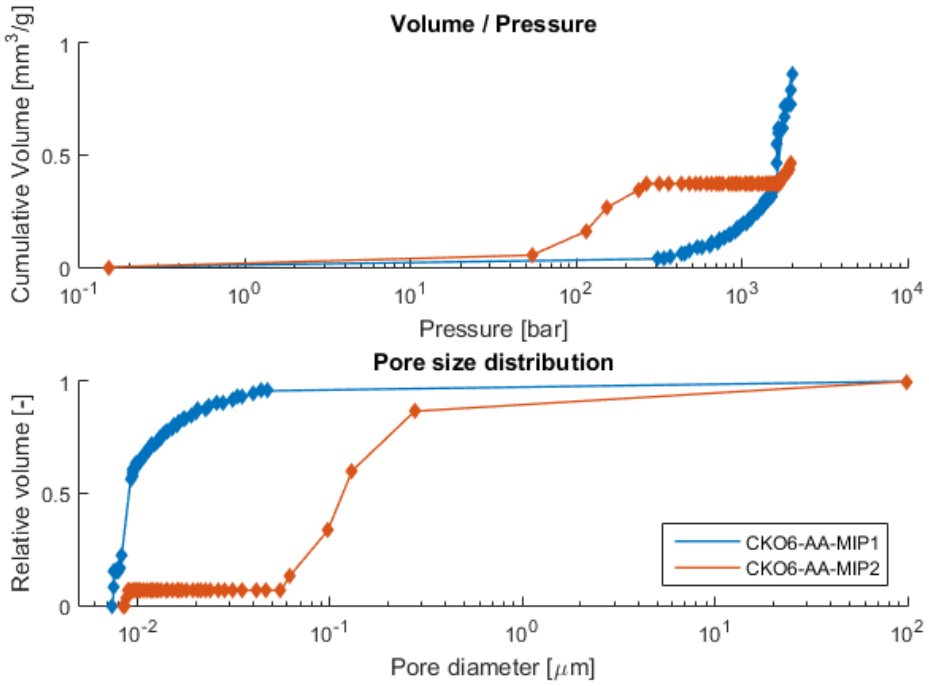

The porosity is determined by three different methods: Mercury Intrusion Porosimetry, Helium pycnometry and by the hydrostatic weighing method. All methods show porosity values between 0.21 and 1.00%, with a maximal uncertainty of +/- 0.88%. This uncertainty is mainly affected by measuring the sample dimensions (Helium pycnometer and dry/wet method). The MIP method is not dependent on the sample dimensions and is therefore the most accurate method, as indicated by the uncertainty range.

Sample code	Porosity [%]	Uncertainty [%]
	Helium Pycnometer	
CKO6-AA-01-03-18p	0.82	±0.85

The SURE project has received funding from the European Union's Horizon 2020 research and innovation programme under grant agreement No 654662.

CKO6-AA-01-03-13p	0.21	±0.86
CKO6-AA-01-03-15p	1.00	±0.88
Hydrostatic Weighing		
CKO6-AA-01-01-10s	0.82	±0.36
CKO6-AA-01-02-05s	0.87	±0.36
Mercury Intrusion Porosimetry*		
CKO6-AA-MIP1	0.30	±0.3
CKO6-AA-MIP2	0.21	±0.3

All samples show an exponential decrease of the pore volume. At a confining pressure of 20 MPa, the average pore volume change is 0.14 cm 3 with a maximum at 0.18 cm 3 and the minimum at 0.11 cm3. The CKO6-AA-01-03-01p and CKO6-AA-01-03-06p samples show a more volatile behavior, which can be explained by the temperature sensitivity of hydraulic pumps: the larger the amount of liquid in the cylinder, the larger the error due to temperature variations within the laboratory. Based on the volatility of the curve, the error is determined at ± 0.03 cm 3 for the parallel samples and ± 0.01 cm 3 for the perpendicular samples. At a confining pressure of 20 MPa the pore volume change corresponds to a porosity decrease between 0.04% and 0.097%. Based on the obtained average porosity of 0.8% of the intact rock, the relative porosity change is between 5% - 12%.

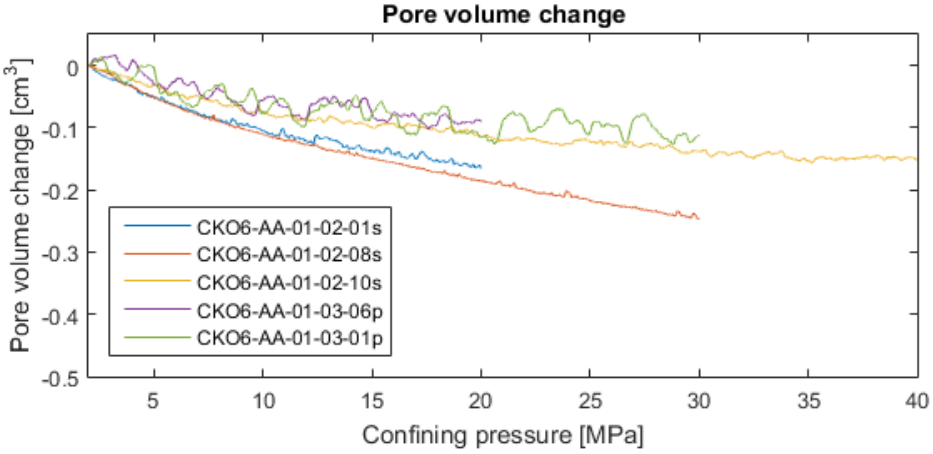

4.9.7. Permeability Measurements

The SURE project has received funding from the European Union's Horizon 2020 research and innovation programme under grant agreement No 654662.

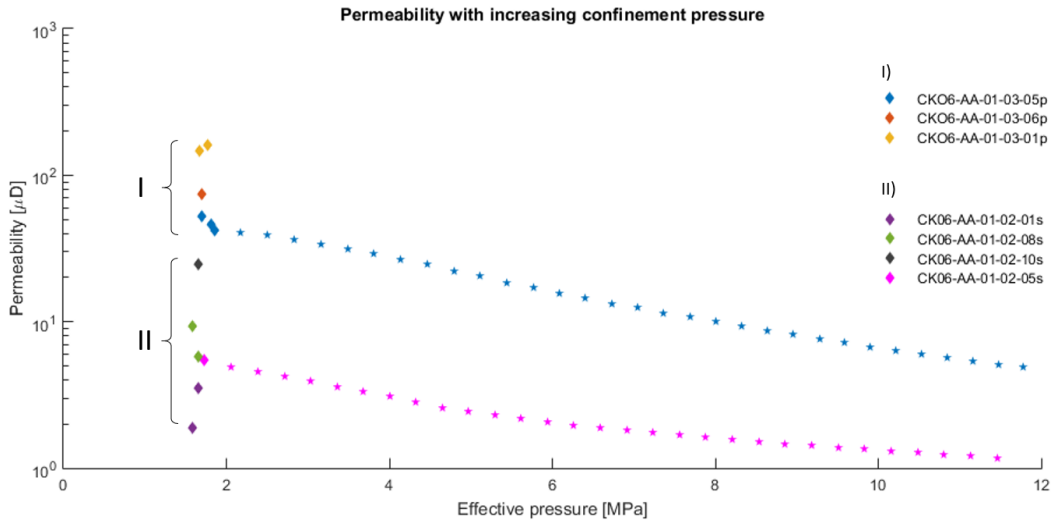

There is a clear distinction between the sample orientation and the permeability. In case the flow is parallel to the bedding, the permeability is ranging from 3 to 24 µD. In case the flow is parallel to the bedding the permeability is ranging from 47 to 154 µD. The minimum measurable permeability is about 1 µD.

Sample code	Confining Pressure [MPa]	Permeability (Pc ~ 2MPa) [µD]
CKO6-AA-01-03-06p	20	74
CKO6-AA-01-03-01p	30	154
CKO6-AA-01-03-05p	40	47
Average + Standard deviation		*92 \ 56*
CKO6-AA-01-02-01s	20	3
CKO6-AA-01-02-08s	30	8
CKO6-AA-01-02-10s	40	25
CKO6-AA-01-02-05s	50	5
Average + Standard deviation		*10 \ 10*

Two rock samples were investigated at four different steady state flow rates. A flow rate was kept constant for around 30 minutes in order to ensure a stable flow. The confining pressure is kept constant at 8 MPa for the duration of the entire experiment. Using Darcy's law and the Klinkenberg correction a fluid permeability of 0.31 µD and 0.17 µD is obtained.

The SURE project has received funding from the European Union's Horizon 2020 research and innovation programme under grant agreement No 654662.

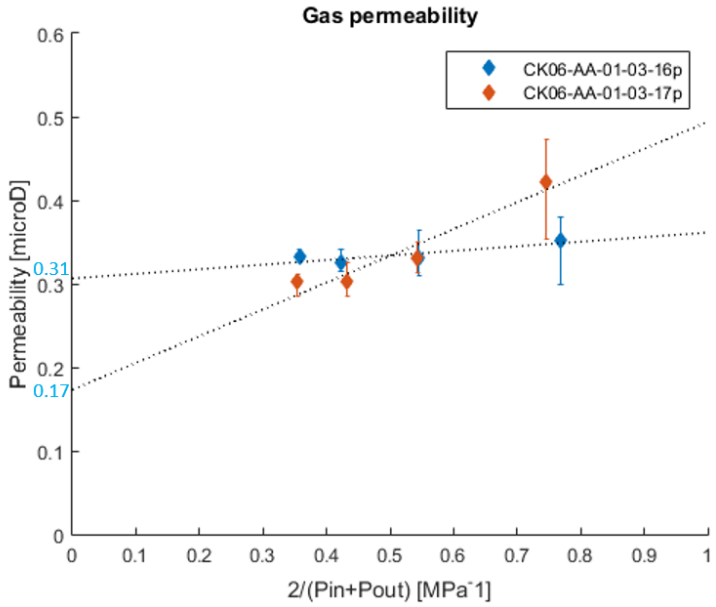

The SURE project has received funding from the European Union's Horizon 2020 research and innovation programme under grant agreement No 654662.

4.10. SWD6_OK – Oberkirschner sandstein

4.10.1. UCS

Sample: SWD6_OK_50_X3

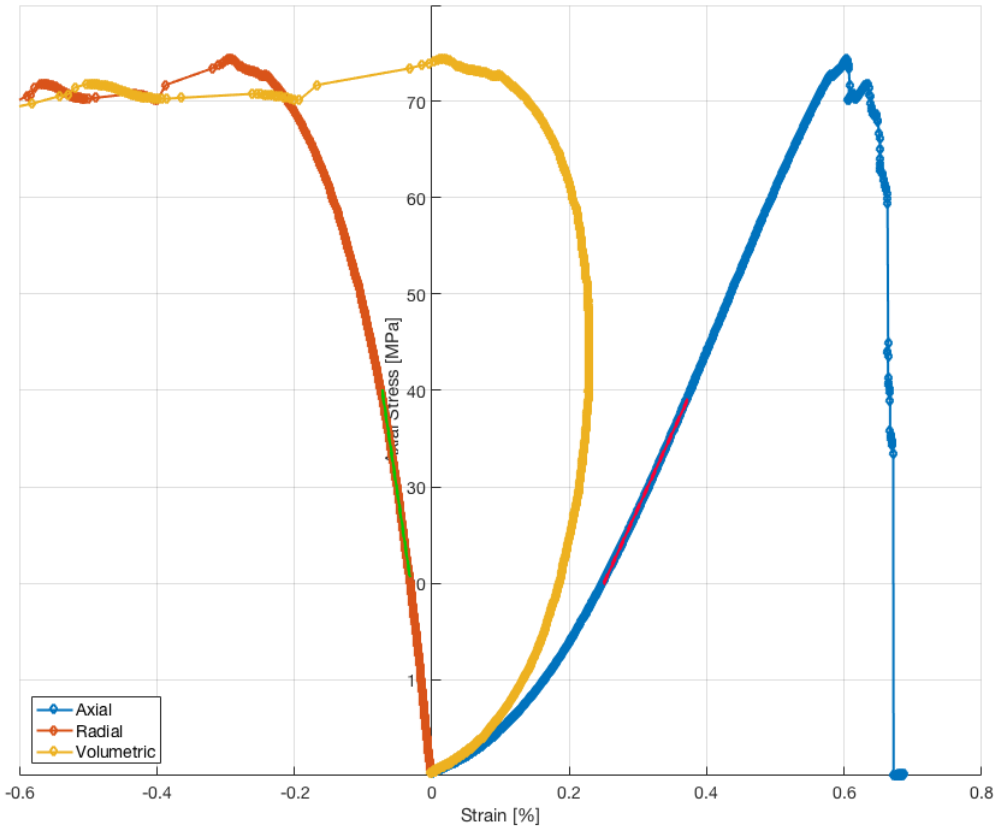

Peak stress: 75 [MPa]
Yield stress: 69 [MPa]
Young's Modulus: 15.6586 +/- 0.043426 [GPa]
Poisson's ratio: 0.32602 +/- 0.0026761, [-]

The SURE project has received funding from the European Union's Horizon 2020 research and innovation programme under grant agreement No 654662.

Sample: SWD6_OK_50_Z3

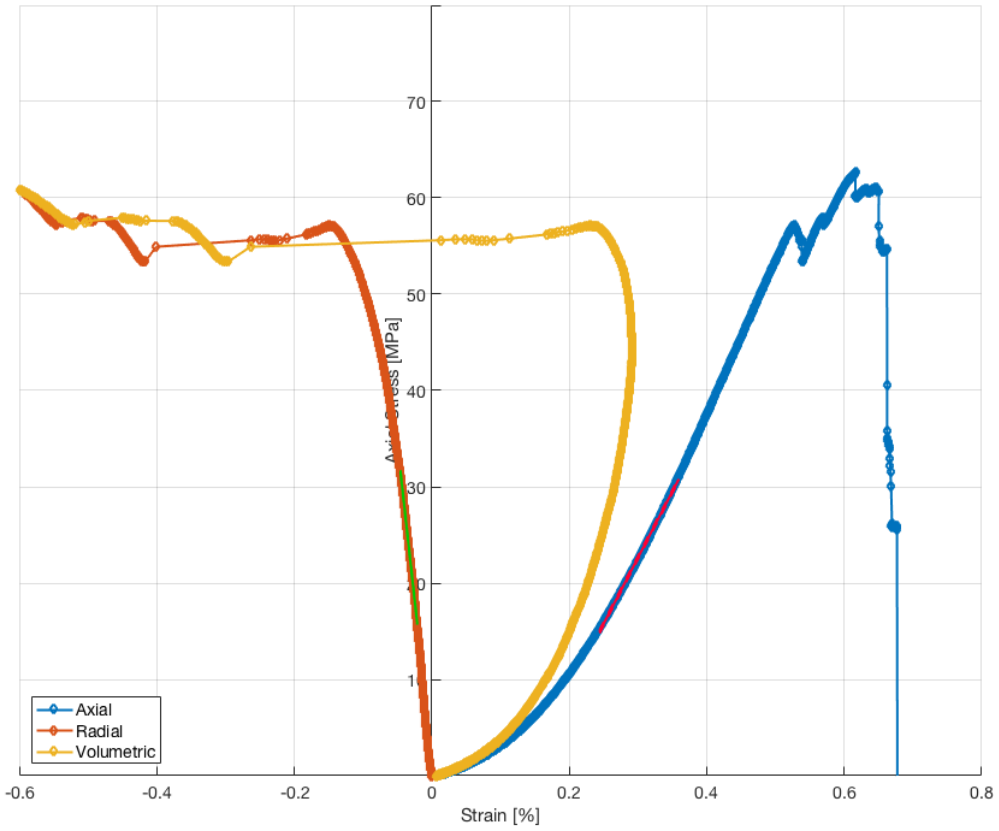

Peak stress: 63 [MPa]
Yield stress: 53 [MPa]
Young's Modulus: 13.7241 +/- 0.051983 [GPa]
Poisson's ratio: 0.21232 +/- 0.0016281,

4.10.2. Tri-axial deformation

At the moment of writing there is too little data to plot Mohr circles. Performed tests: unconfined tests and one test at P_c = 20 MPa (failure at a differential stress of 131.5 MPa, which were done before the project focused on specific rock types. Representative stress/strain curve is shown below.

The SURE project has received funding from the European Union's Horizon 2020 research and innovation programme under grant agreement No 654662.

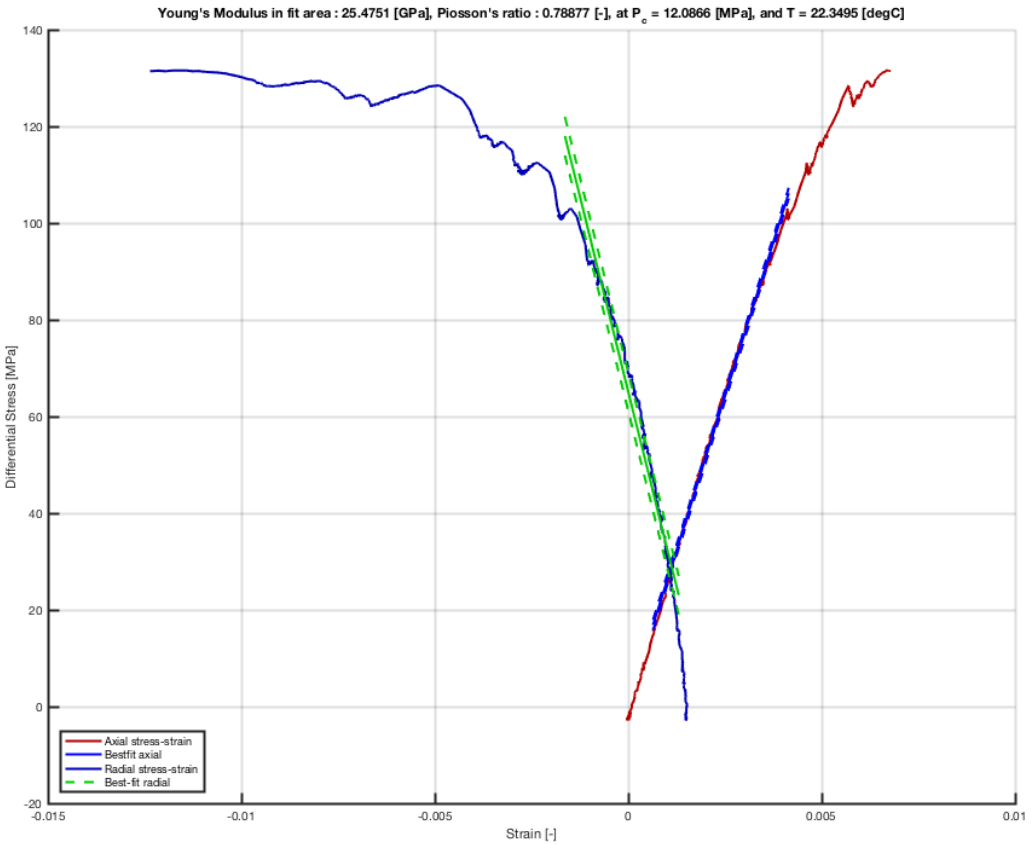

4.10.3. Permeability

Permeability range of sample SWD6_OK_50_X2 (sample orientation: axis along bedding): 6.3 x 10^{-15} to 2.2 x 10^{-15} m^2 in a hydrostatic effective pressure range: 2.5 to 30 MPa. Sample permeability is not recoverable (at least not significantly) during depressurization

The SURE project has received funding from the European Union's Horizon 2020 research and innovation programme under grant agreement No 654662.

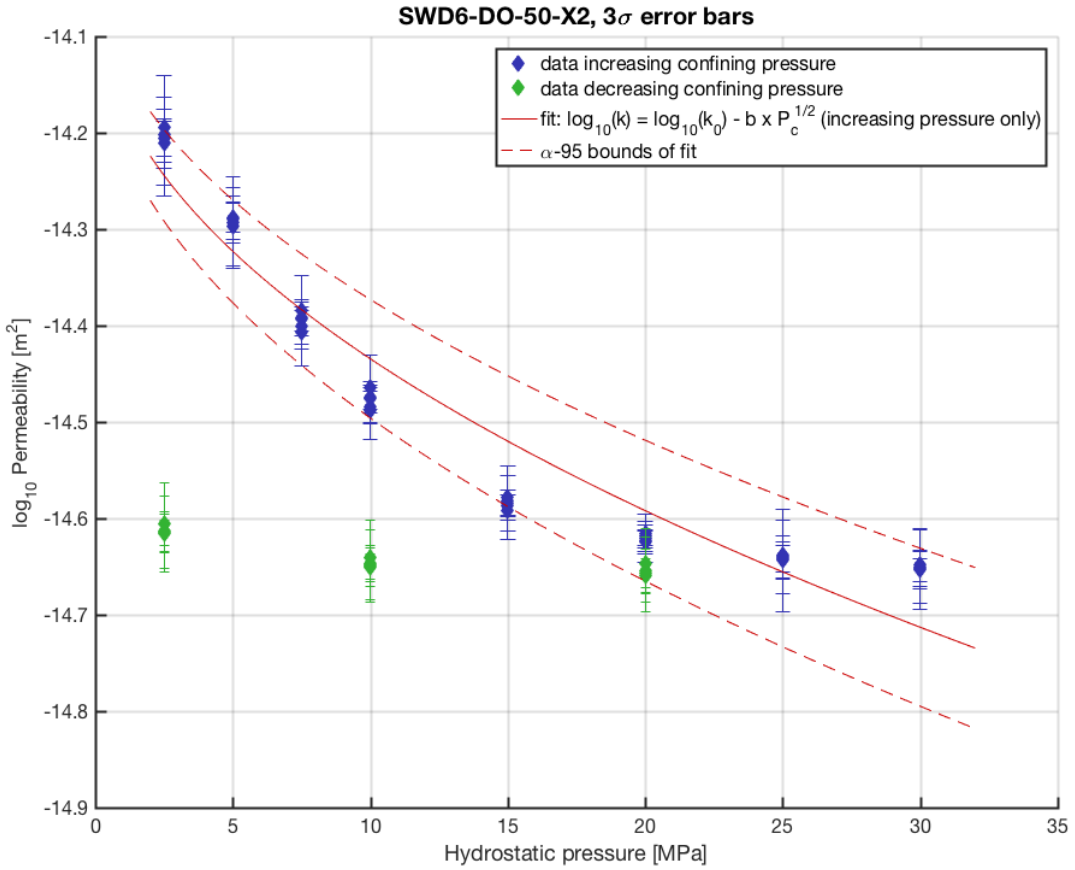

4.10.4. Acoustic velocities

Sample code	v_p [km/s]	v_{s1} [km/s]	v_{s2} [km/s]
SWD6_OK_50_X3	2.8739	1.9991	1.9343
SWD6_OK_50_Z3	3.0515	2.0056	2.0229

The SURE project has received funding from the European Union's Horizon 2020 research and innovation programme under grant agreement No 654662.

4.11. SRG6_RU - Ruethener Gruensandstein

4.11.1. UCS

Sample: SRG6_RU_50_X3

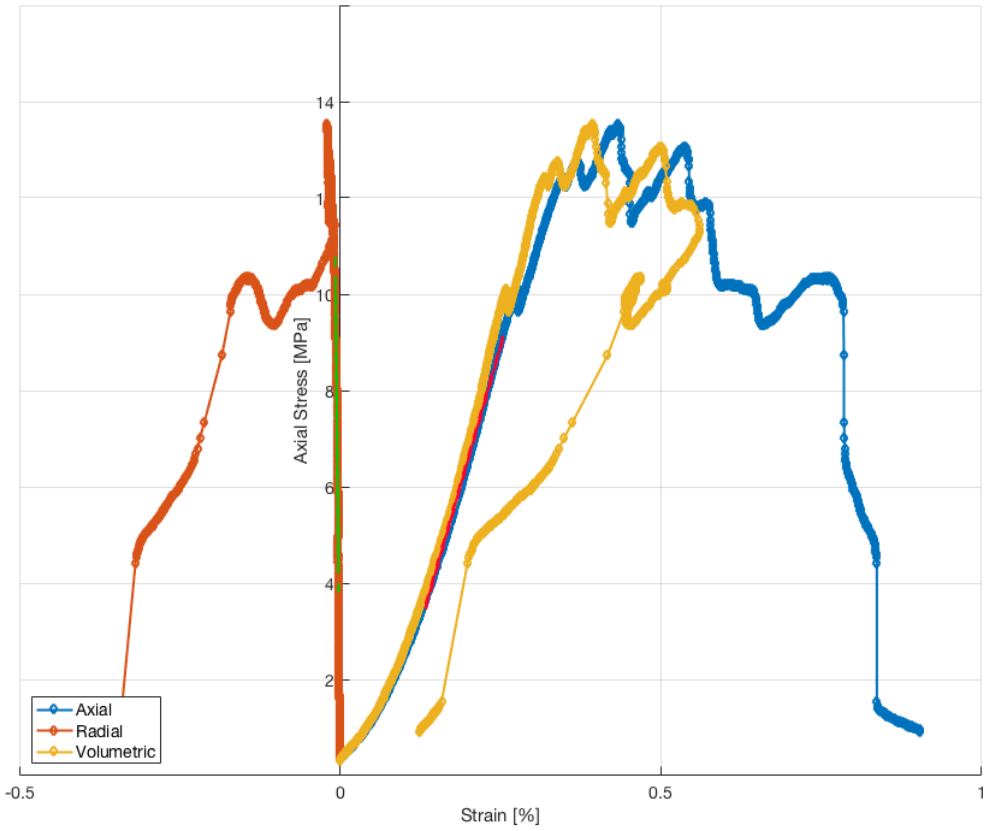

Peak stress: 13.5 [MPa]
Yield stress: 9.4 [MPa]
Young's Modulus: 4.4264 +/- 0.023062 [GPa]
Poisson's ratio: 0.030472 +/- 0.0011655, [-]

The SURE project has received funding from the European Union's Horizon 2020 research and innovation programme under grant agreement No 654662.

Sample: SRG6_RU_50_Z3

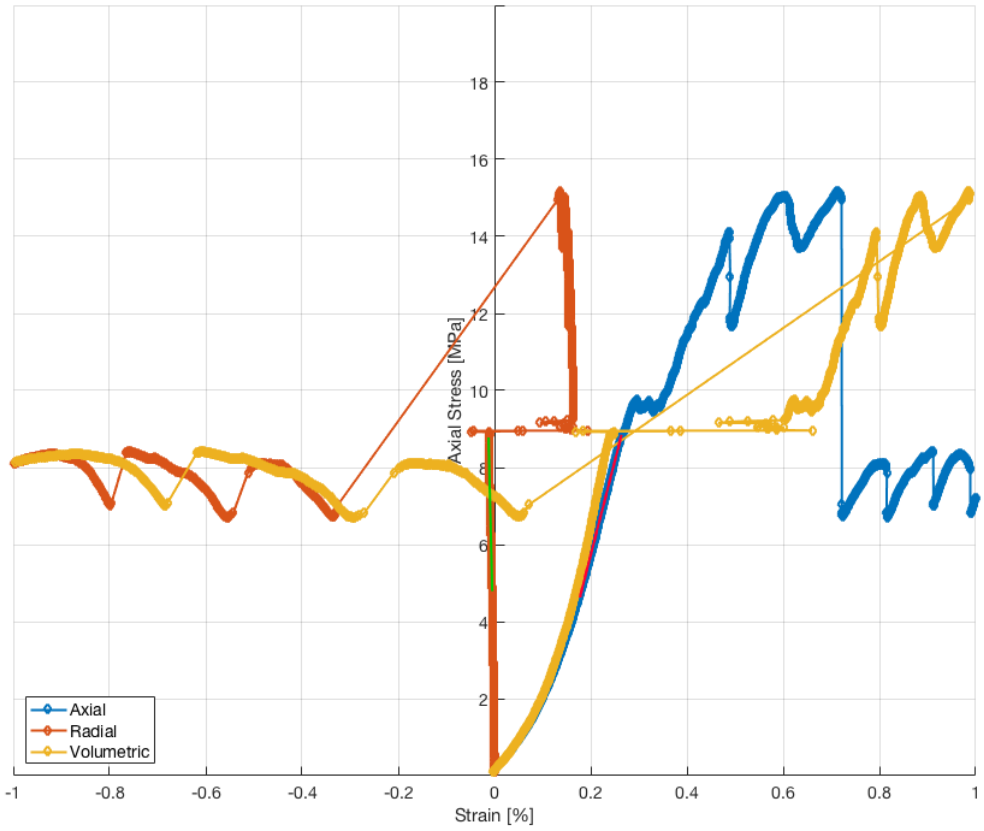

Radial strain gage mounted improperly. Poisson's ratio not measured, yield and peak strengths not identified.
Young's Modulus: 4.7439 +/- 0.018374 [GPa]

The SURE project has received funding from the European Union's Horizon 2020 research and innovation programme under grant agreement No 654662.

4.11.2. Permeability

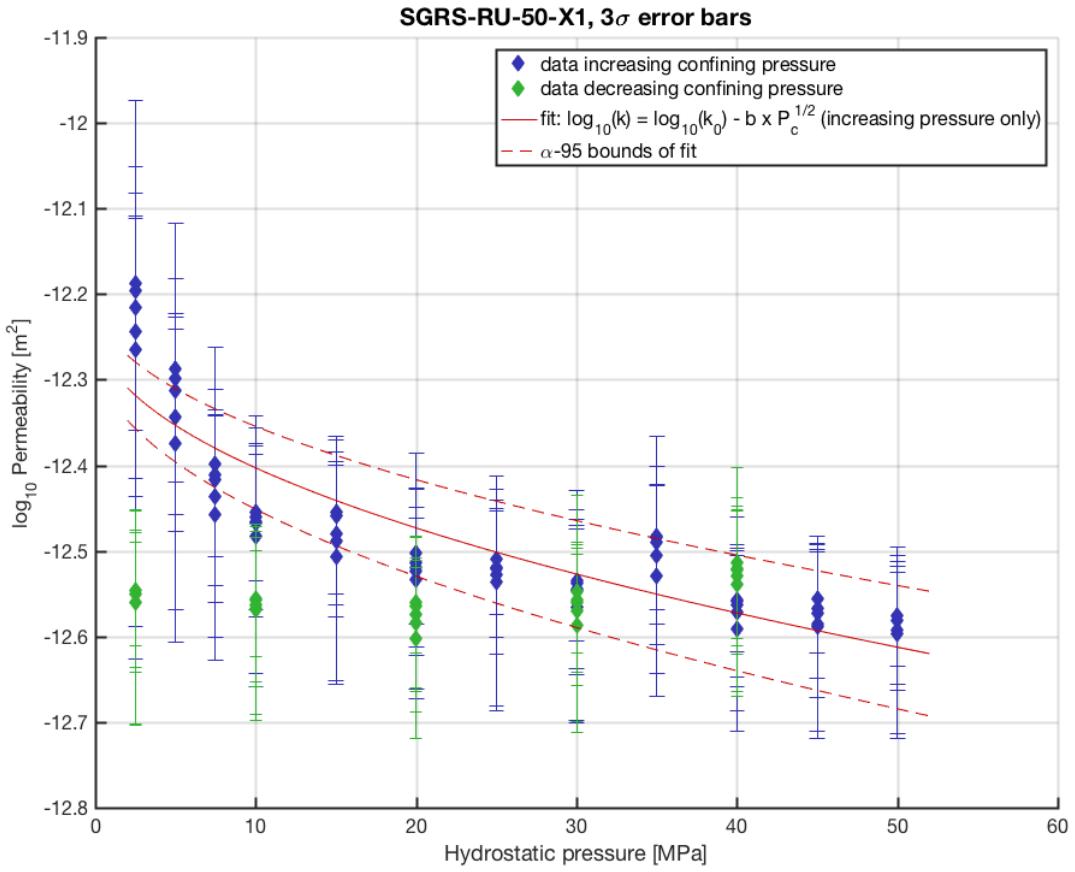

4.11.3. Acoustic velocities

Sample code	v_p [km/s]	v_s [km/s]
SRG6_RU_50_X3	2.5430	1.6649
SRG6_RU_50_Z3	2.6403	1.7322

The SURE project has received funding from the European Union's Horizon 2020 research and innovation programme under grant agreement No 654662.

4.12. VBA6_IC – Iceland Basalt

4.12.1. UCS

Sample: VBA6_IC_03_1A

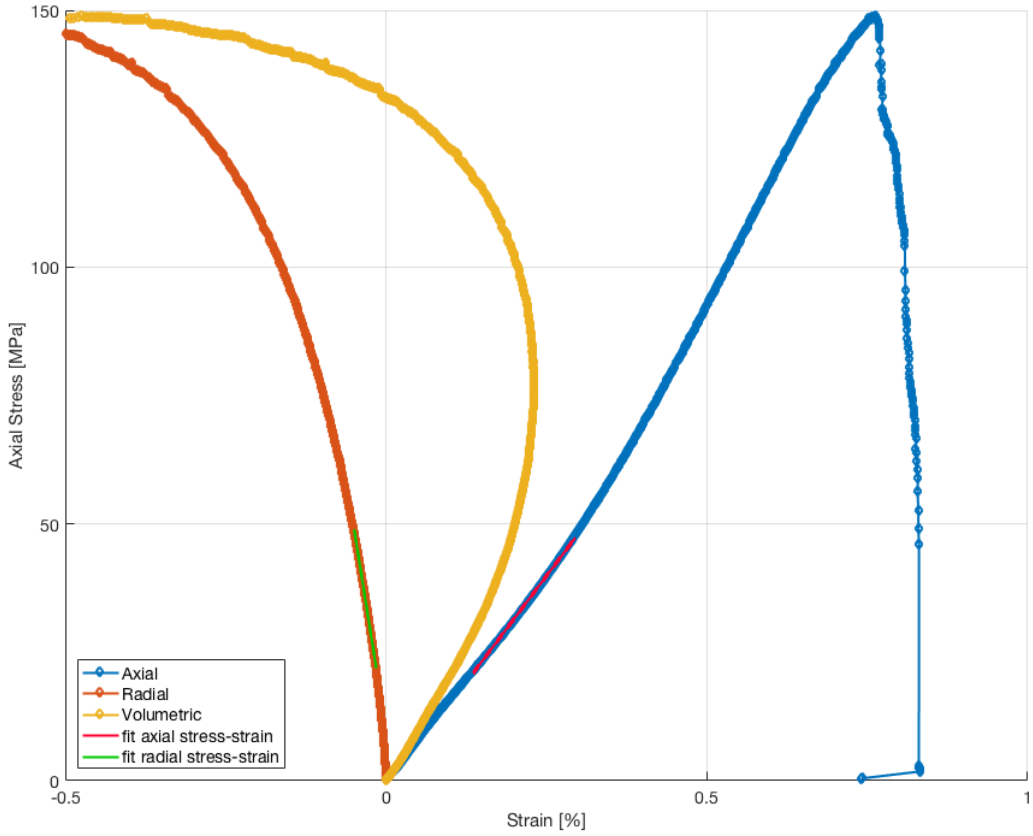

Peak stress: 149 [MPa]
Yield stress: 131 [MPa]
Young's Modulus: 16.5494 +/- 0.05104 [GPa]
Poisson's ratio: 0.21116 +/- 0.0014131, [-]

The SURE project has received funding from the European Union's Horizon 2020 research and innovation programme under grant agreement No 654662.

Sample: VBA6_IC_03_2A

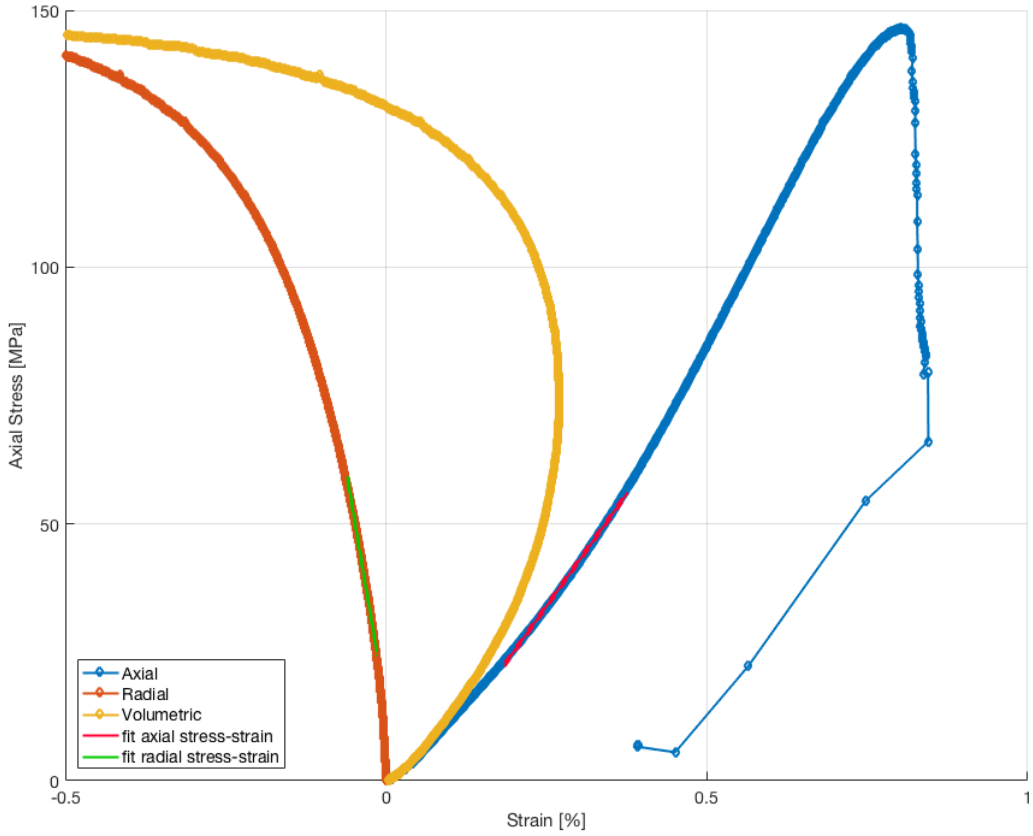

Peak stress: 146 [MPa]
Yield stress: 129[MPa]
Young's Modulus: 17.4498 +/- 0.066713 [GPa]
Poisson's ratio: 0.23717 +/- 0.0023319, [-]

4.12.2. Brazil disk indirect tensile strength

Tensile Strength Mean: 7.1575 [MPa]
Standard deviation: 0.2359 [MPa]
Data range: 6.8253 – 7.5690 [MPa]
Number of samples: 8

4.12.3. Acoustic velocities

Sample code	v_p [km/s]	v_{s1} [km/s]	v_{s2} [km/s]
VBA6_IC_03_1A	3.7505	2.3973	2.4199
VBA6_IC_03_2A	3.6015	2.3297	2.3226

The SURE project has received funding from the European Union's Horizon 2020 research and innovation programme under grant agreement No 654662.

4.13. VIB8-IC - Interlayered sediments

4.13.1. UCS

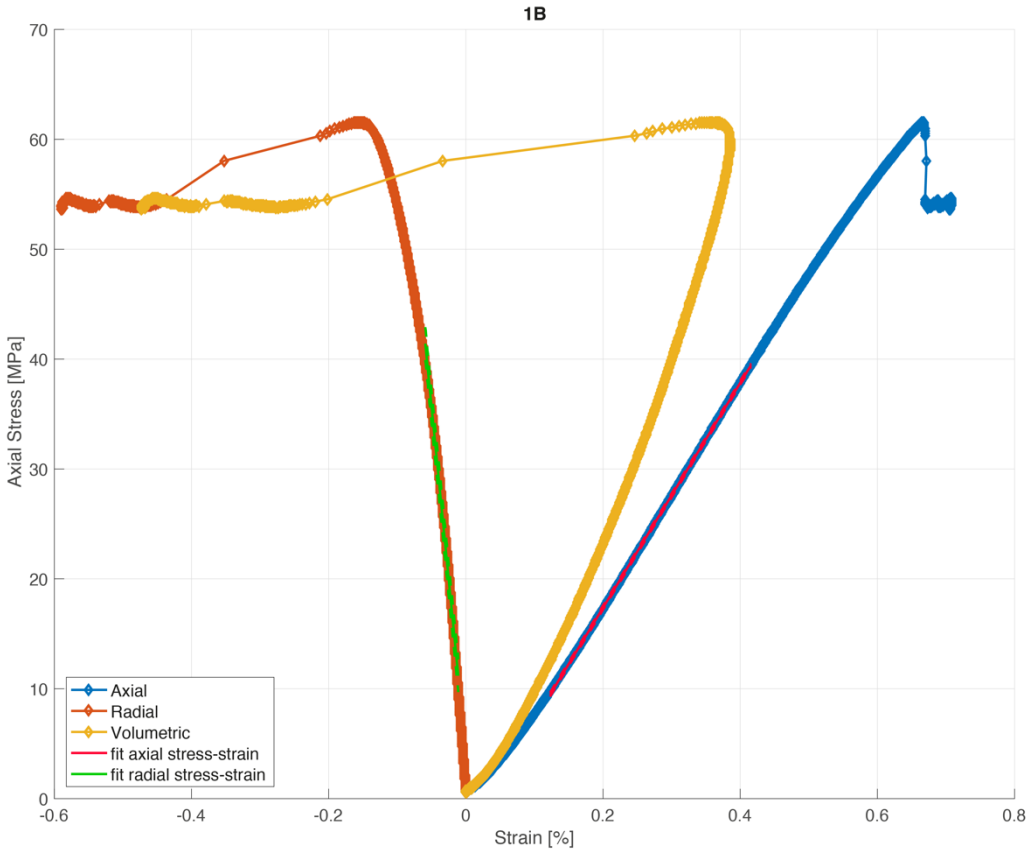

Peak stress:	61.55 [MPa]
Yield stress:	45 [MPa]
Young's Modulus:	10.26 [GPa]
Poisson's ratio:	0.198 [-]

The SURE project has received funding from the European Union's Horizon 2020 research and innovation programme under grant agreement No 654662.

4.13.2. Triaxial Strength

The following data points were available to construct a failure envelope at the time of preparing this document: 4 unconfined tests and 2 confined tests (at 10 and 20 MPa). These data yielded a failure envelope with a coefficient of internal friction of 0.710 and 16.3 MPa for cohesion. See figure below.

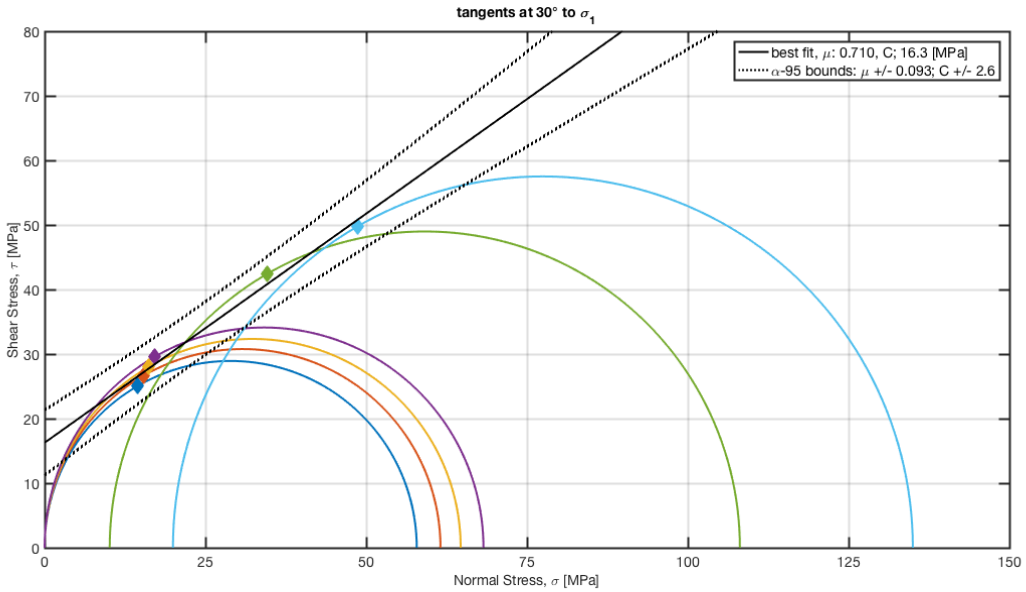

The SURE project has received funding from the European Union's Horizon 2020 research and innovation programme under grant agreement No 654662.

4.13.3. Permeability

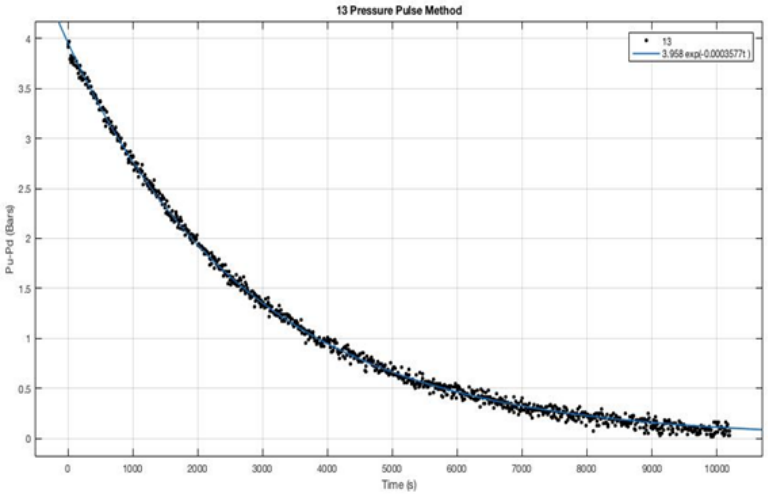

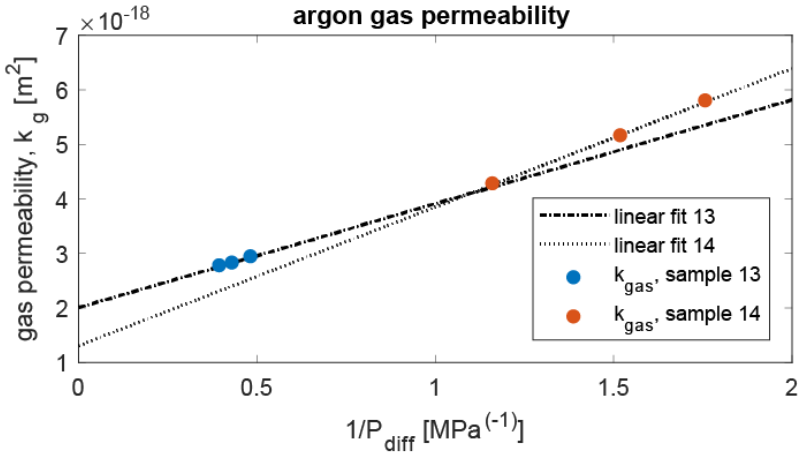

Permeability was measured using the pulse-decay method (example of decay shown upper diagram) and corrected for gas slippage effects (Klinkenberg correction, lower diagram). Initial results show a permeability in the order of 10^{-18} m^2. Data was acquired within the Bsc. Project of Thasya Arysanto (GFZ, TU Berlin), supervised by C. Kluge. More tests pending.

The SURE project has received funding from the European Union's Horizon 2020 research and innovation programme under grant agreement No 654662.

4.13.4. Brazil disk indirect tensile strength

Tensile Strength Mean: 8.66 [MPa]
Standard deviation: 1.52 [MPa]
Data range: 6.37 - 10.94 [MPa]
Number of samples: 18

4.13.5. Acoustic velocities

Sample code	v_p [km/s]	v_{s1} [km/s]
VIB8_IC_01_1A	3.672	2.065
VIB8_IC_01_1B	3.293	1.995
VIB8_IC_01_2A	3.345	2.033
VIB8_IC_01_3A	3.278	2.047
VIB8_IC_01_4A	3.432	2.105
VIB8_IC_01_4B	3.351	2.124

The SURE project has received funding from the European Union's Horizon 2020 research and innovation programme under grant agreement No 654662.

4.14. Chalk Outcrop – Austin (US) and Welton (UK)

4.14.1. UCS

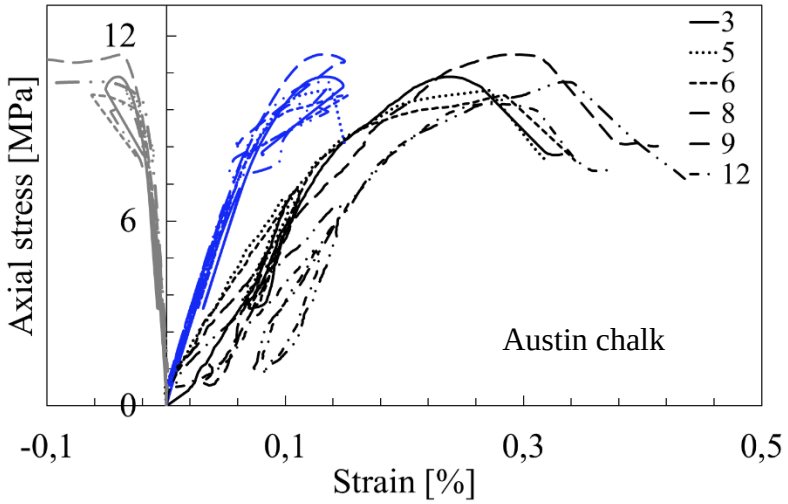

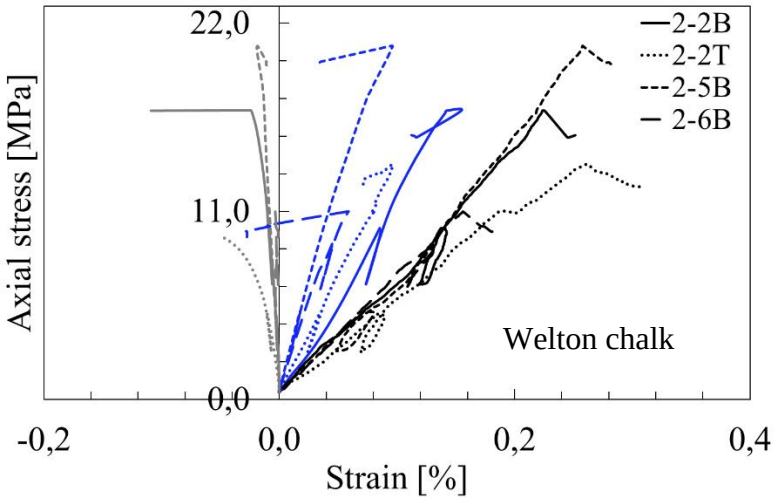

The SURE project has received funding from the European Union's Horizon 2020 research and innovation programme under grant agreement No 654662.

Table 1 Summary of the rock mechanics properties from UCS test for the Austin and Welton outcrop chalks

ID	ρ_b	φ	v_p	v_s	C_0	E_{s*}	E_s	E_d	ν_s	ν_d
	g/cm^3		m/s	m/s	MPa	GPa	GPa	GPa		
Austin chalk										
3	1.86	0.31	2905	1624	10.67	8.0	10.7	12.5	0.25	0.27
			2904	1605		9.0	12.0	12.3	0.24	0.28
5	1.87	0.31	3008	1630	10.24	6.2	10.9	12.8	0.23	0.29
			2950	1630		8.9	12.5	12.7	0.22	0.28
6	1.87	0.30	3072	1632	10.08	5.8	11.2	13.0	0.24	0.30
			3023	1607		9.0	12.4	14.3	0.22	0.22
8	1.90	0.29	3055	1669	11.41	5.1	11.5	13.6	0.21	0.29
			3054	1608		8.3	12.4	12.8	0.23	0.31
9	1.90	0.29	3064	1614	10.08	4.4	12.0	12.9	0.22	0.31
			3027	1596		5.7	12.8	14.6	0.23	0.31
12	1.89	0.30	2996	1625	9.80	4.7	10.7	12.9	0.25	0.29
			2973	1642		5.7	11.3	13.1	0.25	0.28
Welton chalk										
2-2B	2.23	0.16	4285	2129	16.9	9.3	13.7	27.0	0.16	0.34
			4319	2079		16.3	22.2	26.0	0.21	0.35
2-2T*	2.22	0.18	4233	2103	13.8	5.9	14.4	28.3		0.34
2-5B*	2.25	0.14	4438	2453	20.7	10.0	22.9	34.7	0.20	0.28
2-6B	2.23	0.15	4217	2294	11.0	7.0	20.3	30.3	0.10	0.29
			4217	2290		10.3	24.6	30.2	0.32	0.29

Averages:
Austin chalk:
Mean Unconfined Strength: 10.4 MPa
Mean Young's modulus static (LVDT): 5.7 GPa
Mean Young's modulus static (strain gauge): 11.1 GPA
Mean Young's modulus static (sonic velocity measurements): 13 GPa
Mean Poisson's ratio (static): 0.23
Mean Poisson's ratio (dynamic): 0.29

Welton chalk:
Mean Unconfined Strength: 15.6 MPa
Mean Young's modulus static (LVDT): 8.0 GPa
Mean Young's modulus static (strain gauge): 17.8 GPa
Mean Young's modulus static (sonic velocity measurements): 30.0 GPa

The SURE project has received funding from the European Union's Horizon 2020 research and innovation programme under grant agreement No 654662.

Mean Poisson's ratio (static): 0.15
Mean Poisson's ratio (dynamic): 0.31

4.14.2. Porosity & Permeability

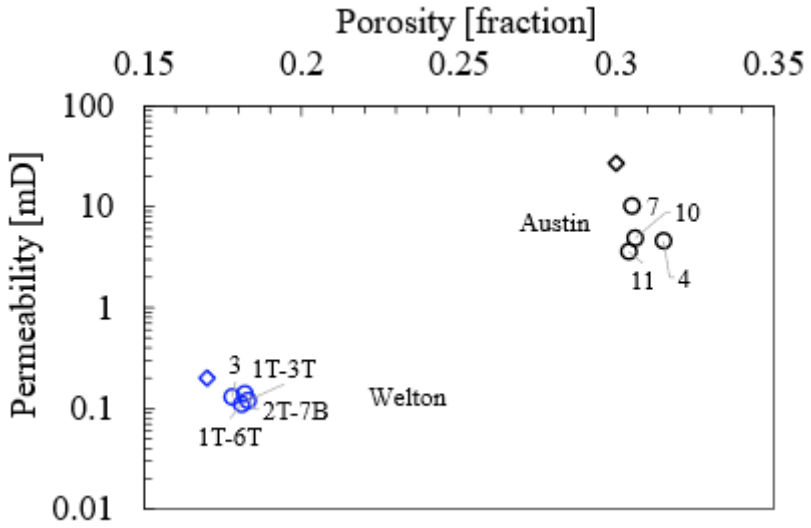

Markers with circle represent measured permeability with chalk tap water flushing in triaxial test set-up. Porosity was estimated from the dry bulk density and grain density measurements. Two diamond markers represent permeability and porosity estimation with gas injection for the Austin 4 and Welton 3 specimens.

Averages:
Austin chalk:
Porosity (gas injection): 0.317
Porosity (chalk saturated tap water): 0.315
Permeability (gas injection): 27 mD
Permeability (chalk saturated tap water flooding): 5.8 mD

Welton chalk:
Porosity (gas injection): 0.17
Porosity (chalk saturated tap water): 0.181
Permeability (gas injection): 0.2 mD
Permeability (chalk saturated tap water flooding): 0.13 mD

The SURE project has received funding from the European Union's Horizon 2020 research and innovation programme under grant agreement No 654662.

4.14.3. Brazil disk indirect test

ID	ρ_b	φ	T_0
	g/cm^3		MPa
Austin chalk			
5	1.93	0.26	1.65
6	1.88	0.29	1.76
7	1.86	0.31	1.71
8	1.86	0.30	1.81
9	1.90	0.29	1.76
10	1.90	0.29	1.80
Welton chalk			
5M	2.19	0.14	2.53
5B	2.20	0.16	3.10
5T	2.21	0.14	3.38
3T	2.26	0.13	2.02
7T	2.20	0.15	2.90
2-5T	2.25	0.13	2.77

Averages:
Austin chalk:
Mean Tensile Strength: 1.8 MPa

Welton chalk:
Mean Tensile Strength: 2.76 MPa

4.14.4. Triaxial compression & compaction testing

Austin chalk specimen 11 tested at 2 and 4 MPa confining stresses during fisrt and second compressive loading, respectively.

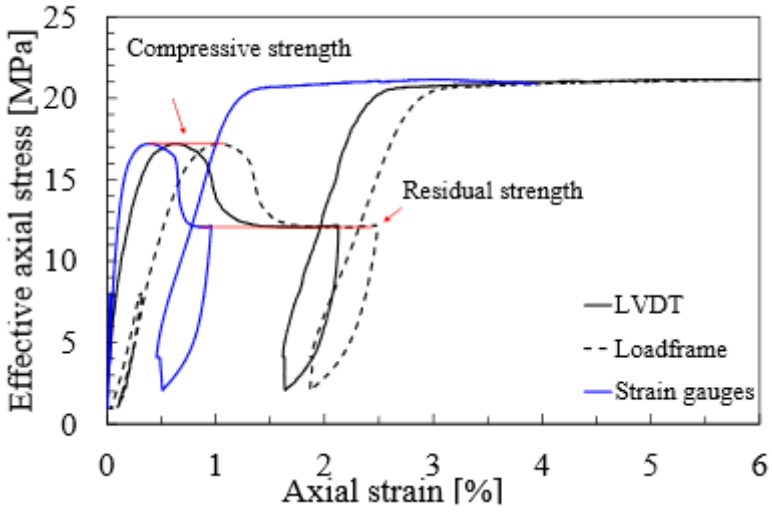

The SURE project has received funding from the European Union's Horizon 2020 research and innovation programme under grant agreement No 654662.

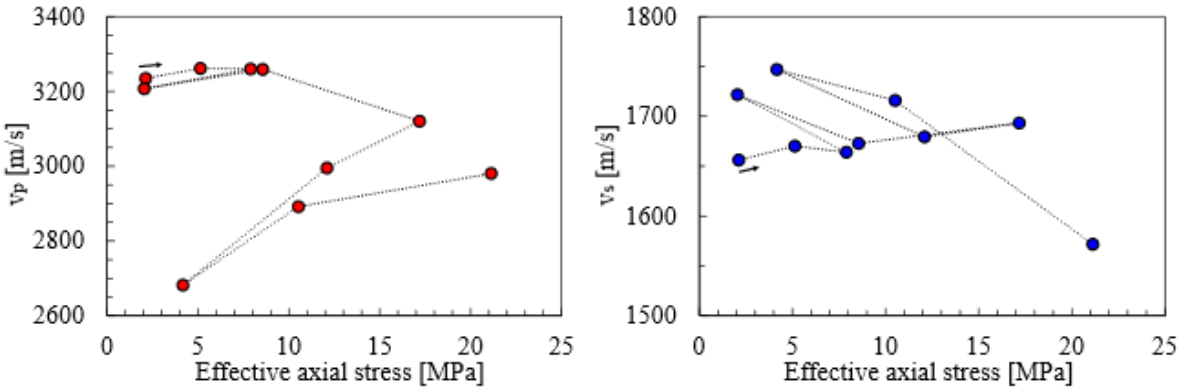

Austin chalk specimen 7 tested at 4 and 2 MPa confining stresses during fisrt and second compressive loading, respectively.

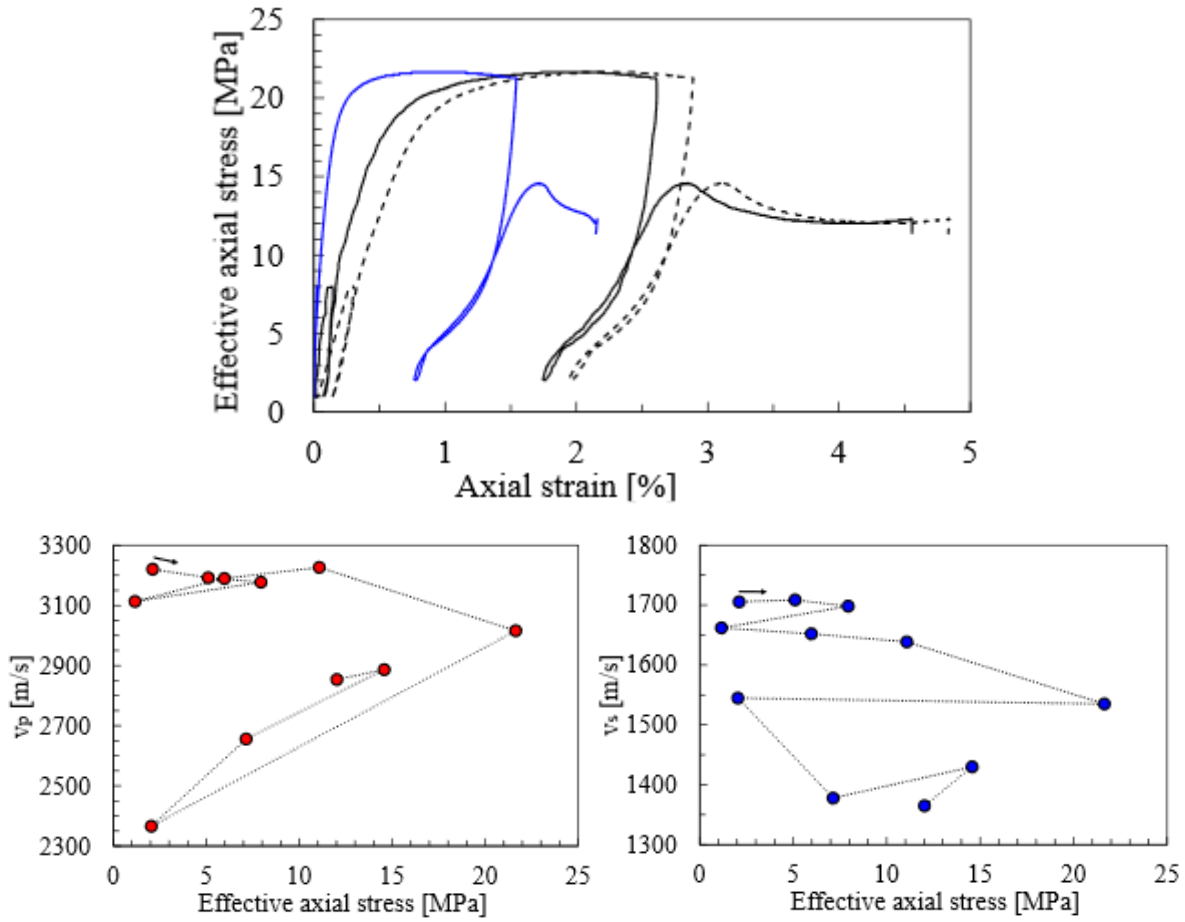

The SURE project has received funding from the European Union's Horizon 2020 research and innovation programme under grant agreement No 654662.

Austin chalk specimen 10 tested at 6 and 4 MPa confining stresses during fisrt and second compressive loading, respectively.

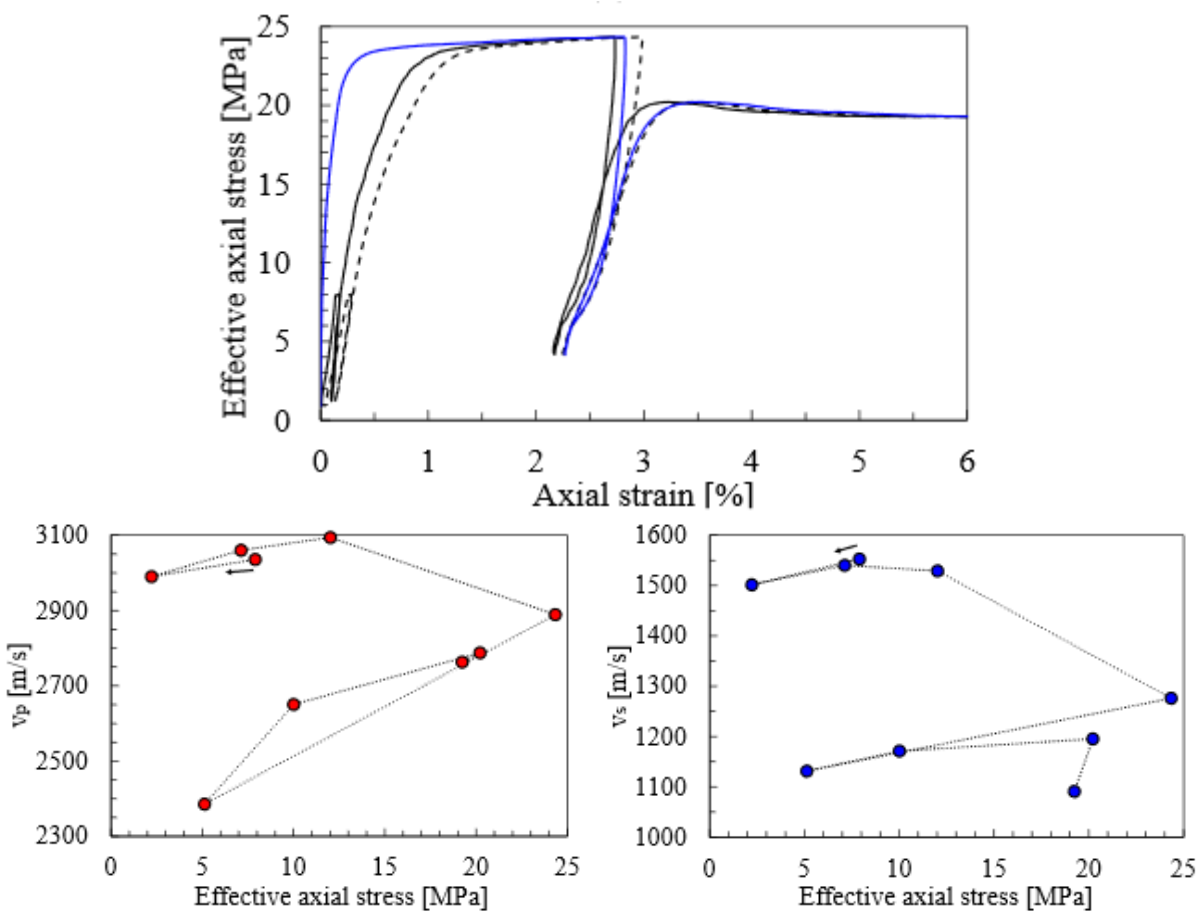

Austin chalk specimen 4 tested under triaxial compation/ hydrostatic loading.

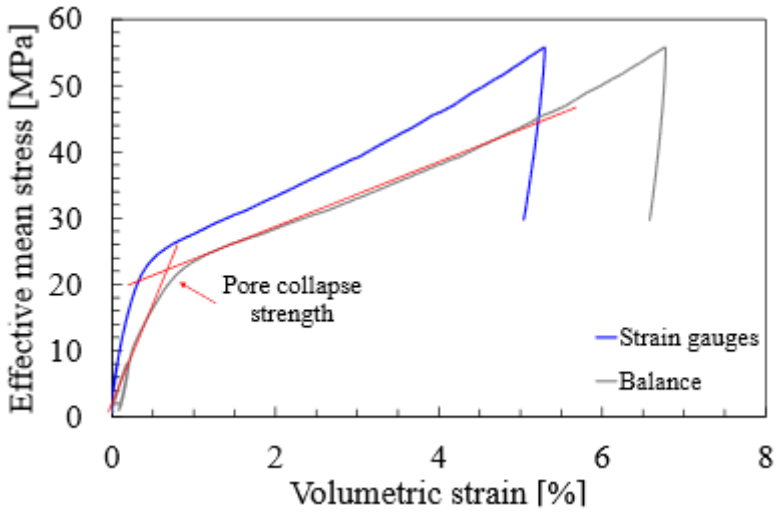

The SURE project has received funding from the European Union's Horizon 2020 research and innovation programme under grant agreement No 654662.

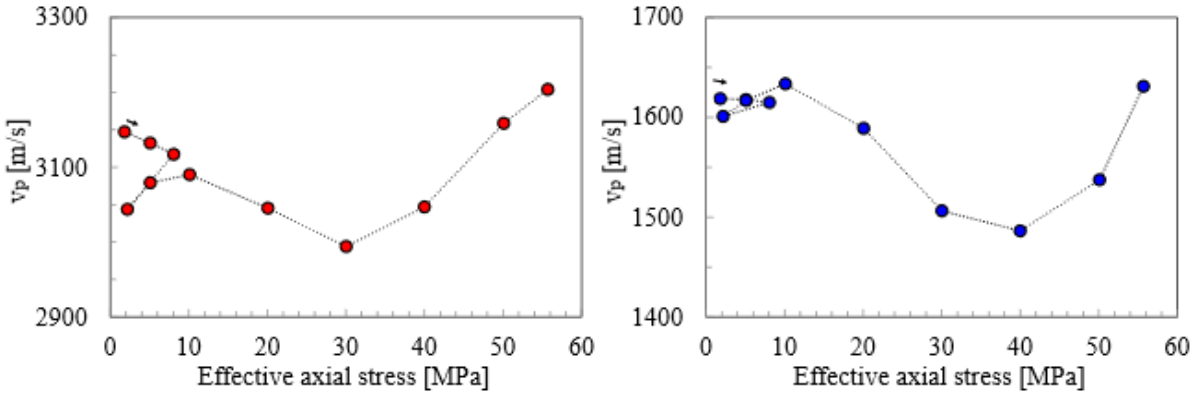

Welton chalk specimen 1T-6T tested at 2 and 6 MPa confining stresses during fisrt and second compressive loading, respectively.

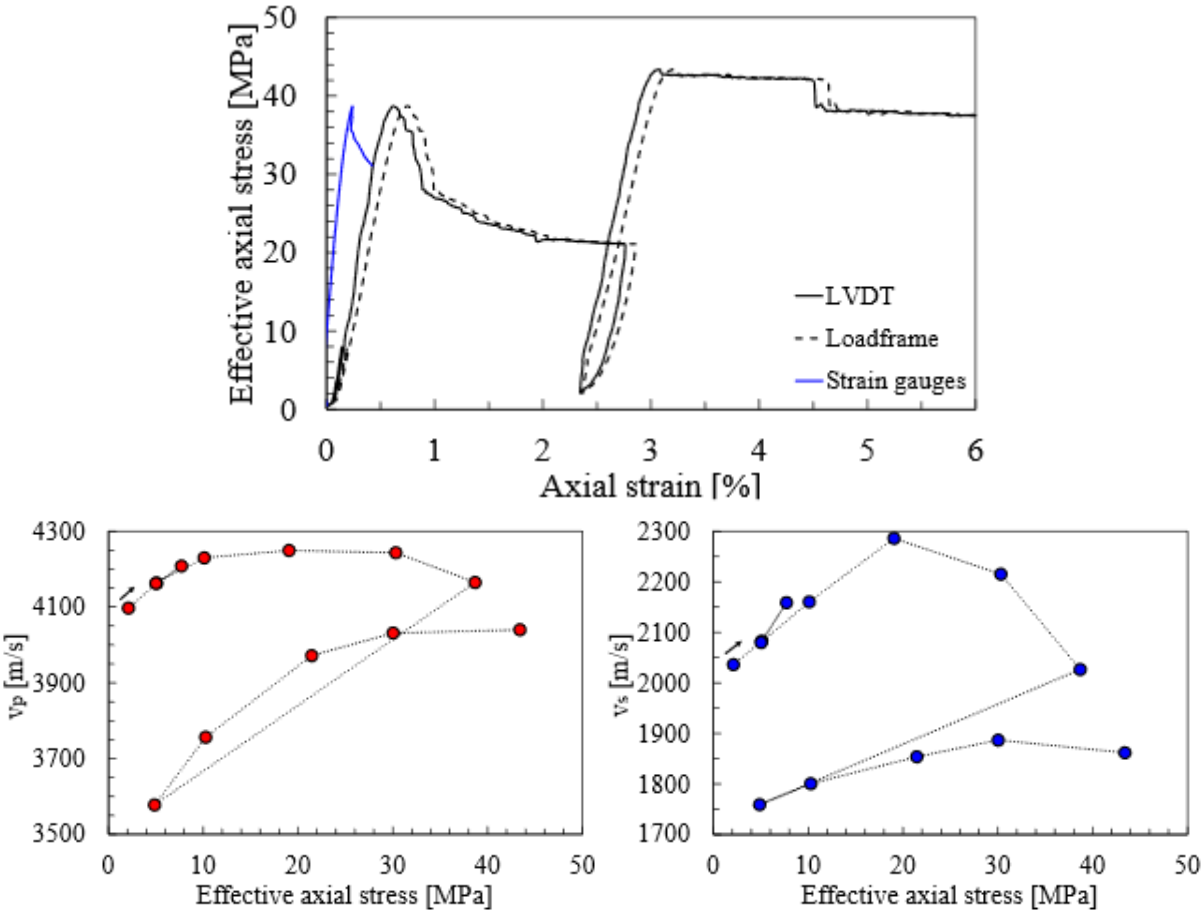

The SURE project has received funding from the European Union's Horizon 2020 research and innovation programme under grant agreement No 654662.

Welton chalk specimen 1T-3T tested at 4 and 2 MPa confining stresses during fisrt and second compressive loading, respectively.

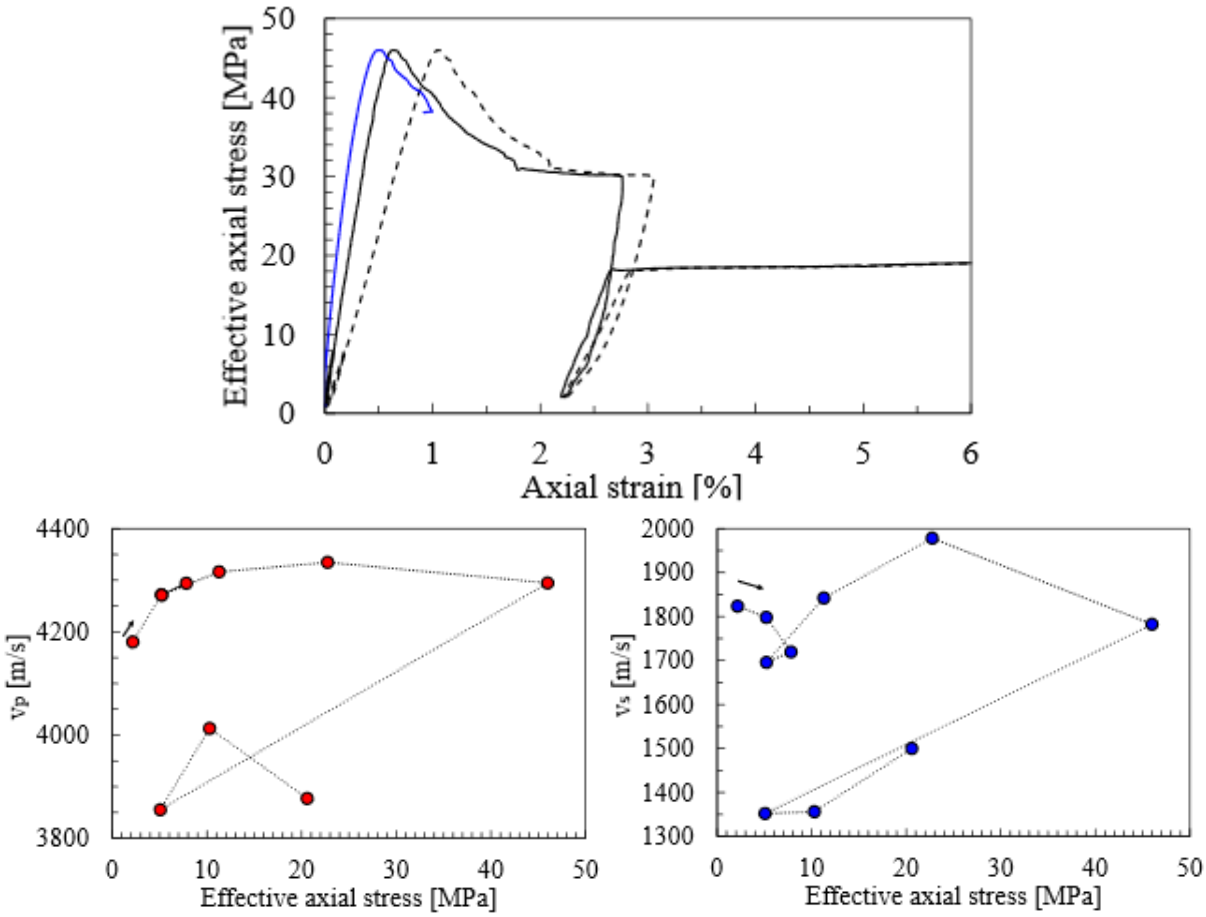

Welton chalk specimen 2T-7B tested at 6 and 4 MPa confining stresses during fisrt and second compressive loading, respectively.

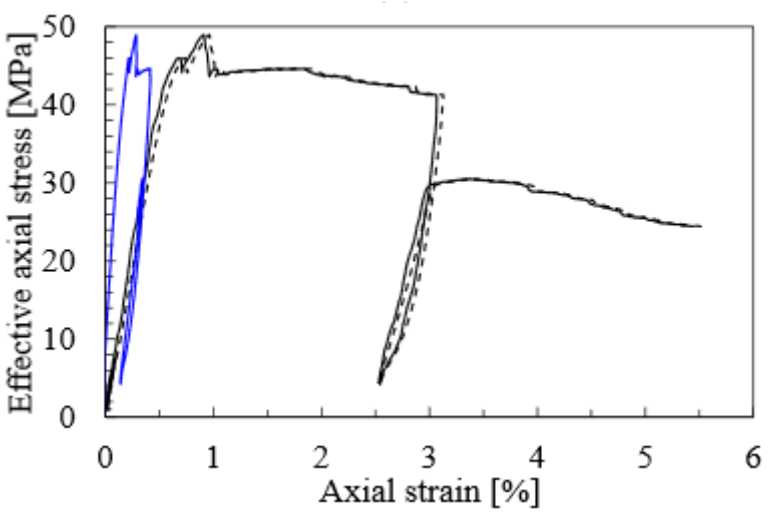

The SURE project has received funding from the European Union's Horizon 2020 research and innovation programme under grant agreement No 654662.

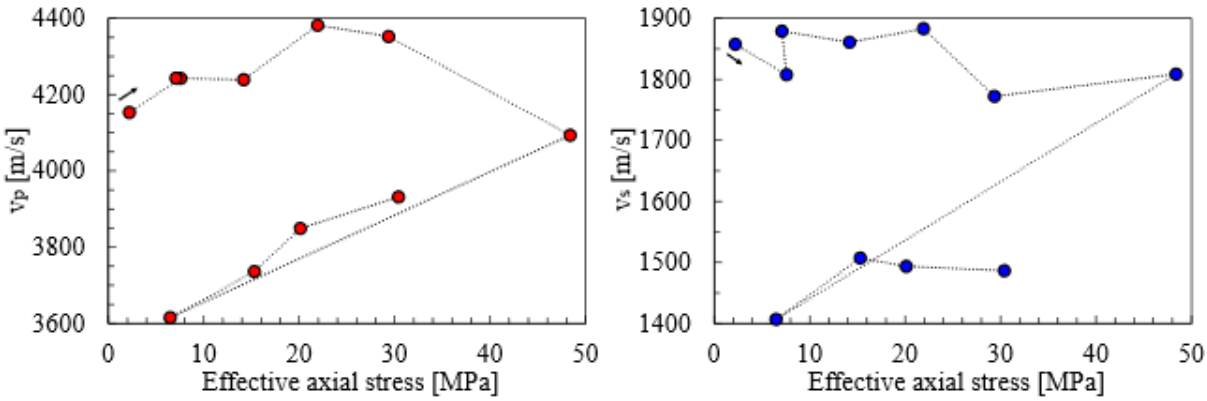

Welton chalk specimen 3 tested under triaxial compation/ hydrostatic loading.

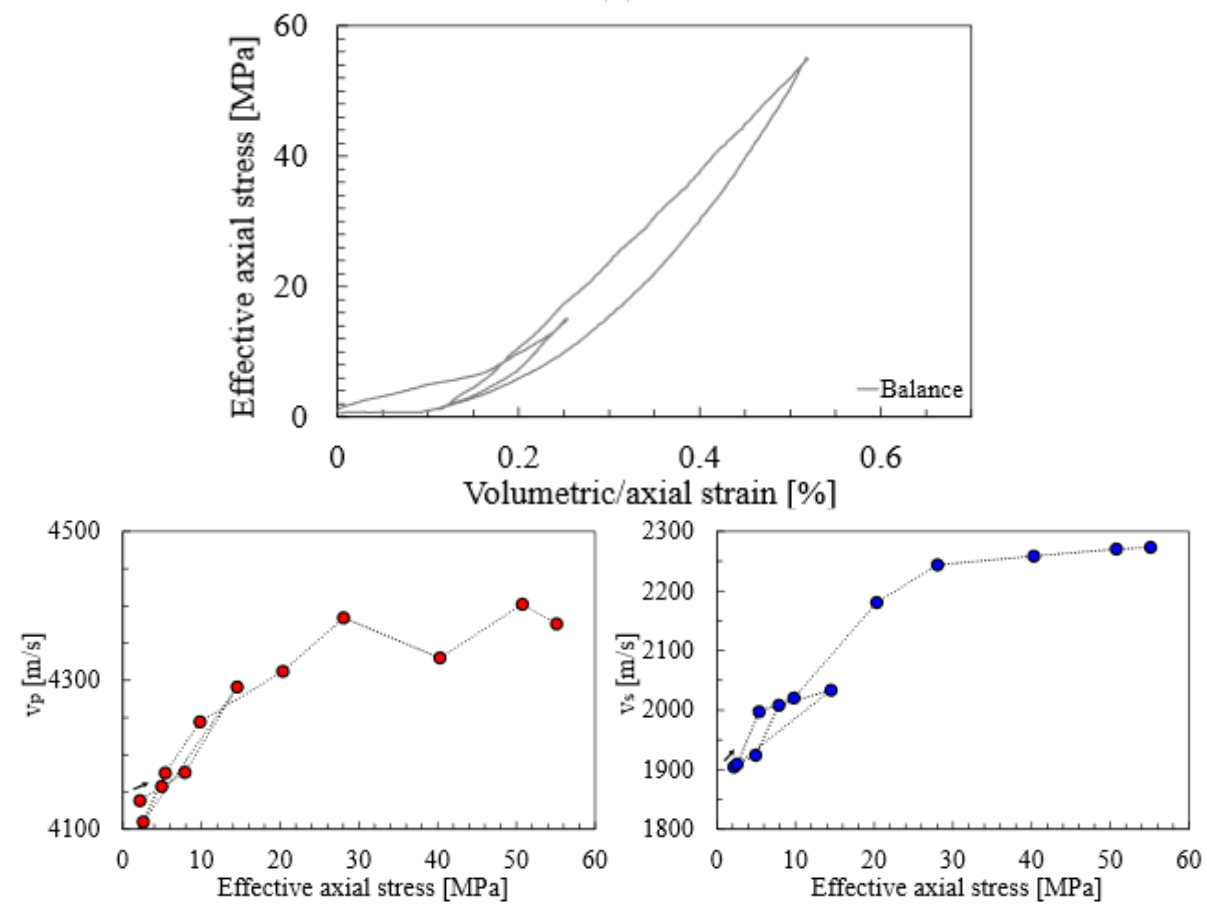

The SURE project has received funding from the European Union's Horizon 2020 research and innovation programme under grant agreement No 654662.

Table 2 Rock properties from triaxial compression test including hydrostatic loading (first raw), first (second raw) and second (third raw) compression phases for the Austin and Welton outcrop chalks.

ID	ρ_b	φ	- σ_{a1} σ_{a2}	- σ_{r1} σ_{r2}	σ_{res}	v_{ph} v_{p1} v_{p2}	v_{sh} v_{s1} v_{s2}	K_s	K_d	- E_{s1*} E_{s2*}	- E_{s1} E_{s2}	- E_{d1} E_{d2}	- ν_{s1} ν_{s2}	- ν_{d1} ν_{d2}
	g/cm^3		MPa	MPa	MPa	m/s	m/s	GPa	GPa	GPa	GPa	GPa		
Austin chalk														
11	1.88	0.31				3260	1664	8.3	13.1					
			17.2	2	12.1	3259	1673			4.5	10.0	13.9	0.27	0.32
			21.2	4		2892	1716			2.1	2.2	13.6	0.24	0.23
7	1.88	0.31				3177	1698	5.1	11.8					
			21.6	4		3226	1639			3.2	9.9	13.4	0.2	0.33
			14.6	2	12.0	2656	1378			1.1	1.2	9.4	0.38	0.32
10	1.88	0.31				3036	1553	5.1	11.3					
			24.3	6		3094	1529			3.3	11.6	11.8	0.17	0.33
			20.2	4		2650	1171			2.2	1.9	7.1		0.38
Welton chalk														
1T-6T	2.22	0.18				4208	2159	8.3	25.5					
			38.7	2	21.4	4249	2286			11.2	16.1	30.1	-	0.30
			43.4	6		3972	1854			5.4	-	20.8	-	0.36
1T-3T	2.22	0.18				4294	1720	8.4	32.1					
			46.0	4	30.2	4335	1978			8.2	11.0	23.7	0.13	0.36
			20.7	2		4012	1356			3.4	-	11.7	-	0.34
2T-7B	2.22	0.18				4243	1808	8.5	30.3					
			49.0	6		4380	2424			7.4	20.8	21.8	0.24	0.39
			30.5	4		3736	1948			6.1	11.2	14.1	0.39	0.40

Table 3 Rock properties from triaxial compaction test for the Austin and Welton outcrop chalks.

ID	ρ_b	φ	v_p	v_s	K_s	K_d	P_c
	g/cm^3		m/s	m/s	GPa	GPa	MPa
Austin 4	1.86	0.31	3117	1615	4.2	11.6	22.0
Welton 3	2.23	0.17	4221	2068	5.0	27.0	52.0

The SURE project has received funding from the European Union's Horizon 2020 research and innovation programme under grant agreement No 654662.

4.14.5. p'-q failure diagram

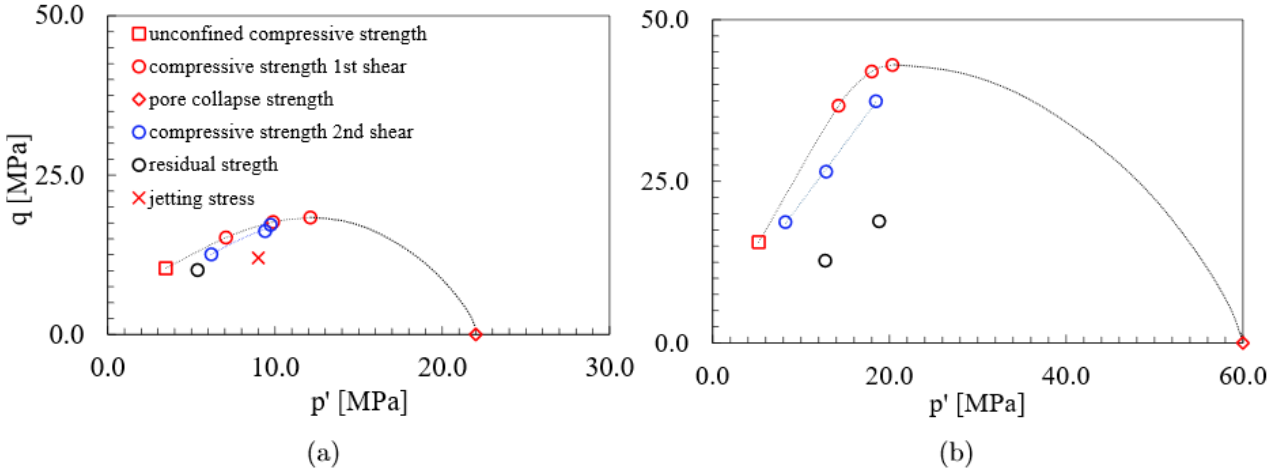

Figure 7 The Chalk model for the a) Austin and b) Welton outcrop chalks depicted on the p'-q diagram. Shear failure surface: red rectangle represent uniaxial compressive strength from UCS test; red and blue circular points represent compressive strength from the first and second shear phases in two-stage triaxial test, respectively; black circular points show residual strength from two-stage triaxial test. End cap: red diamond represents pore collapse strength from triaxial compaction test. Red cross marker shows the state of the stress used in the confined jet drilling experiment.

The SURE project has received funding from the European Union's Horizon 2020 research and innovation programme under grant agreement No 654662.